Design and Control of an underactuated cable-driven robot for agile handling of parts in a manufacturing line

Atal Anil Kumar

UNIVERSITÉ DE LORRAINE

École doctorale IAEM (Informatique-Automatique-Electronique-Electrotechnique-Mathematiques)

Thèse Européen

Présentée et soutenue publiquement pour l'obtention du titre de

DOCTEUR DE l'UNIVERSITE DE LORRAINE

Mention: << Automatique, Traitement du signal et des images, Génie informatique >>

par Atal Anil KUMAR

Conception et Commande d'un Robot à Câbles pour la manipulation dextre de pièces sur des chaînes de production

Version finale

Membres du jury :

Mme. Christine CHEVALLEREAU,	Directrice de recherche CNRS, LS2N, France	**Rapportrice**
M. Olivier BRÜLS,	Professeur, Université de Liège, Belgique	**Rapporteur**
M. Peter PLAPPER,	Professeur, Université du Luxembourg, Luxembourg	**Rapporteur**
M. Jacques GANGLOFF,	Professeur, Université de Strasbourg, France	**Examinateur**
M. Gabriel ABBA,	Professeur, Université de Lorraine, France	**Directeur**
M. Jean-François ANTOINE,	Maître de Conférences, Université de Lorraine, France	**Co-directeur**
M. Patrick ZATTARIN,	Maître de Conférences, Université de Lorraine, France	**Co-encadrant**

N° EA 4495, Laboratoire de Conception Fabrication Commande (LCFC), Université de Lorraine, Arts et Métiers ParisTech Centre de Metz, 4 rue Augustin Fresnel 57078 METZ Cedex 3

UNIVERSITÉ DE LORRAINE

École doctorale IAEM (Informatique-Automatique-Electronique-Electrotechnique-Mathematiques)

European Thesis

This dissertation is submitted in partial fulfillment of the requirements for the degree

DOCTOR OF PHILOSOPHY

Specialization: << Automatic control, Signal and Image Processing, Computer Engineering >>

by Atal Anil KUMAR

Design and Control of an underactuated cable-driven robot for agile handling of parts in a manufacturing line

Final version

Members of the jury :

Christine CHEVALLEREAU, Research Director - CNRS, LS2N, France	**Reviewer**
Olivier BRÜLS, Professor, Université de Liège, Belgique	**Reviewer**
Peter PLAPPER, Professor, Université du Luxembourg, Luxembourg	**Reviewer**
Jacques GANGLOFF, Professor, Université de Strasbourg, France	**Examiner**
Gabriel ABBA, Professor, Université de Lorraine, France	**Director**
Jean-François ANTOINE, Associate Professor, Université de Lorraine, France	**Co-director**
Patrick ZATTARIN, Associate Professor, Université de Lorraine, France	**Co-supervisor**

N° EA 4495, Laboratoire de Conception Fabrication Commande (LCFC), Université de Lorraine, Arts et Métiers ParisTech Centre de Metz, 4 rue Augustin Fresnel 57078 METZ Cedex 3

Abstract

This thesis aims to design and control an underactuated Cable-Driven Parallel Robot (CDPR) with four cables for the agile handling of parts in a manufacturing line. For already installed manufacturing lines, most of the available working space is often used, and adding a new serial robot on the workshop ground is sometimes difficult. Using the ceiling to fix heavy machines is not always possible, and it could be necessary to reinforce the structure. CDPR is a way to achieve the work with a light structure, with low modification of the existing workshop. The novelty of the work lies in the fact that the majority of the existing designs place the actuating motors and the winches on the base platform, whereas in this work, the actuating motors are placed on the moving platform, making it convenient for the CDPR to be fixed in the manufacturing line with simple anchor points.

First, the workspace of the CDPR for the desired environment is investigated. The underactuated nature of the robot and the positive cable tension constraint imposed due to the flexibility of the cable limit the workspace investigation to static equilibrium conditions. The classical static equilibrium equations have been used to calculate the robot workspace and the corresponding behavior of the platform orientation angles have been presented. Several case studies have been shown with different payloads attached to the moving platform. The dimensions of the moving platform and the base structure have also been changed to understand the possible region of the workspace where the robot performance can be satisfactory. The prototype dimensions have been fixed taking into account the workspace performance. Following this, the classical dynamic model developed in the field of CDPR has been used to implement the control law on the CDPR.

The second part of the thesis presents the design and implementation of the control laws for the CDPR. The classical Input-Output Feedback Linearization (IOFL) technique is developed and simulation results have been presented. The role of internal dynamics present in the system because of the underactuation is demonstrated using their phase-plane plots. Two possible solutions have been suggested to reduce the effect of internal dynamics on the system. The first so-

lution is to use appropriate dimensions for the platform and the base structure. Simulation results have been presented to show the behavior of the platform when the dimensions are changed. A Modified Feedback Linearization (MFL) has been proposed as an ad-hoc solution for eliminating the effects of the internal dynamics. The simulation results obtained show that the proposed ad-hoc solution performs efficiently and significantly better than the classical IOFL technique for certain dimensions of the CDPR. The use of this approach for different cases of CDPR needs to be investigated. Experimental results validating the IOFL technique are presented to demonstrate the satisfactory behavior of the CDPR with the control law developed during the thesis.

The overall objective of the project is to develop a CDPR that can work with an operator in a fully functional manufacturing line and aid the worker in lifting heavy or hot objects. This thesis achieves the first step in making a functional prototype of a CDPR which will be improved further to make it collaborative.

Keywords: Cable-driven parallel robots, workspace analysis, input-output feedback linearization, modified feedback linearization, conceptual design, reconfigurable cable-driven parallel robots.

Résumé

L'objectif de cette thèse est de concevoir et de contrôler un système de Robot Parallèle à Câbles (RPC) à quatre câbles pour la manipulation dextre de pièces sur des chaînes de production. Pour une ligne de fabrication déjà installée, l'espace de travail est souvent limité et l'ajout d'un nouveau robot-sériel sur le sol de l'atelier est parfois difficile. L'utilisation du plafond pour fixer une machine lourde n'est pas toujours possible car il pourrait être nécessaire de renforcer la structure. Le RPC est un moyen de réaliser la tâche avec une faible modification de l'atelier existant. La nouveauté du travail réside dans le fait que la majorité des conceptions existantes placent les moteurs d'actionnement et les treuils de la plate-forme de base, alors que dans ce travail, les moteurs d'actionnement sont embarqués sur la plate-forme mobile, ce qui permet de fixer facilement le RPC dans la chaîne de fabrication avec des points d'ancrage simples.

Tout d'abord, l'espace de travail du RPC pour l'environnement souhaité est étudié. La nature sous-actionnée du robot et la contrainte d'une force de tension positive du câble imposés en raison de la flexibilité des câbles limitent sont la base d'une étude sur l'espace de travail respectant les conditions d'équilibre statique. Les équations d'équilibre statique classiques ont été utilises pour calculer l'espace de travail du robot et le comportement correspondant de la plateforme mobile. Les angles d'orientation de la plate-forme ont été présentés. Plusieurs études de cas ont été montres avec différentes charges utiles attachées à la plate-forme mobile. Les dimensions de la plate-forme mobile et la structure de base ont également été modifiées afin de calculer le domaine de l'espace de travail où les performances du robot peuvent être satisfaisantes. Les dimensions du prototype ont été fixées en tenant compte de l'espace de travail. Par la suite, le modèle dynamique classique du RPC a été utilisé pour mettre en œuvre la loi de contrôle.

La deuxième partie de la thèse présente la conception et la mise en œuvre des lois de contrôle pour la RPC. La linéarisation classique de la rétroaction entrée-sortie (IOFL) est développée et des résultats de simulation ont été présentés. Le rôle de la dynamique interne présente dans le système en raison de la sous-

performance ont été démontrés en utilisant leur diagramme de phase. Deux solutions possibles ont été envisagées afin de réduire l'effet des dynamiques internes sur le système. La première solution consiste à utiliser des proportions appropriées pour la plate-forme et la structure de base. Des résultats de simulation ont été présentés pour montrer le comportement de la plate-forme lorsque les dimensions sont modifiées. Une linéarisation modifiée de la rétroaction (MFL) a été proposé comme une solution *ad-hoc* pour éliminer les effets de la dynamique interne. Les résultats de la simulation obtenus montrent que la solution *ad-hoc* proposée fonctionne efficacement et nettement mieux que la technique classique de l'IOFL pour certaine dimensions du RPC. L'utilisation de cette approche pour différents cas de RPC doit faire l'objet d'une étude enquête. Les résultats expérimentaux validant la technique de l'IOFL sont présentés pour démontrer le comportement satisfaisant de le RPC avec le contrôle.

L'objectif global du projet est de développer un robot parallèle à câble qui peut travailler avec un opérateur dans une chaîne de fabrication pleinement fonctionnelle et aider le travailleur à soulever les objets lourds ou chauds. Cette thèse réalise la première étape pour rendre un prototype de RPC qui sera par la suite amélioré pour le rendre collaboratif.

Mots-clés : Robots parallèles à câble, analyse de l'espace de travail, linéarisation par retour d'état de entrée-sortie, conception, robots parallèles reconfigurables commandés par câble.

Contents

List of Figures

List of Tables

Abbreviations

CDPR	Cable-Driven Parallel Robot
CFW	Collision Free Workspace
CoM	Centre of Mass
DFW	Dynamic Feasible Workspace
DoF	Degree of Freedom
FPK	Forward Pose Kinematics
GDP	Gross Domestic Product
IOFL	Input-Output Feedback Linearization
IPK	Inverse Pose Kinematics
IPM	Interpolated Position Mode
MFL	Modified Feedback Linearization
MIMO	Multi-Input Multi-Output
MP	Moving Platform
PD	Proportional-Derivative
PID	Proportional-Integral-Derivative
PWDR	Parallel Wire-Driven Robot
SEW	Static Equilibrium Workspace
SFW	Stiffness Feasible Workspace
SISO	Single-Input Single-Output
WCW	Wrench Closure Workspace
WFW	Wrench Feasible Workspace
WMSD	Work related Musculoskeletal disorder

General Introduction

Cable-Driven Parallel Robots (CDPRs) is a special variant of traditional parallel robots in which the traditional rigid links are replaced by flexible cables to connect the movable end-effector and the fixed base. The position and orientation of the moving platform are controlled by the coordinated retraction and extension of the cables which are driven by a winch consisting of a tensioning motor and spool or a linear actuator moving a pulley system. CDPRs have several advantages compared to the traditional serial-link and other parallel type robots in terms of large load capacity, low inertia, high energy efficiency, large workspace, and so on. In addition to these, they also are easily reconfigurable, less expensive to construct, easy to transport, assemble and disassemble, etc. CDPRs are suitable for many applications where industrial robots cannot be used due to the limitation of their workspace, payload, and the required cycle time.

The concept of developing underactuated CDPRs has recently attracted much interest from the research community. They are suitable for several applications in which the task to be performed requires a limited number of controlled degrees of freedom or a limitation of dexterity is acceptable to decrease complexity, cost, set-up time, the likelihood of cable interference, etc. They also pose exciting research challenges in terms of their kinematics, workspace, and control theory.

This thesis focuses on the design and development of an underactuated cable-driven robot with four cables that can be installed in a working environment of a manufacturing unit with simple attachment points. It is well known that the working space of most of the production lines is used to its limits. Adding a

new robot to the existing set-up would be a difficult task and could cost a lot to the company. Cable-driven parallel robots could be one of the solutions for such situations. To make the solution more feasible, the actuation unit for the cables (motors, winches, control units, etc.) is placed on the moving platform of the prototype developed in this thesis. The cables are fixed in the working environment with the help of simple anchor points. This simplification can help in strengthening the practical application of the fabricated prototype.

The underactuated design presents several challenges from a control perspective as the number of actuators (4) is less than the number of degrees of freedom (6). This means that it will not be possible to control two degrees of freedom of the moving platform. Hence, the control law must be designed to ensure the stability of the uncontrolled degrees of freedom while controlling the other outputs (the position x, y, z, and the rotation about $z - axis$). It is also evident that due to the underconstrained nature of the CDPR, a point-to-point movement of the moving platform can lead to the generation of unbounded oscillatory motion. The control laws designed must ensure positive cable tensions at all times during the motion of the platform in the entire workspace.

Several control laws have been developed for underconstrained CDPRs. However, not all of them can be applied in general as the control issues of each configuration depend on the degree of underactuation. One of the most commonly used control approaches is known as Input-Output Feedback Linearization (IOFL) technique. This method is used to produce a control input by linearizing the system using the dynamic model of the robot. A precise model of the system is needed to achieve a good control action using the feedback linearization method.

The theoretical formulation of the IOFL has been done based on an initial selection of dimensions for the CDPR. Several simulations have been performed to get an overview of the performance of the control law and to observe the behavior of the uncontrolled degrees of freedom (in this case the platform orientation

angle about x and y axis). Based on the simulation results, a modified feedback linearization method is proposed for improving the results of control for the initial parameters of the simulation. The performance of the proposed modified feedback linearization has been demonstrated through the simulation plots.

The prototype of the CDPR has been fabricated at the LCFC laboratory at Metz, France, to validate the theoretical results of IOFL control. There is a difference in the initial dimensions (square fixed structure and square moving platform) used for the simulation and the final dimensions of the prototype (rectangular fixed structure and square moving platform). This is because of the constraints in the environment where the CDPR is installed. The tests have been performed on the CDPR to generate a point-to-point motion along the $z - axis$. The results of the tests in general, prove the validity of the IOFL control law formulated in the work. Some issues need to be addressed with regards to the cable oscillations, the addition of other sensors to make the feedback more robust and reliable and using a more advanced model of the cable taking into account the stiffness of the system. These points have been discussed in detail in the thesis.

This manuscript is organized into six chapters :

In **Chapter I**, a brief introduction about the research is presented. The motivation for the thesis and the major objectives of the work are explained.

Chapter II presents the state-of-the-art including the configurations, applications, and importance of CDPRs. The various control techniques developed on CDPRs are explained in detail. A section with particular emphasis on the control of existing underactuated cable-driven parallel robots is presented to understand the existing challenges. The various research areas that will be addressed in this work are highlighted at the end of the chapter.

The static equilibrium workspace of the underactuated CDPR is presented in **Chapter III**. The design of a CDPR requires the computation of the size and shape of its workspace in addition to the other capabilities. The calculation of the

SEW workspace provides an overview of the possible values of platform orientation angles due to the under-constrained nature of the design, and also the values of the cable forces to maintain the CDPR at static equilibrium. Several case studies have been presented to highlight the changes in the workspace size and shape due to the changes in the platform and fixed structure dimensions. The workspace has also been calculated by changing the total mass acting on the platform. This chapter also presents the commonly used equations for the calculation of the geometric, kinematic dynamical model of the CDPRs.

Chapter IV introduces one of the most widely used approaches for nonlinear systems, known as IOFL. This approach is used to control the CDPR fabricated in this thesis. The first part of the chapter presents the general mathematical formulation for the IOFL approach followed by the implementation of the control law on the CDPR. Simulation results have been presented for different conditions to analyze the performance of the CDPR. Since the number of actuators (4) is less than the number of degrees of freedom (6), there is a presence of internal dynamics in the system. These internal dynamics can result in some unwanted behaviors in the moving platform such as oscillations, high cable forces, and unrealistic acceleration values, etc. Hence, it is important to understand the role of internal dynamics for the CDPR studied in this work. The behavior of the uncontrolled internal dynamics has been studied using phase-plane plots. It has been observed that the internal dynamics resulted in oscillations in the platform orientation angles which in turn resulted in high oscillations of the cables forces.

As a possible solution, the role of platform dimensions in reducing the oscillations in cable forces has been highlighted using simulation studies. The complexity of the equations restricted the formulation of a mathematical relationship between the dimensions and the internal dynamics behavior. From a control perspective, a modified feedback linearization method has also been proposed that showed significant improvement in the performance of the CDPR behavior with the initial

dimensions considered. This law was able to reduce the effect of internal dynamics which in turn helped in eliminating the oscillations in the cable forces. The application of this modified control law on other general CDPR systems needs to be verified so that a mathematical stability criterion can be developed accordingly.

The experimental validation of the IOFL control is presented in **Chapter V**. The details of the prototype developed in this work have been presented in the first part. The experimental setup and the procedures followed to perform the tests have been explained. The validation of the control law is done for a translation motion of the moving platform along the $z-axis$. This avoided the addition of any external sensors to obtain feedback about the movement in z. Two sets of point-to-point motions have been studied and the comparison between the desired values and the obtained values are presented. The cable forces have been measured using force sensors and are compared with the estimated values of forces generated using the control law. It was shown that the moving platform was able to achieve the desired motion with satisfactory performance. There are cable oscillations due to the movement and also due to the under-constrained configuration. However, for the cases considered, these oscillations did not impact the position of the moving platform. Further tests will be done on movement in different directions to analyze and improve the behavior of the CDPR. The important inferences from the tests have been discussed at the end of the chapter.

A general conclusion is written in **Chapter VI** on the research work carried out in the framework of this doctoral thesis. This thesis achieved the first step in making a working prototype of an underactuated CDPR to be installed in a manufacturing line. Finally, the topics for future research works are discussed to improve the performance of the CDPR to make it fully functional for a successful installation.

Introduction générale

Les Robots Parallèles à Câble (RPC) sont une variante spéciale des robots parallèles traditionnels dans lesquels les liens rigides traditionnels sont remplacés par des câbles flexibles pour relier l'effecteur final mobile et la base fixe. La position et l'orientation de la plate-forme mobile sont contrôlées par la rétraction et l'extension coordonnées des câbles qui sont entraînés par un treuil composé d'un motoréducteur et d'une tambour de treuil ou d'un actionneur linéaire déplaçant un système de poulies. Les RPC présentent un certain nombre d'avantages par rapport aux robots traditionnels à liaison série et autres types de robots parallèles rigides en termes de grande capacité de charge, de faible inertie, de rendement énergétique élevé, d'espace de travail important, etc. En outre, ils sont facilement reconfigurables, moins chers à construire, faciles à transporter, à monter et à démonter, etc. Les RPC conviennent pour un certain nombre d'applications où les robots industriels ne peuvent pas être utilisés en raison de la limitation de leur espace de travail, de leur charge utile et du temps de cycle requis.

Le concept de développement de RPC sous-actionnéés a récemment suscité un grand intérêt de la part de la communauté des chercheurs. Ils conviennent à plusieurs applications dans lesquelles la tâche à accomplir nécessite un nombre limité de degrés de liberté contrôlés ou dans lesquelles une limitation de la dextérité est acceptable afin de réduire la complexité, le coût, le temps de mise en place, la probabilité d'interférence des câbles, etc. Ils posent également des défis de recherche passionnants en termes de cinématique, d'espace de travail et de théorie du contrôle.

Cette thèse se concentre sur la conception et le développement d'un robot parallèle à quatre câbles, qui peut être installé dans un atelier de fabrication avec des points d'attache simples. L'environnement d'un atelier pouvant être fortement encombré, l'ajout d'un nouveau robot dans l'installation existante est délicat et pourrait coûter très cher à l'entreprise. Des robots parallèles actionnés par câble pourraient être une solution appréciable pour de telles situations. Afin de rendre la solution plus réaliste, l'unité d'actionnement des câbles (moteurs, treuils, unités de commande, etc.) est placée sur la plate-forme mobile du prototype développé dans cette thèse , de sorte que les câbles aient seulement besoin d'être fixés dans l'environnement de travail à l'aide de simples points d'ancrage. Cette simplification peut contribuer à renforcer l'application pratique du prototype fabriqué.

La conception sous-actionnée présente plusieurs défis du point de vue du contrôle, car le nombre d'actionneurs (4) est inférieur au nombre de degrés de liberté (6). Cela signifie qu'il ne sera pas possible de contrôler deux degrés de liberté de la plate-forme mobile. Il est donc nécessaire que la loi de commande soit conçue pour assurer la stabilité des degrés de liberté non contrôlés tout en contrôlant les autres sorties (la position x, y, z, et la rotation autour de l'axe z). Il est également évident qu'en raison de la nature peu contraignante du RPC, un mouvement point à point de la plate-forme mobile peut entraîner la génération d'un mouvement oscillatoire non contrôlé. Les lois de contrôle développées doivent garantir le maintien d'une force de tension positive dans les câbles à tout moment pendant le mouvement de la plate-forme dans l'ensemble de l'espace de travail.

Un certain nombre de lois de contrôle ont été élaborées pour les RPC sous-contraints. Cependant, elles ne peuvent pas toutes être appliquées de manière générale, car les questions de contrôle de chaque configuration dépendent du degré de sous-actionnement. L'une des approches de contrôle les plus couramment utilisées est connue sous le nom de technique de linéarisation par retour d'état entrée-sortie (IOFL). Cette méthode est utilisée pour produire une entrée

de commande en linéarisant le système à l'aide du modèle dynamique du robot. Un modèle précis du système est nécessaire pour obtenir une bonne action de contrôle en utilisant la méthode de linéarisation par rétroaction.

La formulation théorique de l'IOFL a été faite sur la base d'une première sélection de dimensions pour le RPC. Plusieurs simulations ont été réalisées pour obtenir une vue d'ensemble des performances de la loi de commande et pour observer le comportement des degrés de liberté non contrôlés (dans notre cas, les angles d'orientation de la plate-forme autour de l'axe x et y). Sur la base des résultats de la simulation, une méthode modifiée de linéarisation de la rétroaction est proposée pour améliorer les résultats du contrôle pour les paramètres initiaux de la simulation. La performance de la linéarisation modifiée proposée a été démontrée par les tracés de simulation.

Le prototype du RPC a été fabriqué au laboratoire LCFC de Metz, en France, pour valider les résultats théoriques du contrôle de l'IOFL. Il existe une différence entre les dimensions initiales (structure fixe carrée et plate-forme mobile carrée) utilisées pour la simulation et les dimensions finales du prototype (structure fixe rectangulaire et plate-forme mobile carrée). Ceci est dû aux contraintes de l'environnement dans lequel le RPC est installé. Les tests ont été effectués sur le RPC pour générer un mouvement point à point le long de l'axe z. Les résultats des tests en général, prouvent la validité de la loi de contrôle de l'IOFL formulée dans le travail. Certaines questions doivent être abordées en ce qui concerne les oscillations du câble, l'ajout d'autres capteurs pour rendre le retour d'information plus robuste et plus fiable et l'utilisation d'un modèle plus avancé du câble tenant compte de la rigidité du système. Ces points ont été discutés en détail dans la thèse.

Ce manuscrit est organisé en six chapitres :

Dans le **chapitre I**, une brève introduction sur la recherche est présentée. La motivation de la thèse et les principaux objectifs du travail sont expliqués.

Chapitre II présente l'état de l'art, y compris les configurations, les applica-

tions et l'importance des RPC. Les différentes techniques de contrôle développées sur les RPC sont expliquées en détail. Une section mettant particulièrement l'accent sur la commande des robots parallèles à câble sous-actionnés existants est présentée pour comprendre les défis existants. Les différents domaines de recherche qui seront abordés dans ce travail sont mis en évidence à la fin du chapitre.

L'espace de travail en équilibre statique du RPC sous-activé est présenté dans **Chapitre III**. La conception d'un RPC nécessite le calcul de la taille et de la forme de son espace de travail en plus des autres capacités. Le calcul de l'espace de travail statique (SEW) donne un aperçu des valeurs possibles des angles d'orientation de la plate-forme en raison de la nature sous-actionnée de la conception, et aussi les valeurs des forces du câble pour maintenir le RPC en équilibre statique. Plusieurs études de cas ont été présentées pour mettre en évidence les changements de taille et de forme de l'espace de travail dus aux modifications des dimensions de la plate-forme et de la structure fixe. L'espace de travail a également été calculé en modifiant la masse totale supportée par la plate-forme. Ce chapitre présente également les équations couramment utilisées pour le calcul du modèle géométrique, cinématique et dynamique des RPCs.

Chapitre IV présente l'une des approches les plus utilisées pour les systèmes non linéaires, connue sous le nom de IOFL. Cette approche est utilisée pour contrôler le RPC fabriqué dans le cadre de cette thèse. La première partie du chapitre présente la formulation mathématique générale de l'approche IOFL, suivie de la mise en œuvre de la loi de contrôle sur le RPC. Des résultats de simulation ont été présentés pour différentes conditions afin d'analyser la performance du RPC. Comme le nombre d'actionneurs (4) est inférieur au nombre de degrés de liberté (6), il y a présence d'une dynamique interne dans le système. Cette dynamique interne peut entraîner certains comportements indésirables dans la plate-forme mobile, tels que des oscillations, des forces de câble élevées et des valeurs d'accélération irréalistes, etc. Par conséquent, il est important de comprendre le

rôle de la dynamique interne pour le RPC étudié dans ce travail. Le comportement de la dynamique interne non contrôlée a été étudié à l'aide de diagrammes de phase. Il a été observé que la dynamique interne entraînait des oscillations dans les angles d'orientation de la plate-forme qui, à leur tour, entraînaient de fortes oscillations des forces des câbles.

Comme solution possible, le rôle des dimensions de la plate-forme dans la réduction des oscillations des forces des câbles a été mis en évidence à l'aide d'études de simulation. La complexité des équations a limité la formulation d'une relation mathématique entre les dimensions et le comportement de la dynamique interne. Du point de vue du contrôle, une modification de la méthode de linéarisation par retour d'état a également été proposée, qui a montré une amélioration significative de la performance du comportement du RPC avec les dimensions initiales considérées. Cette loi a permis de réduire l'effet de la dynamique interne, ce qui a contribué à éliminer complètement les oscillations dans les forces du câble. L'application de cette loi de contrôle modifiée sur d'autres cas généraux de RPC doit être vérifiée afin qu'un critère de stabilité mathématique puisse être développé en conséquence.

La validation expérimentale du contrôle de l'IOFL est présentée dans **chapitre V**. Les détails du prototype développé dans le cadre de ce travail ont été présentés dans la première partie. Le dispositif expérimental et les procédures suivies pour effectuer les tests ont été expliqués. La validation de la loi de commande est faite pour un mouvement de translation de la plate-forme mobile le long de l'axe z. Cela a permis d'éviter l'ajout de tout capteur externe pour obtenir le retour d'information sur le mouvement en z. Deux ensembles de mouvements point à point ont été étudiés et la comparaison entre les valeurs souhaitées et les valeurs obtenues est présentée. Les forces des câbles ont été mesurées à l'aide de capteurs de force et sont comparées aux valeurs estimées des forces générées à l'aide de la loi de commande. Il a été démontré que la plate-forme mobile était capable

d'effectuer le mouvement souhaité avec des performances satisfaisantes. Il y a des oscillations des câbles dues au mouvement et aussi à la configuration sous contrainte. Cependant, pour les cas considérés, ces oscillations n'ont pas eu d'impact sur la position de la plate-forme mobile. D'autres tests seront effectués sur le mouvement dans différentes directions pour analyser et améliorer le comportement du RPC. Les conclusions importantes tirées de ces tests ont été discutées à la fin du chapitre.

Une conclusion générale est écrite dans le **chapitre VI** sur les travaux de recherche effectués dans le cadre de cette thèse de doctorat. Cette thèse a permis de réaliser la première étape de la fabrication d'un prototype fonctionnel de RPC sous-activé destiné à être installé dans une chaîne de fabrication. Enfin, les sujets des futurs travaux de recherche sont abordés afin d'améliorer les performances du RPC pour le rendre pleinement fonctionnel pour une installation réussie.

Chapter 1

Introduction

Contents

The rapid technological advances in computation, communication, and miniaturization have led to the tremendous growth of robotics and its application in various fields. Robotic systems gained importance because of their exceptional help to humans in doing the 4-D tasks (Dirty, Dull, Dumb, and Dangerous). The demand for robots that are simpler to program and easier to integrate with the technologies is on the rise, and collaborative robots are considered to be the solution for such requirements. Therefore, it is essential to classify and understand the existing system of robot manipulators to help in the continuous development of the new design of robots.

1.1 Context of the work

The proposed work started in January-2017, is a part of the project of Robotix Academy, which is a cross-border research center for industrial robotics and human-robot cooperation and is being funded by the INTERREG V-A Grand Region program that supports cross-border cooperation projects between local and regional agencies from the territories that make up the Grand region.

Figure 1.1: Logo of Robotix Academy[Rob]

1.2 Motivation and Objectives

Work related Musculoskeletal disorders (WMSDs) are the most common occupational health problem in Europe, affecting millions of workers [Wor10]. Most of the processes in manufacturing plants involve automated, semi-automated, and manual, repetitive tasks. Even though a large part of manual work has been replaced by automation, there remain many tasks performed manually. It has been found in various studies that these WMSDs are mainly due to the x repetitive industrial tasks and handling of heavy parts by the workers. In addition to these, the exposure of workers to the heat of the metal when handling hot parts also adds to their discomfort. WMSD problems result in low worker productivity as it tends to slow them physically.

WMSDs are reported to cause approximately 34% of the annual lost time in a company resulting in an overall productivity loss of 7% [NDD]. In addition to the discomfort caused to the workers, it also resulted in high costs to the individual company due to the medical and social security expenses and lost productivity. In some European countries, around 40% of the costs of the worker's compensation are caused by WMSDs and up to 1.6% of the Gross Domestic Product (GDP) of the country itself.

The objective of the proposed work is to develop a solution to help the worker with Cobots (Collaborative robots) to reduce the WMSDs amongst the workers, thus leading to the reduction of compensation costs to the companies. Collaborative robots are a recent trend to allow the interaction of the workers and robots in a safe way making use of the worker's experience. The working space of an already installed manufacturing line is often used to its maximum possible extent and adding a new serial robot in the existing setup would be a very difficult task and would cost a lot to the company. Installing the robots on the ceiling would require reinforcement of the structure, again making the task costlier. A parallel wire-driven robot is a way to achieve the work with a light structure and with low modification of the existing set-up. Hence the main objective of the proposed work is to design and control a parallel wire-driven robot for agile handling of

parts in a manufacturing line.

The wire driven robot is desired to have the following requirements:
1) The number of cables is 4.
2) Motorization to be done on the moving platform, unlike the other designs in which the motors are placed in the base or fixed structure.
3) Simple anchors that can be attached to the environment.
4) An optimum number of actuators to get good control of the moving platform.

1.3 Contribution of the thesis

The research work presented in this manuscript aims mainly at fabricating an underactuated cable-driven robot with four cables and defining a set of control laws that can be used to control and stabilize its motion. The design proposed in this work is different from the other existing designs in the fact that the actuator unit (motors, the controller, and the gears) of each cable is placed on the moving platform. This approach adds considerable mass and inertia to the moving platform. The design also makes use of simple anchors, which can be easily attached to the fixed structure. Several contributions have been made in this thesis to realize the prototype of the robot. These contributions are listed in the subsections below.

1.3.1 Static Equilibrium Workspace

The idea about the possible workspace for the robot is needed for the fabrication of the prototype. With this objective, the initial contribution of the thesis is the implementation of the well-established static equilibrium conditions in the literature to calculate the Static Equilibrium Workspace (SEW) of the CDPR to be designed. These conditions have been imposed on various configurations to obtain an idea about the possible shape and size of the workspace. Limits have been imposed on the cable tension that can be handled by the cables. Additional payload mass has been added to the moving platform to observe the changes in the workspace. Different dimensions (rectangular, square) have been used for the platform shape and the fixed structure shape to fix a satisfactory working area for the robot. Using the observation and inferences from these results, the prototype dimensions are selected. Following this, the standard dynamic model of a CDPR is used to establish the relationship between the CDPR acceleration and the cable forces. For the dynamic model formulated, this work takes into account: (i) the inertia of the moving platform; (ii) the centrifugal and the Coriolis forces induced

by a constant moving platform twist.

1.3.2 Contribution from Control perspective

The significant contribution of the work is the design and implementation of the IOFL technique for the control of the robot. The classical IOFL approach has been formulated to control the four degrees of freedom namely, the three translations along $x-axis$, $y-axis$, $z-axis$ and the Euler angle rotation about the $z-axis$, also known as γ. The internal dynamics of the robot due to the uncontrolled degrees of freedom namely, rotation about $x-axis$, also known as α, and rotation about $y-axis$, also known as β, is analyzed using simulations. The behavior of the robot is stable with smooth values of cable forces for point-to-point motion. However, at certain points in the working environment, the cable forces and the platform orientation angles (α and β) were found to be oscillatory. These oscillations are dangerous for the robot and its actuation unit. It is challenging to calculate the mathematical equations representing the zero dynamics of the CDPR due to the positive cable tension constraint and a lesser number of cables than the number of degrees of freedom of the moving platform. Phase-plane plots have been observed from the simulation studies to infer the oscillatory nature of the internal dynamics. The initial calculation of the internal dynamics equations with some simplifications shows a strong dependence of the internal dynamics on the physical parameters (the platform dimensions, the fixed structure dimensions, the center of mass of the moving platform). Based on the simulation results, two solutions have been proposed to reduce the oscillations due to the internal dynamics behavior.

The first solution suggested is based on changing the physical parameters (MP dimensions, Centre of Mass (CoM) of the moving platform, and the base platform or the dimension of the room where the robot is mounted). Several case studies have been presented by changing each of the parameters and the IOFL has been implemented on the modified dimensions. The results have shown a huge difference from the initial results obtained as the oscillations on the cable forces reduced by a big margin. This solution can be considered by the researchers before the fabrication or mounting of the robot. This can help in avoiding unwanted internal dynamics behavior. The relationship between the dimensions and the internal dynamics behavior, however, is not established as more studies are needed to quantify the relation.

A modified feedback linearization (MFL) technique is proposed as an ad-hoc solution for the initial configuration considered where at certain positions in the

working environment, the robot behavior was found to be unstable due to the internal dynamics. The motivation for this approach is taken from the various control laws existing where the researchers have combined two different control techniques to control and stabilize a system. This approach makes use of two control branches that act simultaneously on the dynamic model of the robot to stabilize the platform orientation angles. One of the control branch acts on x, y, z, and α while the other control branch acts on x, y, z, and β respectively. Each branch is formulated to act on half of the total wrench acting on the moving platform (the total mass of the platform in this thesis). The working of the proposed MFL has been demonstrated using simulations. The proposed approach was successful in eliminating the cable oscillations and also in stabilizing the platform orientation angles. The performance is very good compared to the classical IOFL method for the same configuration. Several case studies have been presented where different conditions have been imposed on the platform by changing the mass of the moving platform. These case studies prove the efficient working of the proposed control law. The use of this modified approach on a general CDPR system needs to be tested for further developing a global stability condition.

The experimental tests have been performed on the prototype fabricated at the LCFC laboratory at Metz, France, to validate the theoretical results. The test results present the point-to-point movement along the $z - axis$ (translation along $z - axis$) where the control law can be implemented measuring only the motor positions. These motor positions have been used to approximate the cable lengths at the particular position. The pose of the robot is then re-built solving a nonlinear optimization problem to implement the feedback to reach the desired value. Two different control modes (interpolated position mode and position mode) offered by the electronic controller are used for the implementation of the feedback. The obtained results have been compared with the theoretical values obtained.

1.4 Thesis organization

This thesis is organized as follows. Chapter II presents the literature review of the existing research on CDPRs. Chapter III introduces the geometric, kinematic, and dynamic models used for studying the performance of CDPRs. This chapter also presents the static equilibrium workspace analysis for the four cable-robot considered. Chapter IV describes the formulation of the classical input-output feedback linearization control technique developed for the implementation on the CDPR. The experimental validations are presented in chapter V. Chapter VI

concludes this manuscript by summarizing the main contributions of this doctoral thesis and by discussing the future research perspectives.

Chapter 2

Literature Review

Contents

This chapter gives a brief introduction to classical industrial manipulators with their advantages and disadvantages. Following this, the concept of cable-driven parallel robots is presented along with their advantages and applications. The various techniques developed for the control of CDPRs are also highlighted. Finally, a section dedicated to the state-of-the-art in the control of under-constrained CDPRs is presented.

2.1 Classical robots

Industrial robotic manipulators are primarily classified into serial and parallel robots based on their structural topology. A serial manipulator consists of an open-loop kinematic chain of one or several links connected in series through actuated joints that are mostly revolute or prismatic [KD04]. Serial robots are often referred to as robotic arms or articulated robots due to their kinematic similarity with the human arm. A parallel manipulator, on the other hand, is a closed-loop kinematic chain mechanism whose end-effector is linked to the base by several independent kinematic chains. These chains are typically referred to as legs or limbs,

while the end-effector is commonly called the platform [Mer06]. A parallel robot with n-degrees of freedom has at least two independent kinematic chains connecting the end-effector, and the fixed base [Mer06]. The actuation of the kinematic chains takes place through n simple actuators. A planar parallel manipulator mostly uses revolute or prismatic joints while the spatial systems use universal and spherical joints [Tsa99]. Examples of a typical serial and parallel manipulator are shown in Fig. 2.1. Serial manipulators have a compact design in general, in addition to their high dexterity and large achievable workspace compared to that of traditional parallel manipulators. However, their limited payload-to-weight ratio, along with their cantilevered structure, results in lower positioning accuracy and lower stiffness. These shortcomings are improved upon by parallel manipulators largely as their structure allows the platform's weight to be distributed through each of the supporting kinematic chains resulting in greater rigidity and positioning accuracy. The primary disadvantage of parallel manipulators is their limited workspace, mainly due to the geometrical and mechanical limits of the design and its joints. This workspace is prone to singularities and causes the system to gain uncontrollable degrees of freedom [AA02b]. In addition to this, the analysis and control of parallel manipulators are, in general, more complex.

(a) A serial manipulator from KUKA robotics[Kuk] (b) A parallel manipulator from ABB[Abb]

Figure 2.1: Classical industrial manipulators

2.2 Cable-Driven Parallel Robots

A new class of parallel robots emerged in the late 1980s and early 1990s from the works of Landsberger [Lan85], Higuchi and Ming [Hig88], and Albus [ABD93] with a major modification in the structure of the traditional parallel robot. This

class of manipulators has been commonly referred to as the Cable-Driven Parallel Robots (CDPRs) or Parallel Wire-Driven Robots (PWDRs) in which the rigid links of the parallel robot is replaced by cables. A simple sketch of a CDPR is given in Fig. 2.2. A cable-driven parallel robot (CDPR) is composed of four basic

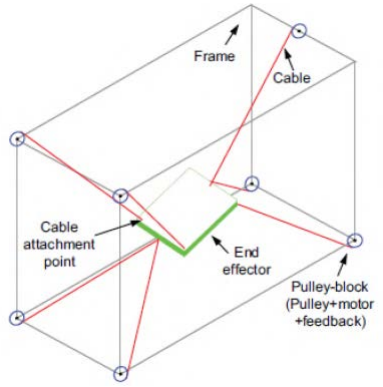

Figure 2.2: Schematic representation of CDPR

components. A platform or end-effector, which is positioned within a workspace to fulfill a specific task, cables to control and move the platform, winches which change the cable length, and a frame upon which these cables are fixed. As the name implies, the platform of the CDPR is driven by a set of cables whose length is adjusted by a winch consisting of a tensioning motor and spool or a linear actuator moving a pulley system [MD10a]. The position and orientation of the platform are controlled by coordinated retraction and extension of cables.

One of the important features of CDPRs is that the cables can be used only when they are in tension. Because of this unilateral nature of cables, it has been reported that in order to design a fully controllable robot with n DoFs, to prevent stability and control being dependent on gravity, at least $n + 1$ cables are needed [Cho96; SOA94].

2.2.1 Classification of CDPRs

CDPRs can be mainly classified according to:
1) Number of the driving cables(m) and degrees of freedom(n)
2) Arrangement of cables
3) Number of controlled degrees of freedom

1) According to number of the driving cables(m) and DoFs(n)

One of the earliest classifications of CDPRs was proposed in [Min94a] and was extended by Verhoeven et al. in [VHT98]. A review of this classification is given here.

A CDPR with m-cables and n-DoF is said to be completely restrained or fully-constrained ($CRPM$) if it has one cable more than the number of degrees of freedom, i.e. $m = n + 1$ (Fig. 2.3b). In such a type of arrangement, all degrees of freedom can be controlled through the cables. An incompletely restrained or

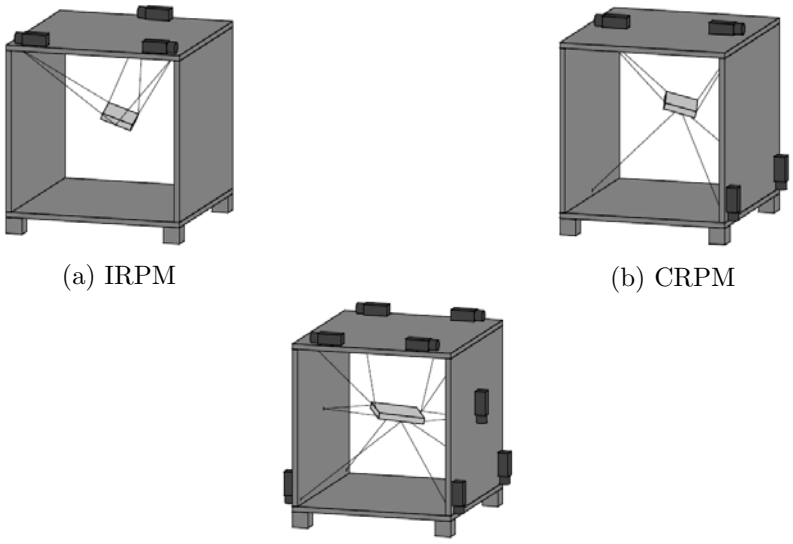

(a) IRPM (b) CRPM

(c) RRPM

Figure 2.3: Classification of CDPRs based on number of controlled DoF[VHT98]

under-constrained cable robot ($IRPM$) is one in which the number of cables is less than or equal to the number of degrees of freedom, i.e., $m \leqslant n$ (Fig. 2.3a). Such systems have one feasible solution for cable tensions and mostly rely on gravity for keeping the cables taut.

A CDPR is said to be redundantly restrained or over-constrained if it has $m > n + 1$ cables (Fig. 2.3c). Such robots have an extended workspace, reduced singularity, and increased stiffness. It also leads to the redistribution of payloads to more cables, which reduces the tension of the driving cables. However, it increases the complexity of workspace analysis and control along with increased cable interference with each other and also with the surroundings.

2) According to arrangement of cables

According to the arrangement of cables, the CDPRs are classified as Suspended CDPRs and Non-suspended CDPRs [Yua15]. A CDPR is said to be suspended when all the driving cables are above the end-effector, and gravity acts as a virtual cable to maintain equilibrium (Fig. 2.4a). Such CDPRs usually have a big load capacity and minimal possibility of cable interference with other objects in the environment. These properties of suspended CDPRs make them suitable for pick and place applications. However, they have a very low stiffness which results in

vibrations and instability of the end-effector. A CDPR is said to be non-suspended

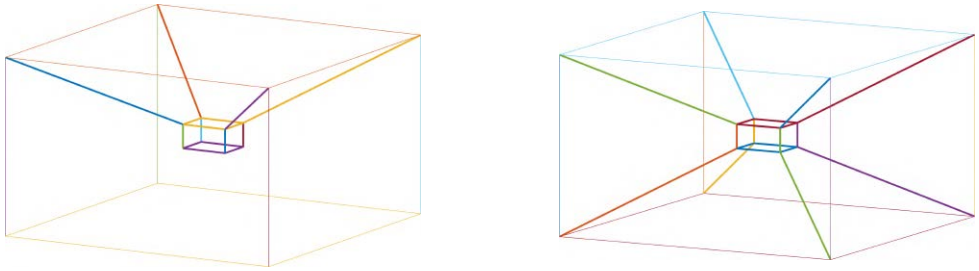

(a) Suspended CDPR (b) Non-suspended CDPR

Figure 2.4: Classification of CDPRs based on number of cables [Yua15]

when at least one driven-cable is below the end-effector (Fig. 2.4b). Also, CDPRs working on a horizontal plane are classified as non-suspended CDPRs. In this case, gravity has no effect on the equilibrium of the end-effector as the weight of the end-effector is balanced by the support of the plane. Non-suspended CDPRs exhibit better performances in high velocity/acceleration applications compared to suspended CDPRs along with improved stiffness and positioning accuracy. However, there may be a significant increase in energy consumption because of the increased number of actuators.

3) According to number of controlled degrees of freedom

Verhoeven proposed a different classification of robot depending on the number of controlled dofs as given below where T is for translation, and R is for rotation [Ver04].

Table 2.1: Table of classification

Type	Motion
1T	Linear motion of a point
2T	Planar motion of a point
1R2T	Planar motion of a body
3T	Spatial motion of a point
2R3T	Spatial motion of a beam
3R3T	Spatial motion of a body

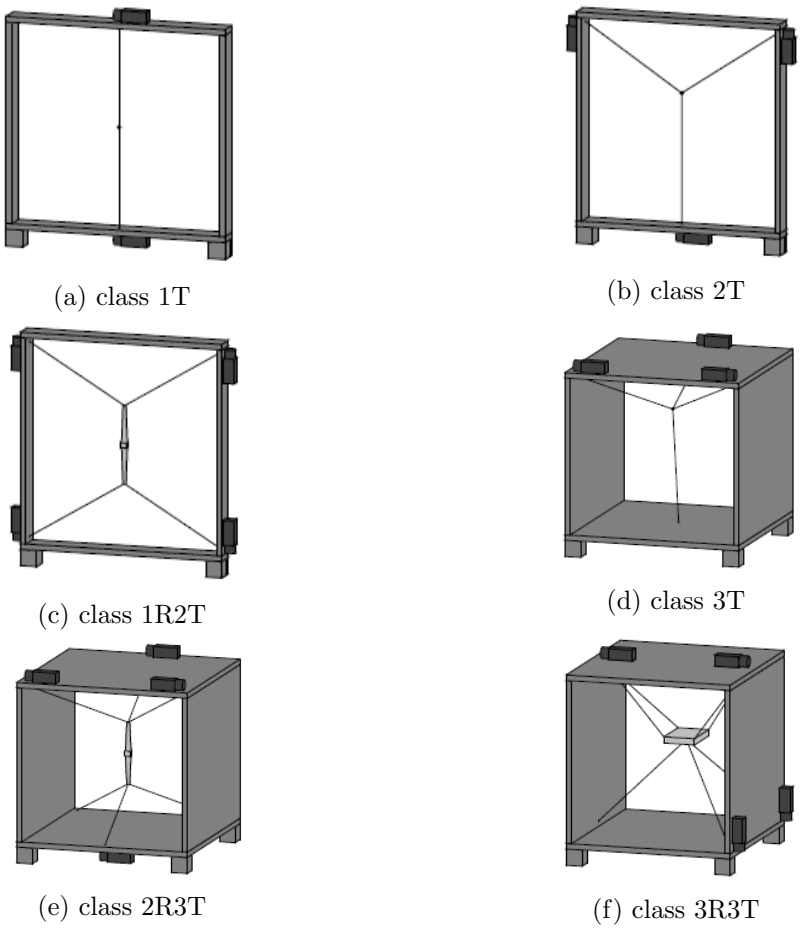

(a) class 1T (b) class 2T

(c) class 1R2T (d) class 3T

(e) class 2R3T (f) class 3R3T

Figure 2.5: Classification of CDPRs based on number of controlled DoF [Ver04]

Various other classifications have been done by the researchers, for example, cable-driven planar robot and cable-driven spatial robot, cable-driven serial robot and cable-driven parallel robot, purely cable-driven robot and hybrid cable-driven robot [Pot18], and so on. However, the major classifications given above covers all the types of CDPRs and is sufficient for the proposed work.

2.2.2 Advantages and Applications of CDPRs

CDPRs offer many advantages when compared to the traditional parallel manipulators.

1) **Large workspace** - One of the most important advantages provided by CDPRs over the classical robots is the large workspace depending on the configuration of the CDPR used for the application. Since the cables are actuated mostly by winches, a large range of length change on the cables can be provided, which is not possible by robots with rigid links [TN08; Con85].

2) **Low inertia** - Since the rigid links of a traditional parallel robot is re-

placed by cables, it reduces the mass and inertia of the manipulator, which in turn maximizes the use of material strength and reduces the mass and inertia of the manipulator. It is known that when the materials are under tensile loading, they provide their highest strength to mass ratio. Since the cables in a CDPR can only be in tension for their application, this results in low inertia, which is desirable in several applications where high speed is desirable [BK06].

3) **Structural simplicity** - The flexible property of cables is utilized as kinematic joints in the robot structure, which reduces the fabrication cost and also keeping the entire structure simple [BFV16].

4) **Reconfigurability** - The winch assemblies can be relocated and reconfigured based on the end-user need to adjust the workspace and configuration [HW06].

5) High-speed manipulation, High payload to robot weight ratio, ease of transportability, high energy efficiency, and low cost are other advantages of CDPRs [ABD93; KKW00]. These advantages are not true for all CDPRs and apply to the configuration of the CDPR considered and the application of the CDPR.

The need for new ideas for applications is typically driven by replacing a mostly manual or mechanized process with a robotic solution that allows for fully/semi-automatic operation. The applications in which CDPRs are implemented successfully make use of the strengths highlighted earlier [Pot18]. A brief description of the various applications is explained in the following paragraphs.

Figure 2.6: Skycam

Figure 2.7: NIST Robocrane

Logistics

CDPRs are being used efficiently in handling, sorting, and palletizing operations because of their large workspace and fast dynamics. One of the earliest high-speed pick and place CDPR was designed by Kawamura [KKW00]. Handling of boxes weighing up to 500 kg in automatic operations was done by CoGiRo CDPR [LG13].

A low-cost and efficient robotic solution combining mobile robots and CDPR

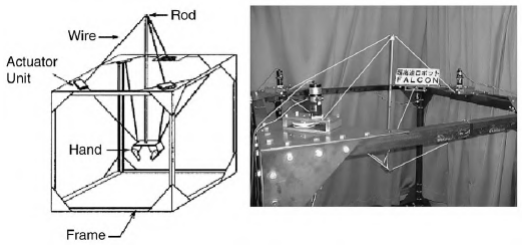

Figure 2.8: High-speed CDPR - FALCON [Kaw+97]

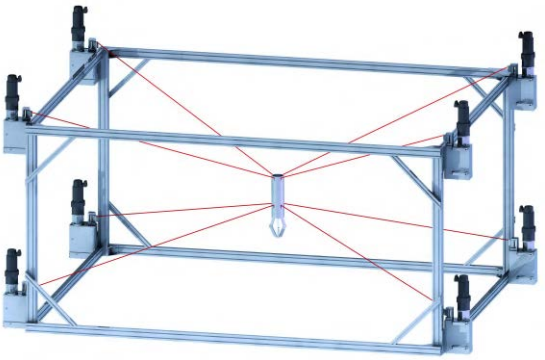

Figure 2.9: IPANEMA robot [Pot18]

has been done for fast picking and kitting operations in existing storage facilities by the FASTKIT project [Ras+18]. The concept of transporting people across river has been addressed by Castelli [COR14]. Other notable CDPRs in logistics is the CABLAR system developed by Bruckmann [Bru+12] used as a storage-retrieval machine, a portable crane for handling heavy loads designed by Merlet, and CDPR design proposed by Bauer in his patent to move optical and radio sensors through shelf storage systems for inspection purpose.

Medical and Rehabilitation Applications

CDPRs have been used widely for the rehabilitation of injured people and post-stroke patients. Some of the well-known research works include the Multi-Axis Cartesian-based Arm Rehabilitation Machine (MACARM) [May+05], Sophia-3 [Zan+14] and wearable exoskeleton CAREX [MA12]. The majority of the CDPRs focus on upper limb rehabilitation even though there are exceptions like STRING-MAN, which is meant for gait rehabilitation in which the CDPR is connected to the patient where the patient's skeletal structure acts analogously to the rigid links of an MCDR [SZB07]. Merlet et al. have designed a family of CDPRs known as MARIONET, which includes MARIONET-ASSIST (used to assist elderlies or people with motion disabilities), MARIONET-REHAB (used for rehabilitation or fast displacement of small payloads), and MARIONETCRANE, which is used in search and rescue operations [Mer08; MD10b]. Practical tests were performed

Figure 2.10: Carex:wearable exoskeleton [MA12]

Figure 2.11: Cogiro prototype [LG13]

with these manipulators for lifting elderly and disabled humans in an ambient assisted living environment.

Construction

The large operating workspace and low mechanism inertia facilitates the use of CDPRs as cranes [ABD93; Hig88; Mae+99]. Through a suitable reconfiguration strategy, Gagliardini et al. have designed a reconfigurable CDPR for the problem of painting and sandblasting large structures [Gag+15]. Bosscher et al [Bos+07] and Barnet and Gosselin [BG15] developed large scale 3D printing facilities for additive manufacturing applications taking advantage of the easy transportability of CDPRs. The project MEDIA-TIC equipped the end-effector of a CDPR with atmospheric sensors to be integrated into the building facades for the concept of intelligent building [Iza+13].

Entertainment

(a) MARIONET ASSIST

(b) MARIONET REHAB

(c) MARIONET CRANE

Figure 2.12: The cable robots of the Marionet family [Mer08; MD10b]

Amusement parks worldwide, such as Disney, have used suspended CDPRs to present thrill rides for the people visiting the parks [CN12]. Another successful commercial application is the use of CDPRs to suspend cameras used at various sporting and entertainment events and cinematography. This technology was developed as early as 1980 [Con85] and has since then developed further to provide spectacular video footage from an excellent point of view.

Other Applications

Several other applications of CDPRs are also found such as Haptic interfaces [IS94; Ho+15; DPL07], teleoperation [KI93], locomotion interfaces [PG08; Oti+08], artistic painting,sport training [MKK97; MKK98], actuation of underwater vehicle-manipulator systems [EGGC15], aerostat positioning systems [LNC07], etc.

2.3 Control of CDPRs

Extensive research has been done on the control of parallel manipulators. While a number of these works can be used for CDPRs, care has to be taken to ensure positive cable tension at all times because of the unilateral cable tension constraint imposed due to its mechanical characteristics. Stabilization of the platform and moving the platform in the desired trajectory are the two main issues in the control of CDPRs. Several studies have been done to address these questions, some of which are explained in this section.

Although control laws have been developed specifically for CDPRs, these remain few. Most of the control strategies used for CDPRs are based on either nonlinear decoupling or feedforward control techniques. Nonlinear decoupling is used to produce a control input by linearizing the system using the dynamic model of the robot. It is one of the most commonly used control methods and is also well-known as feedback linearization or computed torque control. The implementation of this approach requires a thorough knowledge of the system and a good identification of the system parameters. Feedforward control consists of anticipating the future behavior of the system. This type of control requires prior knowledge of the system behavior and is combined with a feedback loop for improving the robustness of a system.

One of the earliest control schemes dedicated to CDPRs was proposed by Ming in [Min94b]. The proposed control law compares the measured cable length to the desired length generated by a trajectory generation algorithm. A nonlinear decoupling law based on the dynamic model of the CDPR was realized with a proportional controller on the error. Kawamura et al.[Kaw+97] used a Proportional-Derivative (PD) controller in the joint space to control the FALCON-7 CDPR to compensate for the weight of the platform known in advance.

A control scheme similar to the previous one is proposed in [AA02a; OA05] compensating for the dynamic effects. A Proportional-Integral-Derivative (PID) controller was developed in cascade to control the robot platform by Khosravi and Taghirad in their work [KT13]. This controller is composed of two loops, the first loop to control the position of the robot in joint space and the second loop to meet the voltage requirements to maintain the positive cable tension by comparing the output of the first loop with the current voltage in the cables. A control scheme with PD corrector was proposed in the joint space of the robot by Gholami et al. [GAT08] by using the torque calculated in the operating space to take into account the dynamics of the platform.

A control strategy of a fully-constrained CDPR is proposed in [AY17]. It consists of determining the motor torque allowing to minimize the errors between the measured cable tensions and the desired ones. The latter is defined by the outer-loop controller, which manifests in an adaptive robust feedback controller with bounded feed-forward compensation terms. Bounded positive cable tensions are generated by the outer-loop controller, utilizing the integral of the sign of the error (RISE) approach.

In [CLP18], the control of CDPR in the operational space is presented, where the CDPR model is derived using Lagrange equations of motion for constrained

systems while considering non-elastic but sagging cables through the Assumed Mode Method. A discrete-time control strategy is proposed in [Mer17] to estimate the positioning accuracy of the end-effector by taking into account the actuator model, the kinematics, and the static behavior of the CDPR, but dynamic effects are neglected.

Several papers have addressed the issue of control considering cable elasticity and its effect on the dynamic behavior of the platform. A wave-based control approach has been proposed for a large-scale CDPR combining a position control and active vibration damping approach simultaneously [KTH17]. A control strategy assuming flexibility in the longitudinal direction of the cable is proposed in [KT11; KT14; KT16]. The authors have used singular perturbation theory to prevent unwanted vibrations by adding an elongation compensation term to the control law. They have considered a rigid model for the cables in their study and have modeled the cable using linear axial springs with constant stiffness. Another study considering variable stiffness has been proposed in [KT15]. A robust adaptive controller to reduce vibrations due to the presence of uncertainties has been proposed in [BKT15]. The authors used exteroceptive measurements to measure the cable length and platform pose. However, the external-measurement-based control methods add complexity to the cable-driven manipulators and restrict the application conditions due to the need for additional devices [Cui+13].

Feedforward control has been implemented to improve the accuracy of the CDPR using a CDPR reference model without exteroceptive measurements [ZSC17]. Bruckmann et al. [Bru+13] presented a model-based control of a CDPR used in high rack storage. The authors integrated the elasticity of the cables in the reference signal to enhance the performance of the CDPR.

Adaptive control has been used by some researchers to control the platform as it is a very robust technique that does not require the linearization of the system or the prior knowledge of the range of system uncertainties. Babaghasabh et al. [BKT15] considered vibrations as uncertainties added to the position measurement. They have then used adaptive control to modify the behavior of the control law in response to the disturbances generated by vibrations. They developed another control in [BKT16] where in addition to the adaptive control, they added a term to control the longitudinal vibrations in the cable. The stability of this approach was demonstrated by using the theory of singular perturbation.

A frequency-dependent control technique known as input shaping has also been proposed for CDPRs. This method uses the convolution of the desired command signal with a sequence of impulses resulting in a new reference control signal for the

robot. The new reference signal helped in the cancellation of the oscillations. The effectiveness of this approach has already been demonstrated for serial as well as parallel robots [Par+06; Zha+16; Li+09; ÖKO16; RHK15; Yi+16] . This control strategy has also been implemented in some CDPRs. [Yoo+16] have used input-shaping for redundantly actuated CDPRs. [BFV16; Hwa+16a; LL16b; MV17] have used this method for the control of under-constrained CDPRs as the conventional control methods are limited for such CDPRs. It has been shown that the use of such filters results in a significant reduction of the platform oscillations. It has also been shown that an accurate calculation of the robot's natural frequency resulted in improved performance of the robot control.

Baklouti et al. [BCC19] used a feedforward control to control the vibrations of the platform due to the elasticity of the cables. They calculated the feedforward term using the inverse of the elasto-dynamic model of the CDPR, which takes into account the stiffness of the CDPR. They combined this feedforward term with a PID feedback controller to compensate for the oscillatory motions of the moving platform due to cable elongations. They also proposed another control method [Bak+19] using input-shaping filters into their previous model-based feedforward control to generate signals to make the CDPR self-cancel the residual vibrations.

Finally, other works have used less conventional control methods on CDPR. In Laroche et al., the author explores the use of the robust H_α control on a CDPR by taking into account the elongation of the cables, a dynamic model of the platform which takes into account friction as well as stresses on the tensions. In [Zi+08], a fuzzy logic Proportional-Integral corrector is used to compensate for wind disturbances on cables. Finally, an adaptive control minimizing errors due to uncertainties in the position of the actuators is developed in [Kin+07], but the dynamic parameters of the CDPR are not taken into account.

2.4 Control of under-constrained CDPRs

As the objective of this work is to control an underactuated CDPR, it is important to focus more on the works existing on such CDPRs. This section presents some of the important works done on the control of under-constrained CDPRs to understand the various approaches carried out in this area of research. Under-constrained CDPRs pose interesting challenges for its control design. For a generic underactuated and thus inherently under-constrained CDPR, as the number of cables (m) is less than the number of degrees of freedom of the platform (n), the platform has uncontrollable DoF resulting in the presence of internal dynamics.

These internal dynamics result in unwanted oscillations of the moving platform, limiting the controllable workspace of the moving platform [Hwa+16b]. The control laws designed must also ensure positive cable tensions at all times during the motion of the platform in the entire workspace. Trajectory planning for point-to-point motions is another major topic of research. The characteristics of under-constrained CDPRs lead to the impossibility of bringing the platform to rest once the transition from the starting point to the ending point is completed, and possibly to the generation of unbounded oscillatory motion of the moving platform. Because of the challenges arising from underactuation, most of the papers focus on a specific robot configuration.

One of the earliest controls for under-constrained CDPRs was proposed in [YYM02]. Their analysis was done on a mechanism having three wires, each connected to a manipulator having DoF less than three (using a pulley) as shown in fig.(2.13). The authors presented a control law based on the inverse dynamics

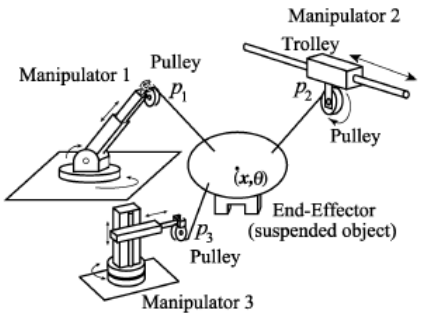

Figure 2.13: Under-constrained CDPR used for study by [YYM02]

calculation to resolve the problem of platform swing not only at the terminal points but also along the whole trajectory of the platform. The length of the cables was controlled by moving the joints of the manipulator according to the desired trajectory. They first designed a feedforward control law by calculating the desired joint angles for a target trajectory of the platform. Using a servo control, they made all the joint angles follow the desired joint angles calculated without swinging. However, the feedforward law was not found to be robust in the presence of external disturbances such as wind or when the joint angles changed quickly. To improve this behavior, they proposed a feedback control by using an internal model to generate the desired trajectory. The feedback control was based on a nonlinear dynamic compensation of the CDPR mechanism using inverse dynamics calculations. By simulations and experiments, they demonstrated that the MP of the CDPR was controllable along a trajectory with no swing. They also showed that the response of the mechanism was never affected by changing

the robot parameters as the inverse dynamics calculation completely compensated the non-linearity of the mechanism.

The authors proposed another control technique in [YYM04] for under-constrained CDPRs using a feedback control method based on exact linearization for a prototype similar to fig.(2.13). However, the major focus was on the formulation of inverse dynamics using which the trajectory of the cable length and trolley positions corresponding to the desired motion of the moving platform was calculated. These calculated values were used for the feedforward control law design to move the platform. To reduce the platform swing during motion, they proposed the design of a feedback controller based on exact linearization. Following this, they introduced a servo controller and a precompensator to achieve smooth motion of the suspended platform even in the presence of disturbances. The experimental and simulation results proved the effectiveness of the proposed control technique. The exact linearization method allowed the control system to be always stable without changing its pole assignment even during the changes in the wire length.

Flat systems

The work of [HW06] used the concept of flat systems to achieve trajectory tracking control of the moving platform. It is shown that when a CDPR is under-constrained but fully actuated, the system is flat. In a flat system, the problem of trajectory planning is completely algebraic. The system state variables (position and orientation) and the control inputs (cable lengths or tension) can be expressed algebraically in terms of the so-called flat output and a finite number of time derivatives of the flat output. The forces for the control are calculated

Figure 2.14: CABLEV prototype [HW06]

from the desired values of the trajectory points and their time derivatives up to the fourth-order. This leads to the design of a feedforward control strategy. A quasi-static state feedback approach is used to achieve exact linearization of the nonlinear dynamics leading to the asymptotic stable tracking behavior of the system variables. Since no extra dynamics is introduced in the control loop in

quasi-static feedback, it can be used in place of dynamic feedback extension in general.

The Winch-Bot

A winch-like robot called "Winch-Bot" was developed to transport a heavy end-effecter swiftly in a large workspace [CA09]. The structure of the robot was simple, compact, and the robot could be fixed to a ceiling or any rigid structure above the workspace. The end-effector of the robot was made to swing by parametric self-excitation, i.e., the end-effector of the robot suspended by a cable was oscillated by extending and reducing the cable length using the winch. The robot was able to generate both point-to-point motions with soft-landing capabilities and also continuous path motion for tracking a trajectory. The authors used dynamic

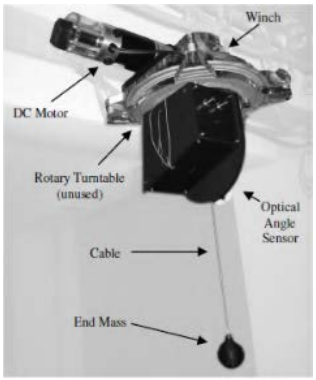

Figure 2.15: Winch-Bot prototype [CA09]

trajectories to increase the workspace of the robot. They succeeded in moving the end-effector from the starting point to the final point by using only a feed-forward control method. They also managed to perform real-time control of the trajectories by varying the driving self-excited oscillations to change the energy. This capability helped them compensate for the errors in the measurement, modeling, and implementation in real-time, thereby improving the controllability of the system. They also showed that continuous point control could be achieved for certain special classes of trajectories depending on the initial condition of the end-effector. However, a non-zero initial condition must be provided to move the end-effector outside a straight vertical line and achieve point-to-point motions.

A 3-DoF underactuated CDPR

The control of an underactuated three DoF CDPR was presented in [ZG12]. The robot consists of two cables to control the moving platform with the actuators placed on the fixed frame. The dynamics of the mechanism proposed were com-

plex because of the absence of pulleys on the end-effector. The authors proposed a

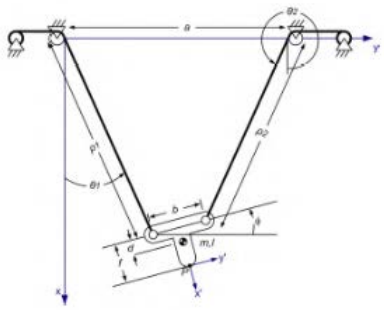

Figure 2.16: Prototype used for study by Zoso and Gosselin [ZG12]

trajectory planning approach based on the natural frequency of the pendulum-like free motion, which was the unconstrained DoF of the mechanism. The frequency and phase delay of sine-like excitation functions were determined using simulations and implemented on the prototype to perform point-to-point trajectories. One of the biggest advantages of their design was that the robot was easier to construct and did not require any hardware on the moving end-effector. On the other hand, the authors could not pre-compute the complete trajectory offline or impose constraints on the transition time. However, the results obtained by the authors confirmed the effectiveness of the planning approach for point-to-point trajectories.

The SpiderBot

The design and control of an innovative mobile under-constrained CDPR, SpiderBot with four cables was presented in [CSS14]. The novelty in the design was that the robot was able to change its grasping points, therefore making it mobile, whereas the traditional CDPRs mostly use stationary attachment points. The

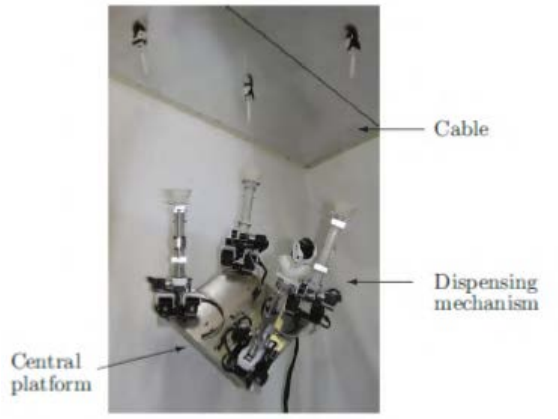

Figure 2.17: Prototype of SpiderBot [CSS14]

main purpose of the robot was to carry equipment and sensors over a disaster

area to help rescue forces. Other potential applications include workshops, warehouses, and floating vessels for transferring parts as a moving crane. The motion planning consisted of two phases. The stance-phase, defined as the period in which all cables remained in contact with the environment, and the stride phase, where the attachment or detachment of one of the grasping mechanisms occurs to move the platform. The position of the moving platform was controlled using three cables, while the fourth cable was used to search the next grasping point for performing the motion during the stride phase. The motion of the platform was based on adjusting the cable lengths and relocating its grasping points. The experimental results showed oscillations in the movement of the platform during the stride phase.

Incompletely Restrained Cable-Suspension Swing System (IRCSWs2) A novel design structure, also known as incompletely restrained cable-suspension swing system (IRCSWs2) for the simulation of actual swing motions, was proposed in [Wan+15] using two cables. The purpose of the work was to improve the reliability of the swing platforms used in construction shafts, marine ships, cars, etc. The authors used external force to maintain all the cables in tension and analyzed

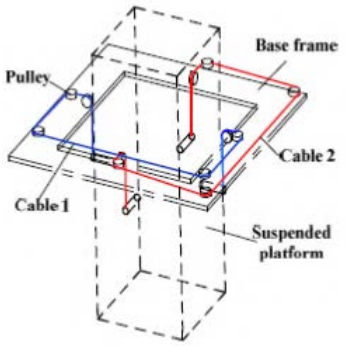

Figure 2.18: A simplified view of the IRCSWs2 prototype [Wan+15]

the performance of the platform during its trajectory and the possible payload that can be applied to it. They developed two models, the ADAMS simulation model, and the physical prototype experimental model to evaluate the analytic expressions formulated in the work. The cable model developed by them did not consider the time-varying inertial effects and instead focused on the kinematics of quasi-static trajectory behavior. They also analyzed the effects of various parameters on the displacement, angles, and cable tensions and observed that the translation of the suspended platform was trivial during its swing. They were able to achieve the easy realization of the swinging angle using a small driving force as the amplitude variation for each cable tension was relatively small.

Oscillation suppression control of four cable CDPR

The work of [LL16a] presented the design of an under-actuated CDPR with oscillation suppression control. The design was modular, easy to install, and reconfigurable. They presented a combined control module to serve as an associate

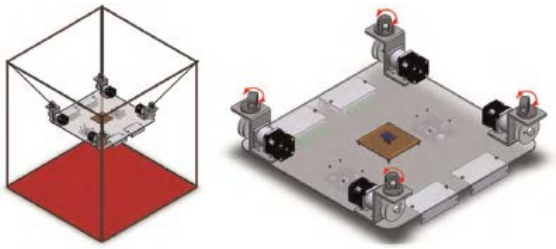

Figure 2.19: Underactuated CDPR prototype used by [LL16a]

controller to stabilize the system. The associate controller helped in the suppression of the oscillations using a feedback controller integrated with a shaping signal. It also helped in the positioning of the moving platform at the desired location with the help of a classical proportional-integral-derivative (PID) controller. The signal generated by the PID controller is modified by the input shaping module to produce a shaped signal to actuate the suspended platform. The shaped signal performs the dual role of driving the suspended platform and also suppressing the motion-induced oscillations. The final control module was derived by constructing a fuzzy controller based on the assistant controller performance-related knowledge. They demonstrated that the proposed control scheme effectively reduced the platform oscillations.

However, the trajectories proposed by the authors were generic. The oscillations of the platform were reduced but not eliminated. Another drawback of the technique was that the nominal path proposed initially undergoes modification by the input shaping filter, thus reducing the precision in the tracking of geometrical paths to be achieved.

Underactuated cable-driven micro-macro robot (u-CDMMR)

Optimal control of a planar under-actuated cable-driven micro-macro robot (u-CDMMR) was proposed in [Bar+17] for applications requiring point-to-point motions inside large workspaces in the presence of obstacles. The system consisted of a two-link passive serial manipulator attached to a CDPR. The specialty of the design was that the serial manipulator was controlled by the same cables driving the CDPR. This increased the reachable workspace of the robot without the addition of actuators on the moving platform and also reduced the risk of interference

with the obstacles. The authors have applied the differential flatness concept to

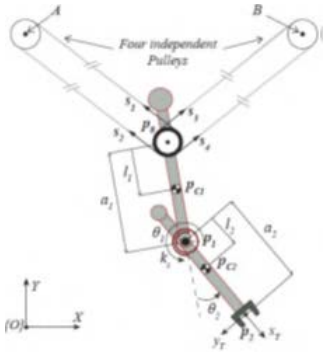

Figure 2.20: Prototype of the u-CDMMR [Bar+17]

control the system for point-to-point motion. Another novel contribution of the work was developing a multi-objective framework to choose the design parameters to minimize the movement time and the control effort needed for a given motion task. The work resulted in defining a set of optimal designs whose performance was compared with a traditional CDPR using optimal control.

Rest-to-rest motion of underactuated CDPR

Eda et al. presented the trajectory planning of underactuated CDPRs in the case of rest-to-rest motions [Idá+18; IBC19]. The geometry of the path and the time for the motion were prescribed in advance. They introduced a novel trajectory planning method based on the solution of a Boundary Value Problem (BVP) arising from the platform dynamics. The authors have also taken into account the effect of swivel pulleys in the prototype on the kinematics and the dynamic model of the platform. The proposed method avoided the geometric modification

Figure 2.21: CDPR prototype developed by Eda et al. [IBC19]

of the path to be tracked by the actuated coordinates and instead focused on a specific design of the motion law that described how these coordinates evolved along the path itself. They formulated the BVP to find a solution to the differential equation described by the dynamic model with constraints on the position and

velocity at start and end times. Following this, they considered the unactuated system states and defined a set of free parameters in the differential equation formulation. The values of these free parameters were calculated by heuristically formulating the problem as a combination of an initial value problem followed by the solution of a system of nonlinear equations. The approach suggested by the authors is suitable to be employed offline as the iterative and approximated nature of the algorithm prevented the prediction of the maximum computational time in advance. They demonstrated that it was possible to bring the platform to rest by accurate planning of the trajectory, taking into account the internal dynamics of the system. They were able to achieve satisfactory results even without a closed-loop control on the platform pose.

The regulation control of an underactuated planar CDPR with three DoF has been presented in [HDT+19]. The dynamic model formulated by the authors does not take into account the platform inertia and cable dynamics. They have analyzed the positions in which the platform of the robot can be maintained with constant inputs. To understand the dynamic behavior of the robot, the zero dynamics of the system were analyzed. They demonstrated that the zero dynamics of the system were stable but not asymptotically stable. To stabilize the internal dynamics behavior, they proposed a control law by combining the classical partial feedback linearization technique with a sliding mode controller and introduced a damping injection term similar to the one proposed in the Interconnection and Damping Assignment Passivity Based Control (IDA-PBC) proposed by Ortega [Ort+02]. They developed a Lyapunov-based controller to ensure the convergence of the system states to the desired values along with the asymptotic stability of the unactuated states. The simulation results were found to be satisfactory and chattering-free because of the damping injection term.

2.5 Research scope

From the elaborate literature review presented on the control of CDPRs with particular emphasis on under-constrained CDPRs, the following points are highlighted to be focused on in this particular thesis.

1) Several underactuated CDPRs have been designed by the researchers. However, a CDPR design with four cables and the motor actuation unit on the moving platform is still not implemented for industrial applications. In this work, a prototype with motors on the moving platform and simple anchor points to be fixed on the environment will be fabricated, and tests will be performed to analyze the

performance. The benefit from this concept is the ease of installing the robot by suitable selection of points in a workshop area. Due to this design, the moving platform cannot be considered as a point mass (as done by most of the works) as the inertia of the platform will play a significant role in the stability of the platform.

2) The problem of underactuation presents exciting control challenges which need to be tackled with efficient solutions to achieve the desired range of motion for the moving platform. The presence of internal dynamics due to the uncontrolled degrees of freedom can induce unwanted behavior in the moving platform. The control law should be able to maintain the stability of the platform by taking into account the internal dynamics. Feedback linearization is the most common control approach used for the control of under-constrained CDPRs. This work will implement this classical control law to study the behavior of the CDPR and attempt to design new control laws to improve the behavior of the CDPR.

2.6 Summary

This chapter highlighted the advantages and the possible areas of application for a CDPR. Particular focus has been given to present an elaborate review on the control of under-constrained CDPRs. It is seen that majority of the works implement feedback linearization and feedforward control techniques to achieve satisfactory point-to-point motion. Some researchers have done design modifications to suppress the oscillations of the platform arising due to the under-constrained nature, while some have combined traditional serial robots with cable robots to obtain the desired characteristics. Several opportunities exist in this field that still needs to be addressed. The effect of other existing nonlinear control techniques for underactuated mechanisms is a potential area of research. The dynamic movement of the attachment points to reconfigure the CDPR to achieve the desired motion and position presents exciting challenges to the researchers from a design and mathematical modeling perspective. These points will be taken into consideration in this work and will be presented in the next chapters.

Chapter 3

Statics, Dynamics and Workspace Analysis

Contents

This chapter presents the mathematical equations needed to calculate kinematics, dynamics, and the workspace of CDPRs. The basic representation of a CDPR structure is introduced in the first section. The kinematic equations are then presented. The equations for the static modeling of the CDPR are also shown in the next section. The standard dynamic model of the CDPR is introduced in the next section. Following this, the workspace analysis of the CDPR to be designed for this work is presented. The final section presents the influence of robot parameters (dimensions, working environment, payload) on the workspace of the robot to aid in the process of selecting the work environment.

3.1 CDPR model representation

A general cable-driven parallel robot with m-cables is shown in Fig. 3.1. As seen in Fig. 3.1, a frame, $\mathcal{F}_b$, with origin O_b, and axes x_b, y_b, z_b is attached to the base

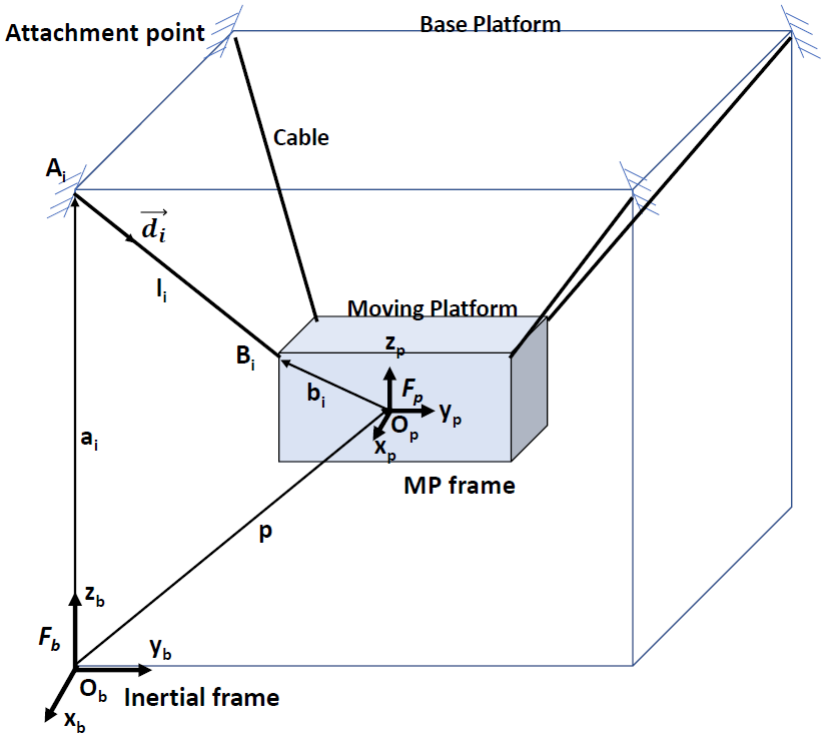

Figure 3.1: Schematic representation of a CDPR

structure of the CDPR and is referred to as the *base* frame or the *inertial* frame. A moving platform frame, $\mathcal{F}_p$, with origin O_p, and axes x_p, y_p, z_p is attached to the mobile platform where, O_p is the reference point of the platform to be positioned by the mechanism and usually coincides with the moving platform CoM.

Point A_i is the point of attachment of the i^{th} cable ($i = 1, 2, ..m$) with the base structure and is assumed to be fixed relative to the base. Similarly, point B_i is the cable attachment point on the mobile platform and is assumed to be fixed relative to the mobile platform. The points A_i and B_i are modeled generally as spherical joints. Vector a_i^b represents the position vector of point A_i expressed in the base frame $\mathcal{F}_b$. Vector b_i^p is the position vector of point B_i expressed in the moving platform frame $\mathcal{F}_p$. The position of the mobile platform is given by p which is the position vector of the origin O_p of moving platform frame $\mathcal{F}_p$.

For a n-DoF CDPR system, $q \in \mathbb{R}^n$ represents the generalized coordinates that describes the pose of the moving platform center of mass. The pose of MP is represented by $[pos^T, \theta^T]^T$ where, $pos^T = [p_x, p_y, p_z]^T$ and is given by the position vector p and θ^T is the orientation vector parameterized by Euler angles α, β, γ. For a CDPR system actuated by m-cables, $l = [l_1, l_2, ..., l_m]^T$ and $\tau = [\tau_1, \tau_2, ...\tau_m]^T$ denotes the vector of cable lengths and cable tensions respectively. Due to the unilateral tension constraint, the condition $\tau_i \geq 0, \quad \forall i$ must be satisfied at all

times.

3.1.1 Assumptions for mathematical modeling

In order to simplify the process of modeling, certain assumptions are made in this study.

- **Assumption 1**:
  The mass of the cables is negligible and the cables are non-elastic.
- **Assumption 2**:
  The i^{th} cable is assumed to be taut between the attachment points and is therefore considered a straight segment.
- **Assumption 3:**
  The MP is assumed to be a rigid body, defined by its mass and inertia matrix.

One of the reasons for these assumptions is due to the objectives formulated at the beginning of the work. The placement of the actuation unit (motors, controllers, winches) on the MP makes the platform heavy. Ottaviano and Castelli in their work have shown that the mass of the cables can be neglected if the ratio of the platform mass to the cable masses is large. Additionally, the choice of stainless steel cables also makes *assumption* 1 reasonable. This condition will be checked after the design of the platform to validate the assumptions. A heavy platform along with the suspended configuration of the CDPR helps in maintaining the cables taut. It also means that the platform will be designed such that its inertia will be significant in the dynamic behavior of the CDPR.

3.2 Kinematics

3.2.1 Inverse Pose Kinematics

The Inverse Pose Kinematics (IPK) problem refers to the determination of cable lengths (l), given the pose of the system, q. There exists a unique solution to the inverse kinematics for CDPRs.

From the description given in section 3.1, the length of the cable can be calculated by using the vector loop equation given by,

$$d_i{}^b = a_i{}^b - b_i{}^b - p \tag{3.1}$$

where, d_i is the vector along cable i pointing from B_i to A_i and $(i = 1, 2 \ldots m)$. Eq. 3.1 is then rewritten as,

$$d_i{}^b = a_i{}^b - Rb_i{}^p - p \tag{3.2}$$

R is the rotation matrix defining the MP orientation and is represented using 3-2-1 intrinsic Euler angle representation and is given by

$$R = \begin{bmatrix} c\beta c\gamma & s\alpha s\beta c\gamma - c\alpha s\gamma & c\alpha s\beta c\gamma + s\alpha s\gamma \\ c\beta s\gamma & c\alpha c\gamma + s\alpha s\beta s\gamma & s\alpha s\beta c\gamma - s\alpha c\gamma \\ -s\beta & s\alpha c\beta & c\alpha c\beta \end{bmatrix} \tag{3.3}$$

where c and s represent *cosine* and *sine* respectively.

The length of the cable is calculated using the 2-norm of the cable vector as

$$l_i = \|d_i\|_2 \tag{3.4}$$

The unit vector, $\hat{d}_i$ associated to l_i, $i = 1, 2..m$, with respect to $\mathcal{F}_b$ is given by

$$\hat{d}_i = d_i{}^b / l_i \tag{3.5}$$

3.2.2 Forward Pose Kinematics

Forward Pose Kinematics (FPK) is the dual of IPK. It refers to the problem of determining the platform pose, given the knowledge of current cable lengths. It is considered to be a more difficult problem where no perfect solving technique, which can be applied for all conditions, exists. In general, the forward kinematic problem produces a system of equations that can have no solution or up to infinitely many solutions, sometimes within distinct bounds, depending on geometry and cable length sets. The number of solutions is dependent on the ratio between the number of cables n and degrees-of-freedom m.

3.3 Static modeling

The analysis in 3.2.1 is purely geometric and does not take into account the ability of the mechanism to maintain positive cable tensions. To address this issue, the concept of wrench matrix is introduced where the statics of CDPR is considered.

When a tension is applied, a pure force $\tau_i \hat{d}_i{}^b$ is exerted on the MP by the i^{th} cable at point B_i where τ_i is the magnitude of the tension in the cable. This pure

force generates a moment $b_i^b \times \tau_i \hat{d}_i^{\,b}$ at the reference point O_p of the MP. The wrench (force-moment pair) applied by the i^{th} cable at O_p is given by $\tau_i w_i$ where the wrench w_i is defined as

$$w_i = \begin{bmatrix} \hat{d}_i^{\,b} \\ b_i^b \times \hat{d}_i^{\,b} \end{bmatrix} \tag{3.6}$$

If w_p denotes the total wrench applied at O_p by m cables of the CDPR, the relationship between τ_i in the cables and the wrench w_p can be written as

$$W\tau + w_p = 0 \tag{3.7}$$

where, $W = [w_1 \quad w_2 \quad ...w_m]$ is the $6 \times m$ pose dependent wrench matrix.

The term W also represents the transpose of the Jacobian matrix of a CDPR (J^T).

The total wrench w_p is a 6-dimensional vector expressed in frame $\mathcal{F}_b$ and is represented by

$$w_p = [f_p^T, m_p^T]^T = [f_x, f_y, f_z, m_x, m_y, m_z]^T \tag{3.8}$$

where, f_x, f_y, and f_z are the x, y, z components of the total force f_p and m_x, m_y and m_z are the x, y, z components of the moment vector m_p, respectively.

The definition of w_p depends on the various situations considered by the researcher. For instance, under static conditions, the platform wrench w_p represents the wrench induced by gravity and platform load on the platform, under dynamic conditions, the platform wrench represents the wrench induced by gravity plus the inertial effects associated with the platform motion.

3.4 Dynamic model

The standard dynamic equation of a CDPR is formulated using the Newton-Euler equations of motion.

$$\begin{bmatrix} m_{MP} I_{3\times3} & 0_{3\times3} \\ 0_{3\times3} & I_P \end{bmatrix} \begin{bmatrix} \ddot{p} \\ \dot{\omega} \end{bmatrix} + \begin{bmatrix} 0_{3\times1} \\ \omega \times I_P \omega \end{bmatrix} + \begin{bmatrix} -mg \\ 0_{3\times1} \end{bmatrix} = -J^T \tau \tag{3.9}$$

In Eq. 3.9, m_{MP} denotes the mass of the MP, I_P is a 3×3 matrix and denotes the inertia tensor of the MP about point O_p in the base frame, $\mathcal{F}_b$, and is calculated as $I_P = R I_{MP} R^T$, where I_{MP} is the inertia tensor of the MP relative to point P expressed in $\mathcal{F}_p$, $I_{3\times3}$ is a 3×3 identity matrix, g denotes the gravity acceleration vector, τ denotes the vector of cables forces, $\omega = [\omega_x, \omega_y, \omega_z]^T$ denotes the velocity

vector of the orientation, $p = [p_x, p_y, p_z]^T$ denotes the position vector.

Considering $X = [x, y, z, \alpha, \beta, \gamma]^T$ as generalized coordinates vector, in which $\theta = [\alpha, \beta, \gamma]^T$ denotes the vector of a set of Euler angles. The angular velocity of the MP can be written in the following form,

$$\omega = E\dot{\theta} \tag{3.10}$$

where,

$$E = \begin{bmatrix} cos(\beta)cos(\gamma) & -sin(\gamma) & 0 \\ cos(\beta)sin(\gamma) & cos(\gamma) & 0 \\ -sin(\beta) & 0 & 1 \end{bmatrix} \tag{3.11}$$

The equations of motion can be written in terms of X using the notations defined above. By substituting the term defined above, the dynamic model is rearranged as,

$$M(X)\ddot{X} + C(X, \dot{X})\dot{X} + G(X) = -J^T\tau \tag{3.12}$$

where,

$$M(X) = \begin{bmatrix} mI_{3\times3} & 0_{3\times3} \\ 0_{3\times3} & I_P E \end{bmatrix}$$

$$C(X, \dot{X})\dot{X} = \begin{bmatrix} 0_{3\times3} \\ I_P\dot{E}\dot{\theta} + (E\dot{\theta}) \times I_P(E\dot{\theta}) \end{bmatrix}$$

$$G(X) = \begin{bmatrix} -mg \\ 0_{3\times1} \end{bmatrix}$$

in which, the matrix $(E\dot{\theta})_\times$ is a skew-symmetric matrix defined by the components of the angular velocity vector.

Eq. 3.12 is finally represented as

$$M(X)\ddot{X} + N(X, \dot{X})\dot{X} = -J^T\tau \tag{3.13}$$

where, $\quad N(X, \dot{X})\dot{X} = C(X, \dot{X})\dot{X} + G(X)$

3.5 Workspace analysis

The workspace of the robot manipulator is defined as the set of points that can be reached by its end-effector [Cao+11]. The translational and rotational abilities of a manipulator are evaluated by analyzing its workspace. The workspace of the CDPR takes into account the change in cable length and the statics of the MP. The workspace of a CDPR is the set of position and orientation of the MP in which [TMC08]:

- The moving platform or the end-effector is controllable;
- Tensions in cables are positive;
- Force value lies between a minimum (greater than 0) because cables must be maintained in tension, and a maximum, in order to avoid the cables break;
- The end-effector is far from singularities;
- Cables wrapping is avoided.

Few of the commonly utilized workspaces for the analysis of CDPRs are introduced to get an overview of the CDPR performance [DD14].

One of the most fundamental workspace is the Static Equilibrium Workspace **SEW** (also known as statically reachable workspace). It is defined as the set of poses in which the manipulator can achieve static equilibrium to sustain its own weight under gravity force and no external wrenches. Since all the postures of the CDPR are not statically attainable, it is a subset of workspace for cable robots.

The **Wrench Closure Workspace (WCW)** (also called the controllable workspace, or force closure workspace) is defined as the set of all poses where the MP of the CDPR can be located and regardless of the exerted wrench, all cables are in tension. This workspace depends only on the geometric parameters of the system (the locations of cable attachment points on the base and MP). It also corresponds to the set of poses for which the MP of the CDPR is fully-constrained or over-constrained by the cables. Hence a WCW only exists for a CDPR, when the number of cables is more than the number of dofs of the platform.

The **Wrench Feasible Workspace (WFW)** is the set of all poses for which the desired wrench set can be produced considering the upper and lower bounds on the cable forces. This workspace takes into account not only the geometric parameters but also the allowable tension ranges, gravitational effects, and the required wrench set.

From the definition of WCW and WFW two important observations can be made:

- WFW is a subset of WCW
- For any bounded set of wrenches and any pose belonging to WCW, there exists a finite set of allowed cable tensions such that it belongs to the WFW.

Dynamic Feasible Workspace (DFW) is the set of all poses for which a desired set of accelerations and velocities can be produced considering the given upper and lower bounds on the cable forces.

Collision Free Workspace (CFW) is the set of poses that can be reached without collision among the end effector to cables, cable to cable, and cable to workpiece. CFW is a subset of dynamic workspace or WCW.

Stiffness Feasible Workspace (SFW) is a set of MP poses belonging to WCW of the robot in which for any value of the internal forces in the range of (0, max) total stiffness matrix of the robot is positive definite [BKA19]. (Minimum eigenvalue of the total stiffness matrix of the mechanism is positive.)

The availability of different types of workspaces for a CDPR gives the user the freedom to design a CDPR choosing one or some of the workspaces and optimize the CDPR performance.

3.5.1 SEW Calculation and Case studies

This work will be focusing on the SEW of an underactuated and thus an inherently under-constrained CDPR. It is not possible to calculate the WCW and WFW for the robot considered as they require the robot to be fully constrained or over-constrained. Hence it is important to understand SEW as it will help in the appropriate determination of the design parameters and present the possible regions of operation for a given working environment.

In order to calculate the workspace, the following parameters need to be defined: a) Dimension of the base platform - $L(m) \times B(m) \times H(m)$ b) Dimension of the moving platform - $l(m) \times b(m) \times h(m)$ c) Total Payload (Weight of the platform + Weight of the object to be lifted) d) Limits on cable tension e) Limits on platform orientation.

The initial dimensions of the room and the platform are given in table 3.1. The cable attachment points are located as shown in table 3.2. The schematic of the MP location, the cable attachment, and the dimensions for the study are shown in Fig. 3.2.

In order to calculate the workspace, the static equilibrium conditions described in Eq. 3.7 are used. As mentioned earlier, SEW is the set of moving platform poses where the CDPR can balance the weight of the possibly loaded moving platform

Table 3.1: Simulation parameters

Room dimension (m)	5∗5∗3
Platform dimension (m)	0.5∗0.5∗0.2

Table 3.2: Cable attachment points @ z=1.5 m

Cable no.	MP	Base
Cable 1	[2.25,2.25,1.7]	[0,0,3]
Cable 2	[2.25,2.75,1.7]	[0,5,3]
Cable 3	[2.75,2.75,1.7]	[5,5,3]
Cable 4	[2.75,2.25,1.7]	[5,0,3]

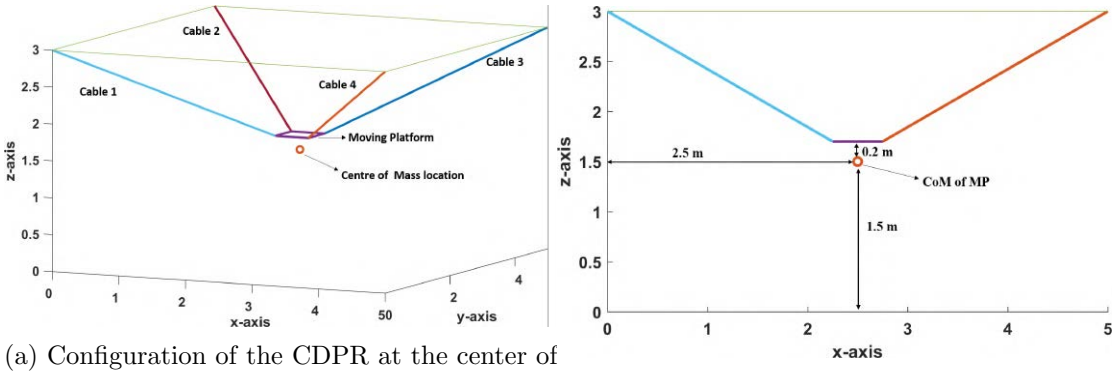

(a) Configuration of the CDPR at the center of the room

(b) View of the CDPR in $x-z$ plane

Figure 3.2: CDPR at the center of the room

according to the cable tension limits, i.e.

$$\begin{aligned} \sum F_x = 0, \sum F_y = 0, \sum F_z = mg \\ \sum M_x = 0, \sum M_y = 0, \sum M_z = 0, \end{aligned} \tag{3.14}$$

where, m is the total payload on the platform, and g is the acceleration due to gravity ($9.81 m/s^2$).

Since the CDPR is underactuated, SEW calculation is formulated as a non-linear optimization problem and is solved using $fsolve$ in Matlab. The solver has been set to use the $Levernberg - Marquardt$ algorithm to solve for the static equilibrium conditions (Eq. 3.14). The limits used for a point to be considered in the SEW are set as shown in Eq. 3.15.

$$\begin{aligned} \underline{\tau} \leq \tau_i \leq \overline{\tau} \\ \underline{\tau} = 10N, \quad \overline{\tau} = 500N \\ \underline{\alpha} = -30°, \quad \overline{\alpha} = 30° \\ \underline{\beta} = -30°, \quad \overline{\beta} = 30° \end{aligned} \tag{3.15}$$

where, $i = 1..4$ (cable number), $\underline{\tau}$, $\underline{\alpha}$, and, $\underline{\beta}$ denotes the lower-limit on cable tensions, orientation about x-axis and orientation about y-axis respectively, and $\overline{\tau}$, $\overline{\alpha}$, and, $\overline{\beta}$ denotes the upper-limit on cable tensions, orientation about x-axis

and orientation about y-axis respectively.

The simulation was done for values of x and y from 0 to 5 m with an increment of 0.1 m. The maximum height (z) of the CoM considered for the simulation was 2.3 m. The number of points tested for the SEW conditions was 71409. The heights at which the SEW conditions were checked are chosen according to the possible heights (in a real work environment) at which the platform could be used for tasks.

The SEW for the conditions in Eq. 3.15 is shown in Fig. 3.3. The 2D image of the SEW (Fig. 3.4) indicates that as the platform is made to go higher, the number of points inside the SEW reduces. This is because of the maximum tension limit set for the simulation. On the other hand, at lower heights, the cable tension values are well below the maximum limit; however, the platform orientation becomes more than the limit set during the simulation.

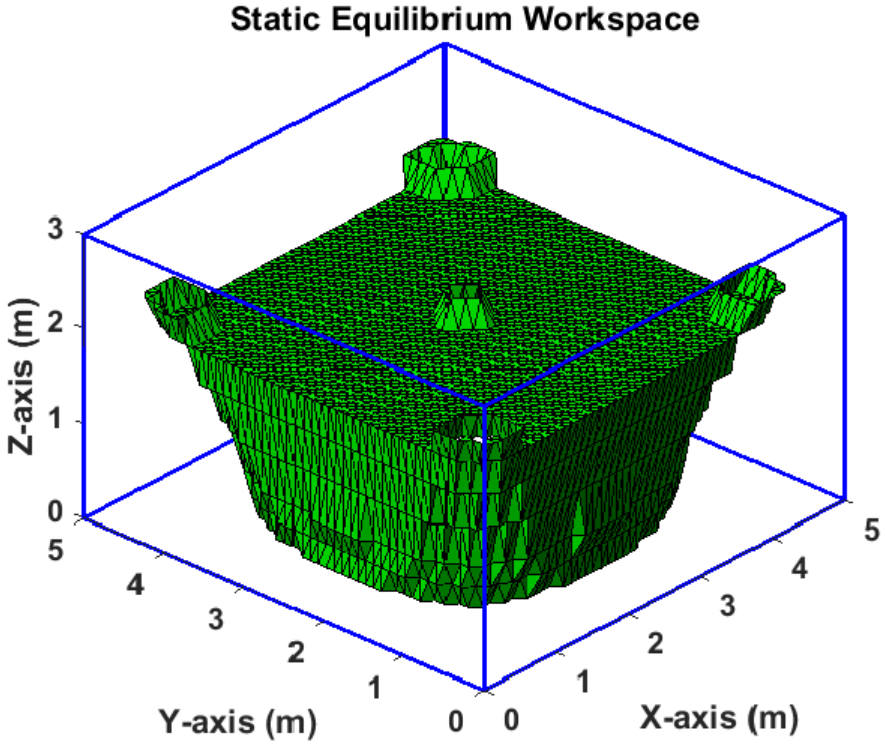

Figure 3.3: SEW of the cable driven robot

The variation of cable forces for the SEW conditions is shown in Fig. 3.5. The maximum value of the cable forces is within the maximum limit.

The variation in the values of α, β, and γ is shown in Fig. 3.6, 3.7, and 3.8. The points inside the red lines in Fig. 3.6 and 3.7 satisfy the limits set for SEW equilibrium conditions (Eq. 3.15).

The results obtained from the initial simulation indicate that the CDPR can

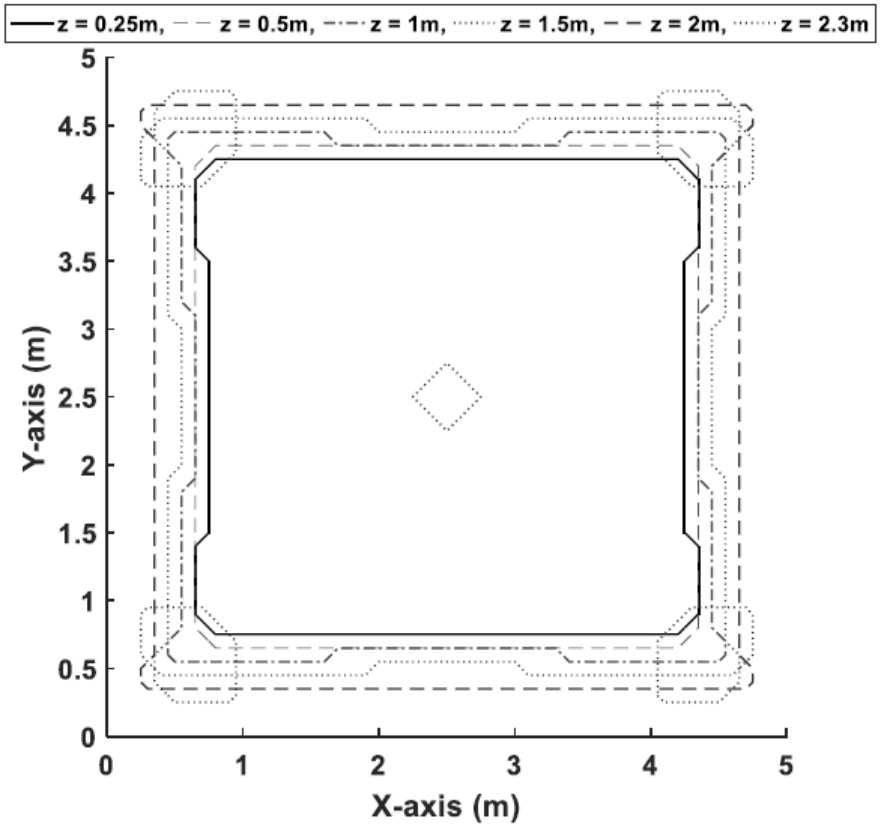

Figure 3.4: SEW of the cable driven robot 2-D view

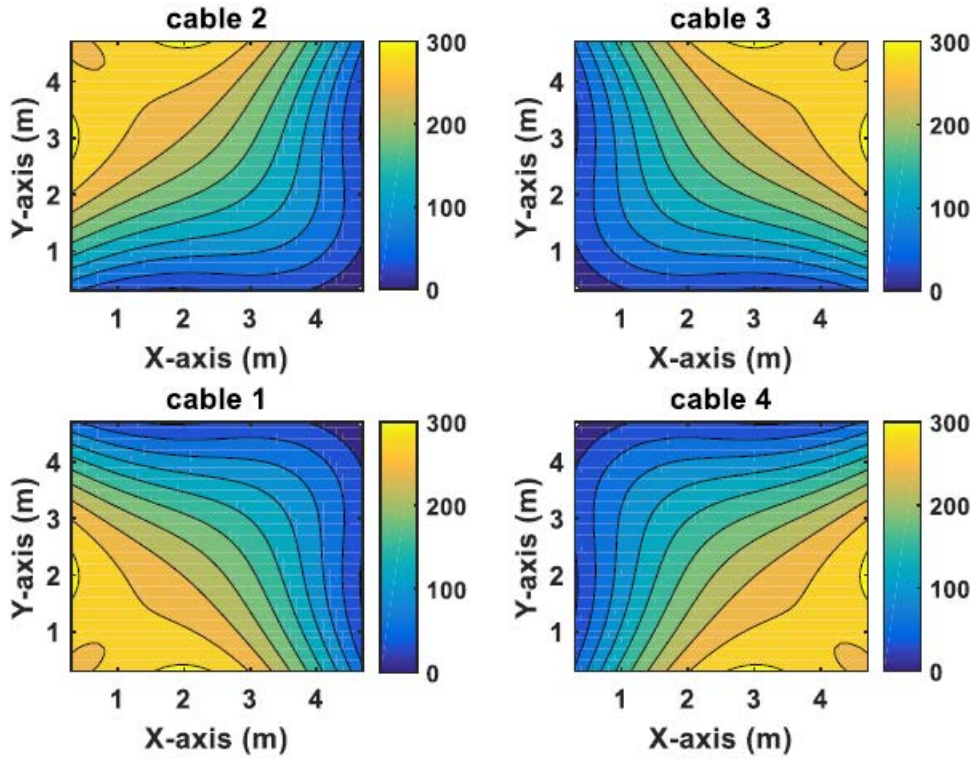

Figure 3.5: Cable tensions at $z = 1.5$ m

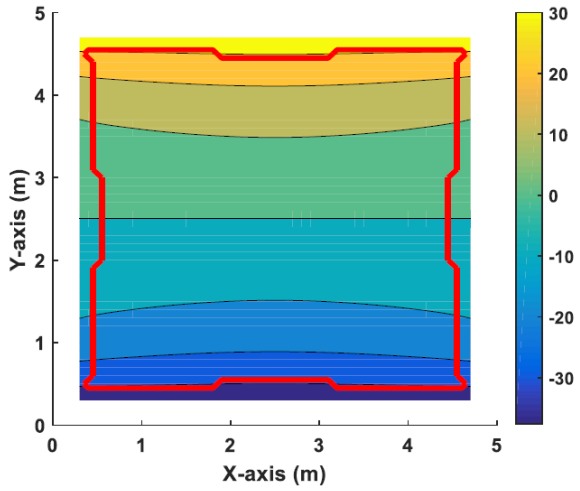

Figure 3.6: Orientation angle (α) at $z = 1.5$ m

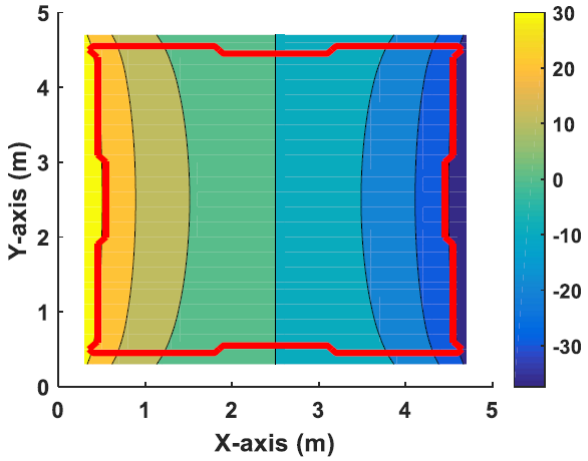

Figure 3.7: Orientation angle (β) at $z = 1.5$ m

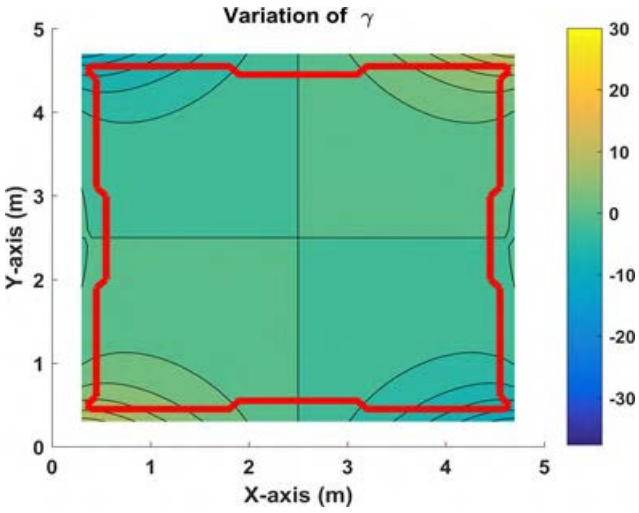

Figure 3.8: Orientation angle (γ) at $z = 1.5$ m

maintain its equilibrium for the defined static conditions at a significant number of points. To further analyze the performance of the CDPR, additional case studies

have been performed. The case studies and their conditions will be presented in the following subsection.

3.5.2 Case studies

The workspace of the CDPR depends on several physical parameters such as the base structure, the moving platform, the mass of payload acting on the platform, and so on. In order to understand their role, some case studies have been presented by changing these parameters.

Case study I: Changing CoM

The first study presents the impact of changing the CoM of the MP. Three different CoMs have been used to calculate the SEW. The simulation is done at the height of 1.5 m for a platform mass of 30 kg. It can be seen from Fig. 3.9 that

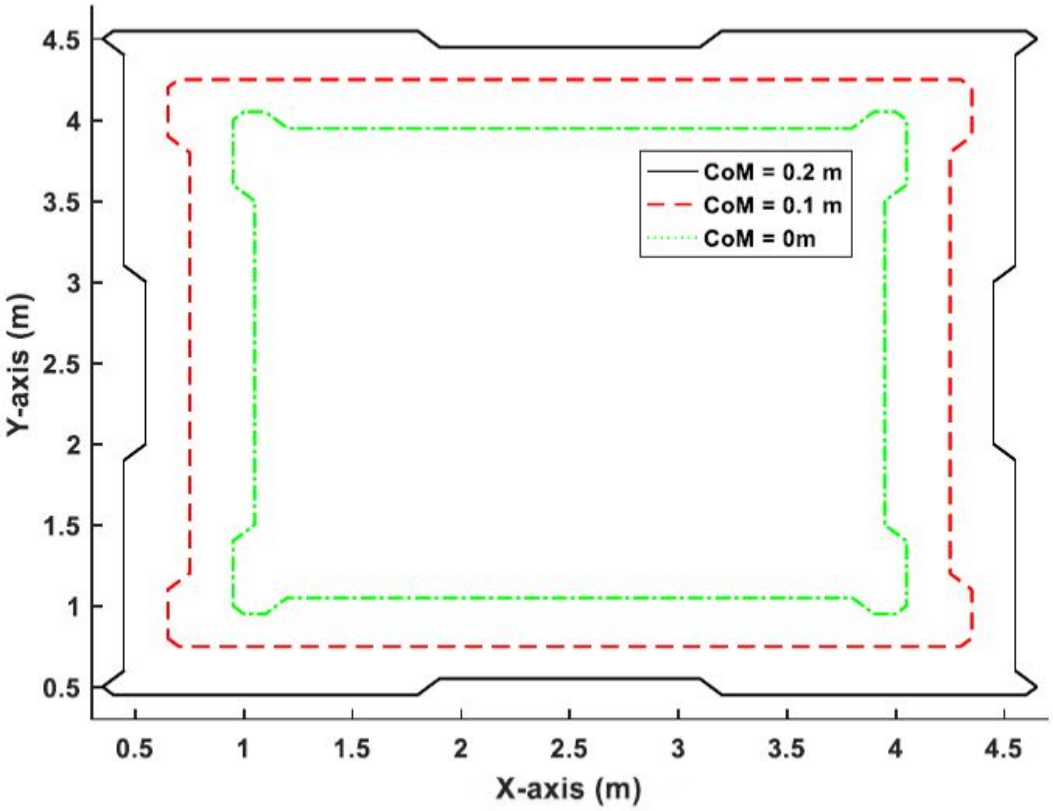

Figure 3.9: Comparison of SEW for different CoM of MP at $z = 1.5$ m

choosing a suitable CoM will help in increasing the workspace of the robot. Points beyond 0.2 m are not checked to limit the height of the MP for the actual prototype. The percentage of points inside the SEW of the CDPR for the different conditions is shown in table 3.3. As the CoM is moved further away from the top

Table 3.3: Percentage of points inside the SEW for different CoM

Condition	SEW %
CoM = 0 m	27%
CoM = 0.1 m	35%
CoM = 0.2 m	46%

surface of the MP, the workspace of the CDPR increases.

Case study II: Changing total payload

The second study presents the impact of changing the total load acting on the MP. Three different loads (25 kg, 35 kg, 40 kg) are tested in addition to the one simulated in section 3.5.1. The dimensions of the platform and the base structure have been kept as shown in table 3.1. The simulation results obtained shows that

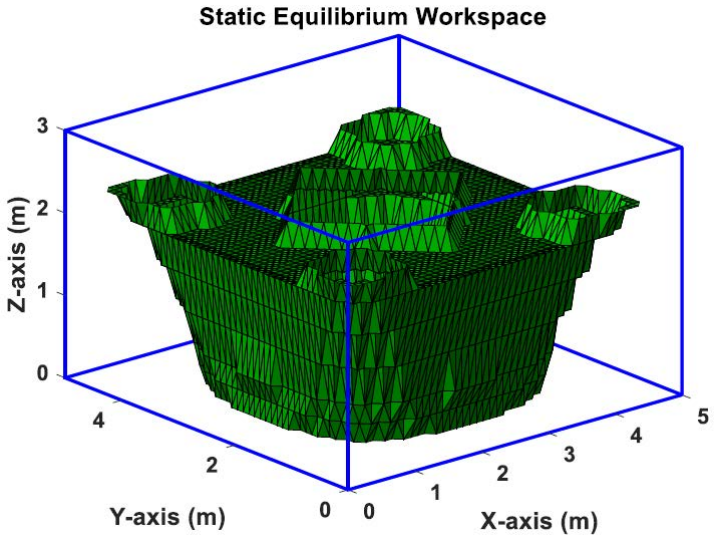

Figure 3.10: SEW for a payload of 25 kg on the MP

as the mass on the MP is increased, the workspace decreases since the tension in the cable exceeds the limits set (500 N).

III: Change in platform shape

The next study presents the impact of platform dimensions on the workspace. Considering the real dimensions of the available space, different combinations were formulated, and the test results are presented in table 3.4. The height of the room is fixed at 3 m for all configurations. The selection of a suitable shape for the platform and the base structure plays a significant role in obtaining a bigger workspace. From the results obtained in table 3.4, it can obtain a satisfactory

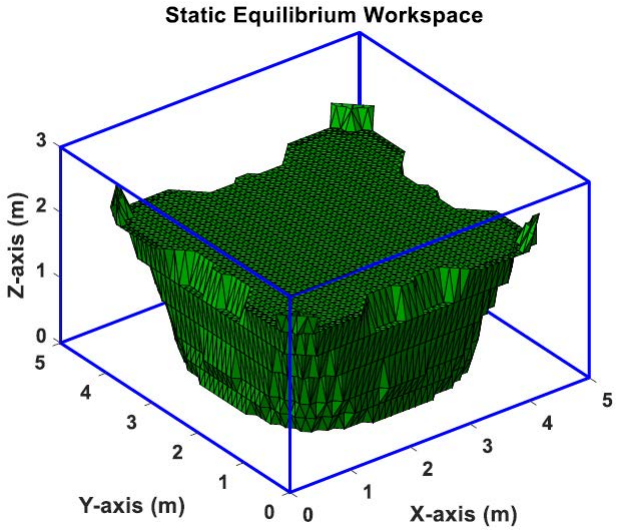

Figure 3.11: SEW for a payload of 35 kg on the MP

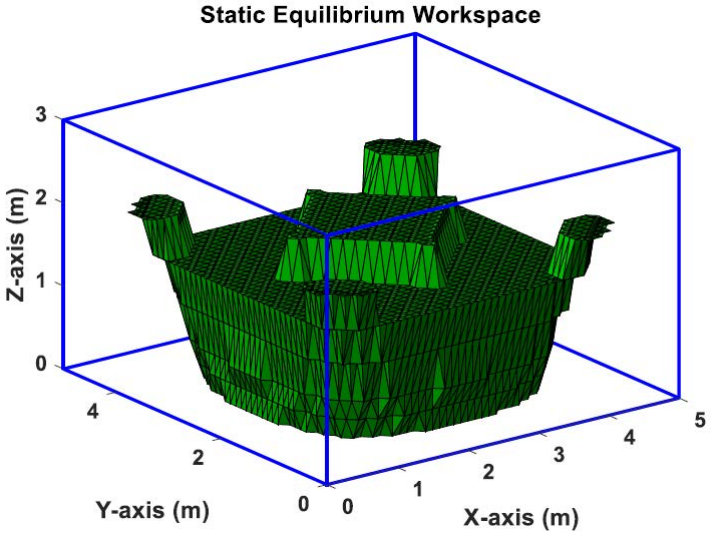

Figure 3.12: SEW for a payload of 40 kg on the MP

workspace for more than one configuration. These insights will be used in the next chapter to verify if these configurations can lead to better control.

3.6 Inferences and Discussion

Based on the workspace calculation and the subsequent case studies performed, certain inferences are presented hereby.

1) The SEW of the CDPR indicates the possible workspace points where the CDPR can maintain its static equilibrium. However, the limits for these points are not fixed and depend on the application of the CDPR. The underactuated

Table 3.4: Different configurations for SEW calculation

Shape of Base Frame	Shape of MP	SEW%
Rectangle (6×4)	Square (0.5×0.5), CoM = 0.2 m	45%
Rectangle (6×4)	Square (0.5×0.5), CoM = 0.1 m	35%
Rectangle (6×4)	Rectangle (0.6×0.4), CoM = 0.2 m	45%
Rectangle (6×4)	Rectangle (0.6×0.4), CoM = 0.1 m	35%
Square (5×5)	Rectangle (0.6×0.4), CoM = 0.2 m	46%
Square (5×5)	Rectangle (0.6×0.4), CoM = 0.1 m	35%

CDPR design for the thesis and the possible application of the CDPR in handling operations resulted in the limits set for the platform orientation angles ($-30°$ to $+30°$ for α, β, and γ) to calculate the SEW calculation in this chapter. The cable forces and cable orientation angles show that the platform can maintain the static equilibrium at a considerable number of points for the considered payload on the MP (30 kg).

2) The shape and size of the SEW are dependent on the limits set on the cable forces, the orientation angles, and the mass on the MP. To analyze the performance of the CDPR, several case studies have been presented in section 3.5.2. It is shown that there are several possible configurations that the user can define to obtain a bigger workspace. The quantification of the relationship between platform, fixed structure, and the SEW could be done to obtain a better performance analysis for the CDPR.

3.7 Summary

This chapter presented the mathematical equations used for the modeling of CDPRs. The equations must take into account the kinematics and the statics of the CDPR due to the unilateral constraint imposed due to the cable characteristics. The dynamic model using the Newton-Euler equations of motions is also presented to design the control laws. The final section of the chapter presented the different workspace studied for a CDPR. A detailed analysis of the static equilibrium workspace for the CDPR (to be designed) with customized static equilibrium conditions was also presented. This will explain the possible orientation of the moving platform and the corresponding cable tension values that the prototype will generate. This will also provide an insight into the possible areas of operation where the operator can work with better performance.

Chapter 4

Non-Linear Control Laws

Contents

This chapter presents the nonlinear control laws implemented for the control of the underactuated CDPR. The first section introduces the concept of classical Input-Output Feedback Linearization (IOFL). The next section presents the implementation of IOFL on the CDPR system. The simulation results are analyzed in the next section to obtain insights into the behavior of the robot for various conditions. A modified control law is then proposed as an ad-hoc solution for improving the control of the robot. The performance of the controller and the stability of the system are shown through simulations.

4.1 Input-Output Feedback Linearization

Input-Output Feedback Linearization is one of the most important nonlinear control design strategies developed during the last few decades [Isi13a]. The main objective of the approach is to algebraically transform a nonlinear dynamic system into a linear dynamic system by using static state feedback and a nonlinear coordinate transformation based on a differential geometric analysis of the system. By eliminating nonlinearities in the closed-loop system, conventional linear control techniques can be applied.

4.1.1 Mathematical Preliminaries

The mathematical approach of IOFL for a nonlinear Multi-Input Multi-Output (MIMO) dynamic system is recalled in this section.

Nonlinear affine-in-input systems

A nonlinear, affine-in-input MIMO of order n with m number of inputs and outputs is represented as follows:

$$\begin{aligned} \dot{x}(t) &= f(x,t) + g_1(x,t)u_1(t) + ... + g_m(x,t)u_m(t) \\ y_1(t) &= h_1(x,t) \\ &... \\ y_m(t) &= h_m(x,t) \end{aligned} \tag{4.1}$$

where, $i = 1, .., m - i^{th}$ inputs, $x(t) \in \mathbb{R}^n$ is the system state vector, $u_i(t)$ is the control input, $y_j(t)$ is the system output ($j = 1, ..., m - j^{th}$ outputs), $f(x,t)$, $g_i(x,t)$, and $h_j(x,t)$ are smooth nonlinear functions.

Lie Derivatives

Consider a Single-Input Single-Output (SISO) nonlinear system (Eq. 4.2).

$$\begin{aligned} \dot{x} &= f(x) + g(x)u \\ y &= h(x) \end{aligned} \tag{4.2}$$

Differentiating the output y with respect to time yields:

$$\begin{aligned} \dot{y} &= \frac{\partial h}{\partial x}\dot{x} \\ &= \frac{\partial h}{\partial x}[f(x) + g(x)u] \\ &= L_f h(x) + L_g h(x)u \end{aligned} \tag{4.3}$$

where, $L_f h(x) = \dfrac{\partial h}{\partial x} f(x)$, and, $L_g h(x) = \dfrac{\partial h}{\partial x} g(x)$.

The function $L_f h(x)$ is called the *Lie Derivative* of $h(x)$ with respect to $f(x)$ or along $f(x)$, and corresponds to the derivative of h along the trajectories of the system $\dot{x} = f(x)$. Similarly, $L_g h(x)$ is called the *Lie Derivative* of h with respect to g or along g, and corresponds to the derivative of function $h(x)$ along the trajectories of the system $\dot{x} = g(x)$.

In case of a MIMO system, the first derivative has the form

$$\dot{y_j} = L_f h_j(x) + \sum_{i=1}^{m} L_{g_i} h_j(x) u_i \tag{4.4}$$

Relative Degree:
A SISO is said to have relative degree r at a point x^0 if
1. $L_g L_f^k h(x) = 0$ for all x in a neighborhood of x^0 and all $k < r - 1$.
2. $L_g L_f^{r-1} h(x^0) \neq 0$.

The relative degree (r) is exactly equal to the number of times one has to differentiate the output $y(t)$ at time $t = t^0$ in order to have the value $u(t^0)$ explicitly appearing. For MIMO systems, the relative degree can be defined pairwise for all of the possible input-output pairs. The resulting derivation takes the form

$$y_j^{r_j} = L_f^{r_j} h_j(x) + \sum_{i=1}^{m} L_{g_i} L_f^{r_j - 1} h_j(x) u_i \tag{4.5}$$

where, r_j represents the number of derivatives needed for at least one of the inputs to appear during the differentiation of the j^{th} output.

Vector relative degree:
The vector relative degree is the sum of the relative degree of each output. For a MIMO system with m outputs, it can be calculated by

$$r = \sum_{i=1}^{m} r_i \tag{4.6}$$

4.1.2 Steps for IOFL

This section presents the steps for implementing the IOFL for a MIMO non-linear system. The basic principle of IOFL method is in finding an input transformation in the shape

$$u_i = \alpha_i(x) + \beta_i(x) v_i \tag{4.7}$$

where, v_i is the new input, $\alpha_i(x)$, and $\beta_i(x)$ are nonlinear functions. Eq.4.7 creates a linear relationship among the outputs y_i and the new inputs v_i decoupling the interaction between the original inputs and outputs. Following this decoupling, control algorithms for subsystem with input and output independent of each other can be synthesized using the conventional linear control laws.

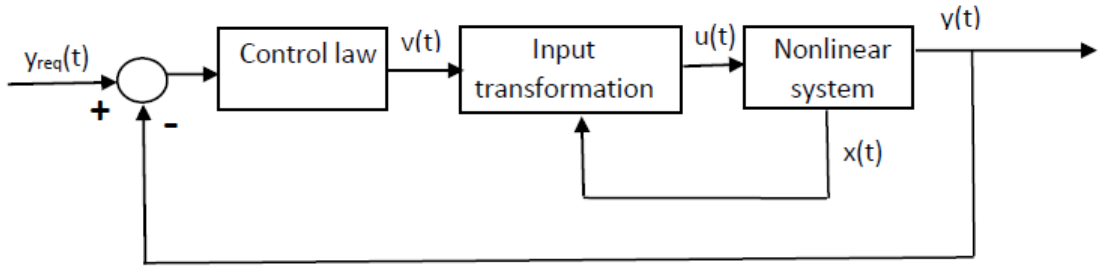

Figure 4.1: Block diagram for IOFL

Step 1: Calculating the Lie derivative for each output (using Eq. 4.3).
Step 2: Calculating the relative degree for each output(using Eq. 4.5).
Step 3: Calculating the vector relative degree for the system (using Eq. 4.6). Following this, for a system with N states
a) if $r = N$, the system can be feedback linearized with simple transformation.
b) if $r < N$, the behavior of internal dynamics needs to be checked for stability.
Step 4: Formulation of the input transformation as shown in Eq. 4.7. For a MIMO system, the approach shown in Eq. 4.5 is followed for each output (y_j). The resulting m equations is written as

$$\begin{bmatrix} y_1^{r_1} \\ ... \\ y_m^{r_m} \end{bmatrix} = \begin{bmatrix} L_f^{r_1} h_1(x) \\ ... \\ L_f^{r_m} h_m(x) \end{bmatrix} + E(x) \begin{bmatrix} u_1 \\ ... \\ u_m \end{bmatrix} \tag{4.8}$$

where,

$$E(x) = \begin{bmatrix} L_{g_1} L_f^{r_1-1} h_1 & ... & L_{g_m} L_f^{r_1-1} h_1 \\ . & ... & . \\ . & ... & . \\ L_{g_1} L_f^{r_m-1} h_m & ... & L_{g_m} L_f^{r_m-1} h_m \end{bmatrix} \tag{4.9}$$

If the matrix $E(x)$ is regular, then it is possible to define the input transformation in the shape

$$\begin{bmatrix} u_1 \\ ... \\ u_m \end{bmatrix} = -E^{-1}(x) \begin{bmatrix} L_f^{r_1} h_1(x) \\ ... \\ L_f^{r_m} h_m(x) \end{bmatrix} + E^{-1}(x) \begin{bmatrix} v_1 \\ ... \\ v_m \end{bmatrix} \tag{4.10}$$

Once the input transformation is completed as shown in Eq. 4.10, the linear control law is used to propose a feedback control for the linear system to ensure the desired behavior of the nonlinear system using the conventional techniques.

4.2 Implementation of IOFL on the CDPR system

The equation for the dynamic model of the CDPR is repeated here in Eq. 4.11.

$$M(X)\ddot{X} + C(X,\dot{X})\dot{X} + G(X) = -J^T\tau \tag{4.11}$$

Eq. 4.11 is then represented as

$$M(X)\ddot{X} + N(X,\dot{X})\dot{X} = -J^T\tau \tag{4.12}$$

where, $N(X,\dot{X})\dot{X} = C(X,\dot{X})\dot{X} + G(X)$.
The terms $M(X)$ and $(N(X,\dot{X})\dot{X})$ are written as M and $\underline{N}$ for ease of representation in further equations. τ represents the four cable forces (in our case the system inputs). The Eq. 4.12 is then simplified as

$$\ddot{X} = -M^{-1}\underline{N} - M^{-1}J^T\tau \tag{4.13}$$

This equation is rewritten as shown in Eq. 4.14.

$$\begin{aligned} \underline{\dot{X}} &= F + \underline{G}u \\ \underline{y} &= h(\underline{X}) \end{aligned} \tag{4.14}$$

where,

$$\underline{\dot{X}} = \begin{Bmatrix} X_{6\times1} \\ \dot{X}_{6\times1} \end{Bmatrix}, F = \begin{Bmatrix} \dot{X}_{6\times1} \\ (-M^{-1}\underline{N})_{6\times1} \end{Bmatrix}, \underline{G} = \begin{Bmatrix} 0_{6\times1} \\ (-M^{-1}J^T)_{6\times4} \end{Bmatrix} \tag{4.15}$$

The terms F and $\underline{G}$ are written as shown:

$$F = [F_1, F_2, F_i....F_N], \quad where \quad N = 12 \tag{4.16}$$

$$\underline{G} = \begin{bmatrix} \underline{G}(1,1) & \underline{G}(1,2) & \underline{G}(1,3) & \underline{G}(1,4) \\ \underline{G}(2,1) & \underline{G}(2,2) & \underline{G}(2,3) & \underline{G}(2,4) \\ \underline{G}(3,1) & \underline{G}(3,2) & \underline{G}(3,3) & \underline{G}(3,4) \\ \underline{G}(4,1) & \underline{G}(4,2) & \underline{G}(4,3) & \underline{G}(4,4) \\ \underline{G}(5,1) & \underline{G}(5,2) & \underline{G}(5,3) & \underline{G}(5,4) \\ \underline{G}(6,1) & \underline{G}(6,2) & \underline{G}(6,3) & \underline{G}(6,4) \end{bmatrix} \tag{4.17}$$

The input vector u represents the cable forces (u_1, u_2, u_3, u_4). The outputs selected for the study are the position x, y, z and the Euler angle about $z-axis$ namely, γ. This is represented as

$$\underline{y_1} = x, \quad \underline{y_2} = y, \quad \underline{y_3} = z \quad \underline{y_4} = \gamma \tag{4.18}$$

The implementation of the IOFL is shown here for one output ($y_1 = x$).

Step 1: The first step is to calculate the Lie derivative as explained in section 4.1.1 for the selected output

$$\underline{y_1} = x \tag{4.19}$$

Differentiating the output $\underline{y_1}$ with respect to time yields:

$$\begin{aligned} \underline{\dot{y_1}} &= L_f h_1(X) \\ &= \frac{\partial h_1}{\partial X} F1(X) \\ &= \dot{x} \end{aligned} \tag{4.20}$$

The output is differentiated till the input (u) appears in the term.

$$\underline{\ddot{y_1}} = \ddot{x} \tag{4.21}$$

Eq. 4.21 can be rewritten as

$$\begin{aligned} \underline{\ddot{y_1}} &= L_f^2 h_1(\underline{X}) + (L_{g_1} L_f^1 h_1) * u_1 + (L_{g_2} L_f^1 h_1) * u_2 + (L_{g_3} L_f^1 h_1) * u_3 + (L_{g_4} L_f^1 h_1) * u_4 \\ &= F7 + \underline{G}(1,1) * u_1 + \underline{G}(1,2) * u_2 + \underline{G}(1,3) * u_3 + \underline{G}(1,4) * u_4 \end{aligned} \tag{4.22}$$

The term F_7 represents the first value of the column vector obtained by the multiplication of the term, $(-M^{-1}\underline{N})_{6\times 1}$.

Step 2: The second step is to calculate the relative degree for the selected output. From the equations 4.14, 4.20 and 4.21, we see that the input appears after differentiating the output twice, i.e.,

$$r_1 = 2 \tag{4.23}$$

Step 3: Calculating the vector relative degree. The vector relative degree is the sum of the relative degree of each output. Following steps 1 and 2 for the other

outputs the relative degree is found to be $r_2 = 2$, $r_3 = 2$, $r_4 = 2$ where, r_i, $(i = 1, 2..4)$ represents the relative degree of the respective output. The vector relative degree is then calculated as

$$\begin{aligned} r &= r_1 + r_2 + r_3 + r_4 \\ &= 8 \end{aligned} \tag{4.24}$$

The number of states of the system (N) is 12 whereas the vector relative degree is 8. This will result in internal dynamics in the system. The stability of the internal dynamics has to be verified for implementing the IOFL.

Step 4: The next step is to formulate the input transformation. The approach given in Eq. 4.21 and 4.22 is followed for the other outputs to be controlled. For a MIMO system, the input transformation is formulated as shown in Eq. 4.25.

$$\begin{bmatrix} u_1 \\ u_2 \\ u_3 \\ u_4 \end{bmatrix} = -E^{-1}(x) \begin{bmatrix} L_f^2 h_1(\underline{X}) \\ L_f^2 h_2(\underline{X}) \\ L_f^2 h_3(\underline{X}) \\ L_f^2 h_4(\underline{X}) \end{bmatrix} + E^{-1}(x) \begin{bmatrix} v_1 \\ v_2 \\ v_3 \\ v_4 \end{bmatrix} [\tag{4.25}$$

where,

$$E(x) = \begin{bmatrix} L_{g_1} L_f^1 h_1 & L_{g_2} L_f^1 h_1 & L_{g_3} L_f^1 h_1 & L_{g_4} L_f^1 h_1 \\ L_{g_1} L_f^1 h_2 & L_{g_2} L_f^1 h_2 & L_{g_3} L_f^1 h_2 & L_{g_4} L_f^1 h_2 \\ L_{g_1} L_f^1 h_3 & L_{g_2} L_f^1 h_3 & L_{g_3} L_f^1 h_3 & L_{g_4} L_f^1 h_3 \\ L_{g_1} L_f^1 h_4 & L_{g_2} L_f^1 h_4 & L_{g_3} L_f^1 h_4 & L_{g_4} L_f^1 h_4 \end{bmatrix}$$

The outputs are related to the new inputs by using Eq. 4.26.

$$\begin{bmatrix} \underline{y_1^2} \\ \underline{y_2^2} \\ \underline{y_3^2} \\ \underline{y_4^2} \end{bmatrix} = \begin{bmatrix} v_1 \\ v_2 \\ v_3 \\ v_4 \end{bmatrix} \tag{4.26}$$

Step 5. Linear feedback equation for calculating the new inputs.
Once the input transformation is done, a classical linear feedback approach is implemented to calculate the new inputs using Eq. 4.27.

$$v_i = \ddot{y_i}^{des} + k_v(\dot{y_i}^{des} - \underline{\dot{y_i}}) + k_p(y_i^{des} - \underline{y_i}) \tag{4.27}$$

where, $\ddot{y_i}^{des}$ represents the desired acceleration value of the i^th output, $\dot{y_i}^{des}$ is the desired velocity of the i^th output, and y_i^{des} is the desired value of the i^th output

given or calculated by the user.

k_v and k_d are $m \times m$ diagonal matrices of positive gains. The values of these gains are normally set by the user applying traditional pole-placement method and then selecting a good value for efficient performance.

4.2.1 Simulation Results

The simulation results of the implementation of the IOFL on the CDPR system are presented in this section. The simulation is done using MATLAB. The following assumptions are made for simulation:
1) All six degrees of freedom are available for measurement.
2) The cable forces are available during the simulation.

4.2.2 Case study : I - Initial Dimensions

This section presents the implementation of the IOFL method on a CDPR with the dimensions given in table 4.1. The attachment points of the cable on the moving platform and the base platform are given in table 4.2.The platform specifications are given in table 4.3.

Table 4.1: Simulation parameters

Room dimension (m)	5∗5∗3
Platform dimension (m)	0.5∗0.5∗0.2
Max. cable force (N)	500
Min. cable force (N)	1

Table 4.2: Cable attachment points @ z=1.5 m

Cable no.	MP	Base
Cable 1	[2.25,2.25,1.7]	[0,0,3]
Cable 2	[2.25,2.75,1.7]	[0,5,3]
Cable 3	[2.75,2.75,1.7]	[5,5,3]
Cable 4	[2.75,2.25,1.7]	[5,0,3]

Table 4.3: Platform specifications

Mass of platform (kg)	Inertia(kgm^2)
30	$\begin{bmatrix} 1.025 & 0 & 0 \\ 0 & 1.025 & 0 \\ 0 & 0 & 1.25 \end{bmatrix}$

a) Moving from x=1, y=1, z=1 to x=2, y=2, z=1:

The point-to-point movement is designed using a quintic polynomial equation to ensure smooth acceleration, velocity, and position. The simulation is done for 25 s, where the time to reach from the starting point to the final is 10 s, and the rest

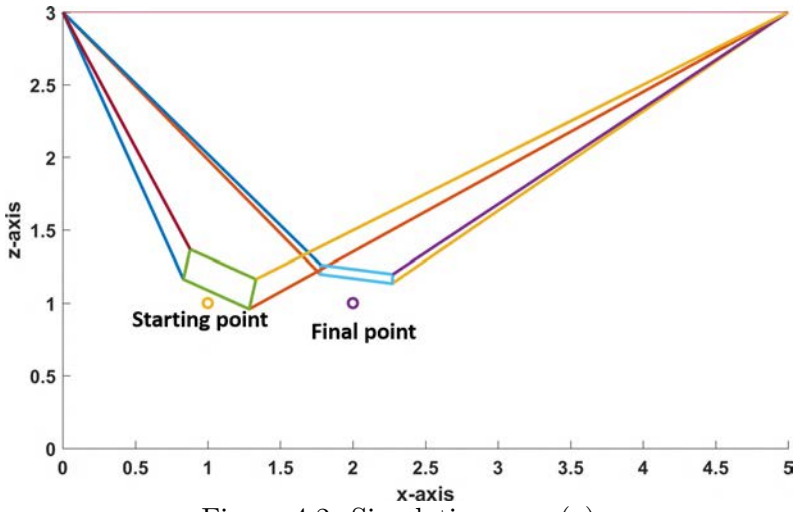

Figure 4.2: Simulation case (a)

time is 15 s. The corresponding values of α, β, γ for the starting and final position are calculated from the static equilibrium program developed by the authors in [Kum+19]. The simulation results are shown in Fig. 4.3 and 4.4. As seen in Fig.

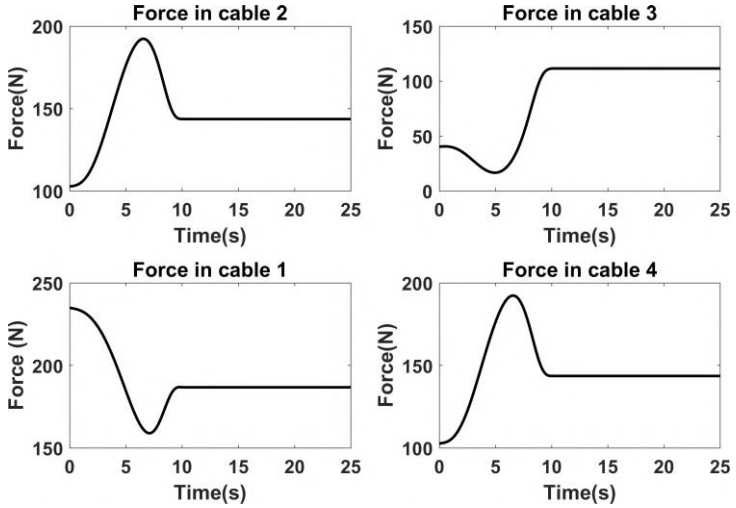

Figure 4.3: Cable forces during the simulation

4.3 and 4.4, the MP is able to attain the desired position while maintaining the stable behavior. The force values generated in the cables are well within limits set for the simulation conditions.

b) Moving from x=3, y=3, z=1.5 to x=4, y=4, z=1:

To ensure the symmetric performance of the robot and also to study its behavior when all the four control outputs (x, y, z, and γ) are made to change simultaneously, the simulation is done as shown in (b). The corresponding values of the cable forces and the platform position and orientation are shown in Fig. 4.6 and Fig. 4.7 respectively. It can be seen that the platform can perform efficiently,

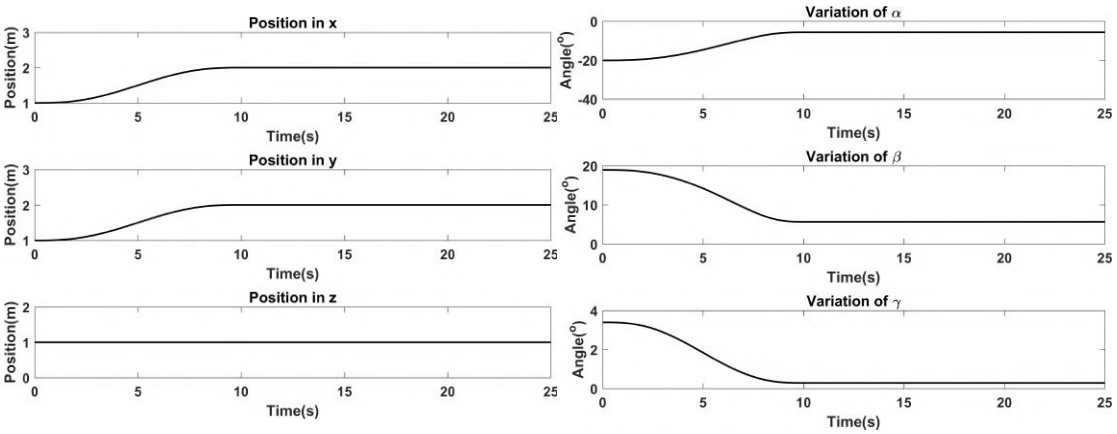

(a) MP position during the simulation

(b) MP orientation during the simulation

Figure 4.4: MP behavior during simulation case a)

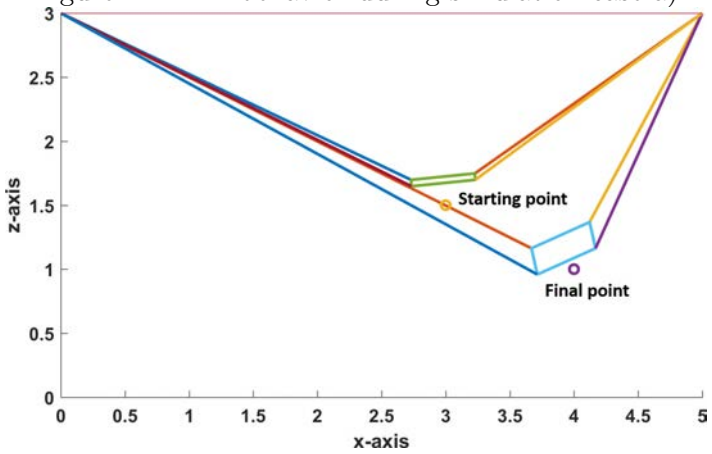

Figure 4.5: Simulation case (b)

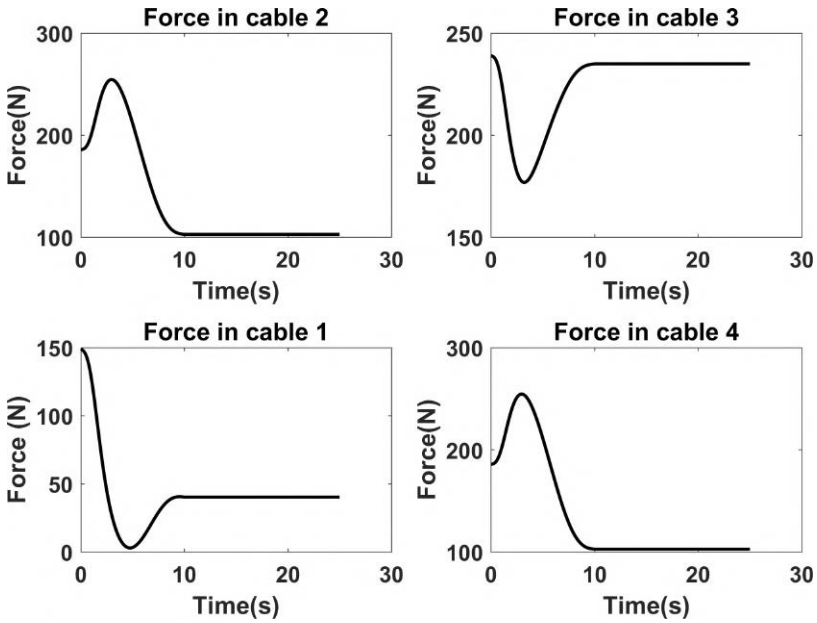

Figure 4.6: Cable forces for the simulation condition (b)

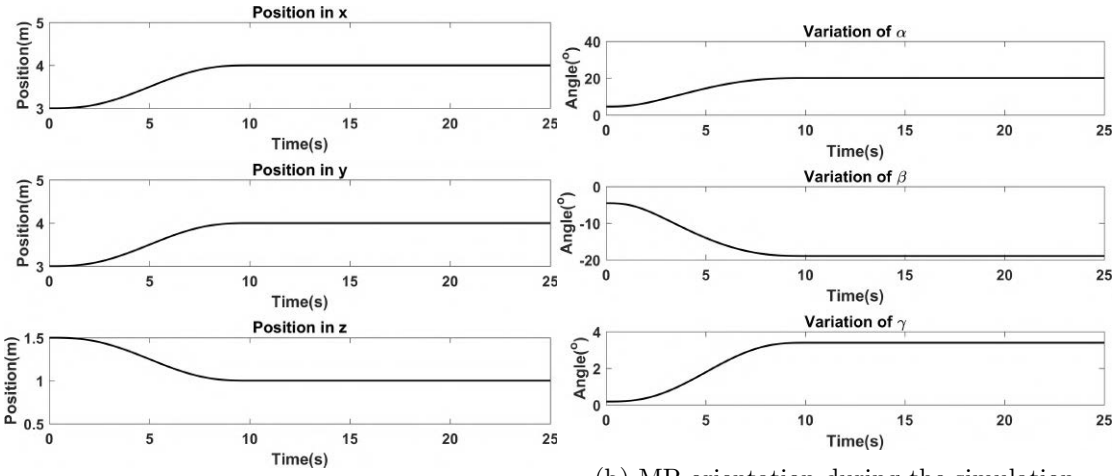

(a) MP position during the simulation

(b) MP orientation during the simulation

Figure 4.7: MP behavior during simulation case (b)

respecting the simulation conditions.

c) Moving from x=2, y=0.5, z=1.5 to x=2, y=2, z=1.5:

The first two cases (a & b) presented the conditions in which the role of internal dynamics was found to be trivial. However, the current condition (c) presents the case where the internal dynamics play a significant role in the system's behavior. The simulation results are presented in Fig. 4.8, and 4.9. As seen in Fig. 4.8, the

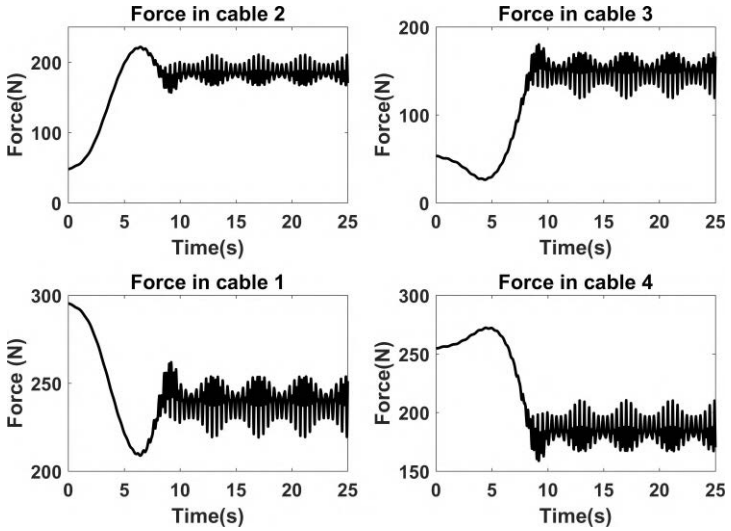

Figure 4.8: Cable forces for the simulation condition (c)

cable forces are oscillatory. The behavior of the CDPR in terms of the position (x, y, z) is found to be stable. However, the uncontrolled DoF (α and β) exhibits oscillations, which affects the forces generated in the cables. In order to get a better idea, the phase-plane plot of α and β is presented in Fig. 4.10a and 4.10b. As seen, the plot shows no convergence and keeps circling, which explains the oscillatory behavior.

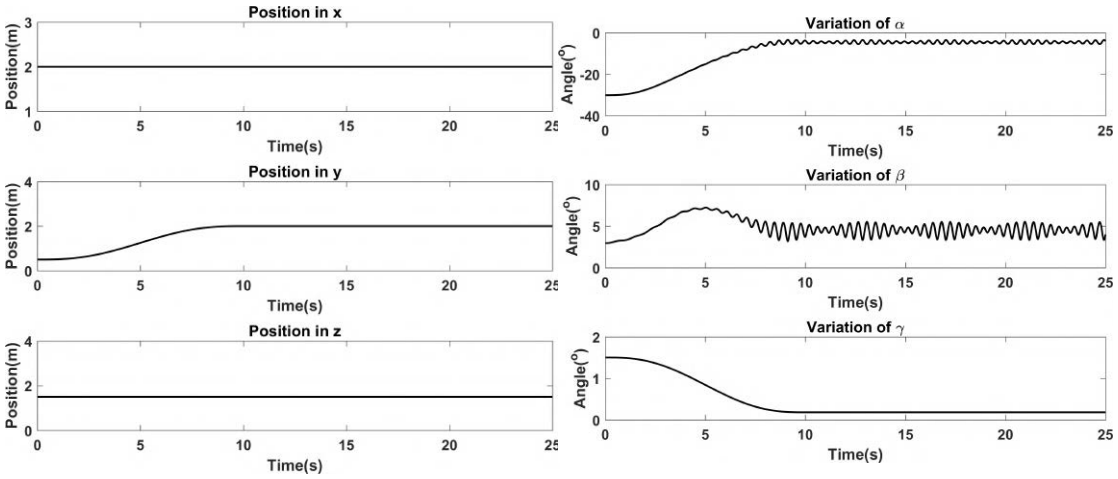

(a) MP position during simulation

(b) MP orientation during simulation

Figure 4.9: MP behavior during simulation case c)

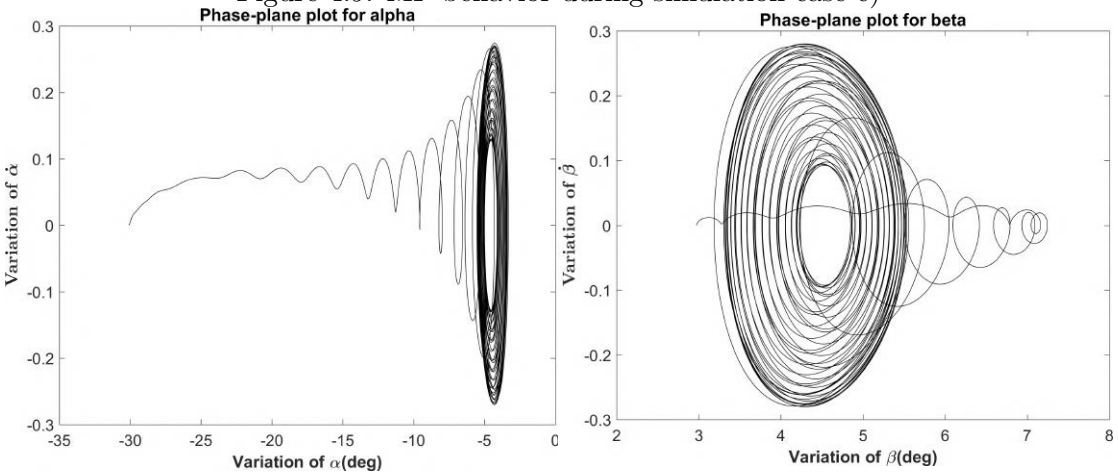

(a) Phase plane plot for α

(b) Phase plane plot for β

Figure 4.10: Phase plane plot for the uncontrolled dof

Internal Dynamics-Further analysis

It is challenging to calculate the equation to analyze the internal dynamics and the zero dynamics due to the positive tension constraint and the number of variables involved in the system. However, an effort has been made to get an idea about the possible role of platform dimensions in the behavior of the internal dynamics. Two different possibilities are considered as given below:

Changing the length and breadth of MP

The length and breadth of the MP have been changed to observe the platform behavior, and the simulation results are shown in Fig. 4.11. This is also similar to the condition where the dimension of the base platform (the room) is changed. It is seen from Fig.4.11a that the values of the cable forces are much less oscillatory due to the change of dimensions. The system behavior was checked at

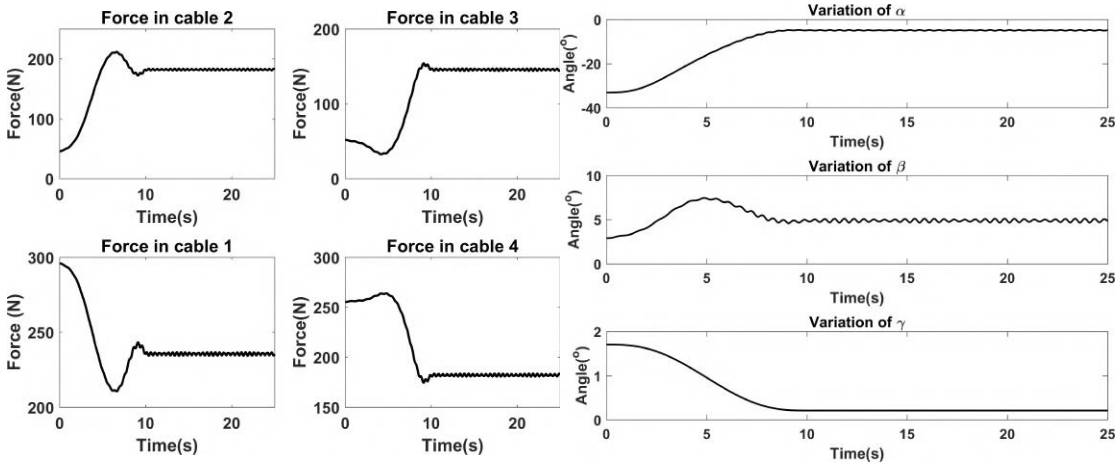

(a) Cable forces (b) MP orientation

Figure 4.11: CDPR behavior when the length and breadth are changed

different heights, and it was found that the MP showed identical behavior at each point selected. Similar performance is observed when the dimensions (length and breadth) are increased, and the CoM is fixed as shown in table 4.1. However, decreasing the size of the MP (with CoM=0.2) caused the CDPR to fail during the simulation due to the generation of unfeasible force values.

Changing the CoM of the MP

The length and breadth of the MP were kept as 0.5×0.5, and the CoM of the platform was changed to observe the CDPR behavior. The simulation behavior is shown in the Fig.4.12. Several different values of CoM were checked from 0.1 m to 0.25 m at heights ranging from $z = 0.25$ m to $z = 2.25$ m, and it was found that the value of 0.1 m produced the most satisfactory performance at all heights considered. The value of CoM was not increased beyond 0.25 m due to the final prototype dimension consideration. It is seen from the simulation results that the highly oscillatory behavior in the cable forces is reduced but is not eliminated. The observations from the simulation study are presented in the inference section (4.4).

Changing the platform and room dimensions to reduce the impact of strong internal dynamics is suitable for cases where they can be implemented before the final prototype is fabricated. However, one drawback of this is that there exist many possible combinations which can result in an efficient prototype dimension. A proper methodology to address this particular issue can be interesting for further research.

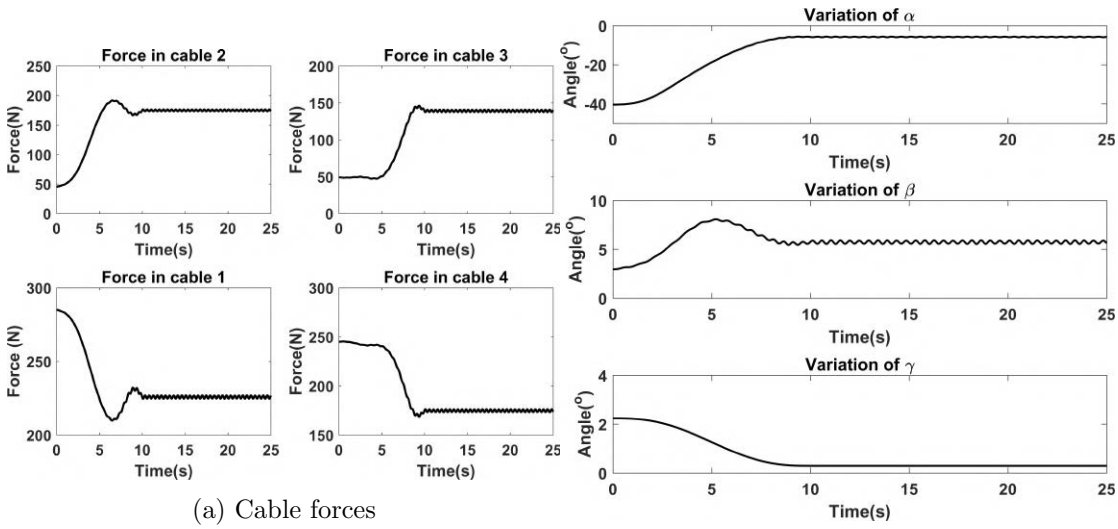

(a) Cable forces

(b) MP orientation

Figure 4.12: CDPR behavior when the CoM is changed

4.2.3 Prototype Dimensions

The final dimension of the prototype and the base platform (the room), taking into account the simulation results from 4.2.2, various physical constraints, and space availability, is given in table 4.4. The final prototype is shown in Fig. 4.13. The red line represents the distance between the cable exit points used in this work. Further explanation about the prototype is given in chapter V. The platform

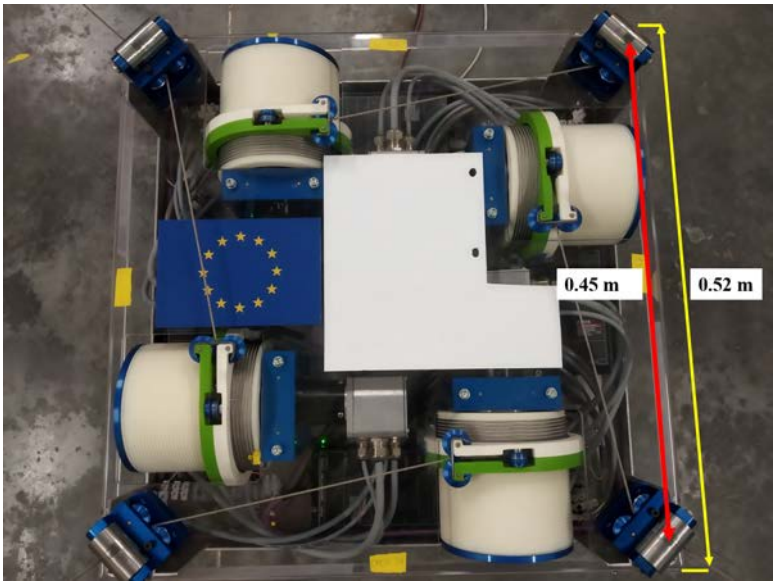

Figure 4.13: Prototype of the CDPR

specifications are given in table 4.6.

Table 4.4: Simulation parameters

Room dim. (m)	5.37∗3.99∗2.97
MP dim. (m)	0.52∗0.52∗0.088
Max. force (N)	500
Min. force (N)	1

Table 4.5: Cable attachment points @ $z = 1$ m

C. no.	MP	Base
1	[2.46,1.77,1.19]	[0,0,2.97]
2	[2.46,2.22,1.19]	[0,3.99,2.97]
3	[2.91,2.22,1.19]	[5.37,3.99,2.97]
4	[2.91,1.77,1.19]	[5.37,0,2.97]

Table 4.6: Platform specifications

Mass of platform (kg)	Inertia(kgm^2)
22.7	$\begin{bmatrix} 0.441659 & 0 & 0 \\ 0 & 0.441659 & 0 \\ 0 & 0 & 0.766125 \end{bmatrix}$

Implementation of the IOFL on the prototype-Simulation

In order to demonstrate the behavior of the prototype using the IOFL, a single simulation study is presented while the experimental results are presented in the later chapter. The simulation is done using the following condition.

a) Moving from x=2.685, y=1.995, z=1.102 to x=4.985, y=1.995, z=1.102:

It is seen from Fig. 4.15 that the behavior of the MP with the dimensions chosen

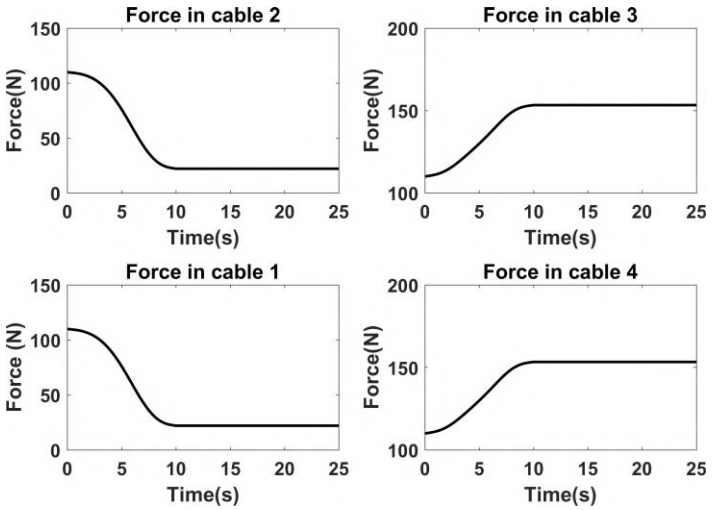

Figure 4.14: Cable forces during the simulation using prototype dimensions

for the prototype is ideal. The force values (Fig. 4.14) are smooth, and the MP can reach the desired position maintaining the stability of the uncontrolled degrees of freedom.

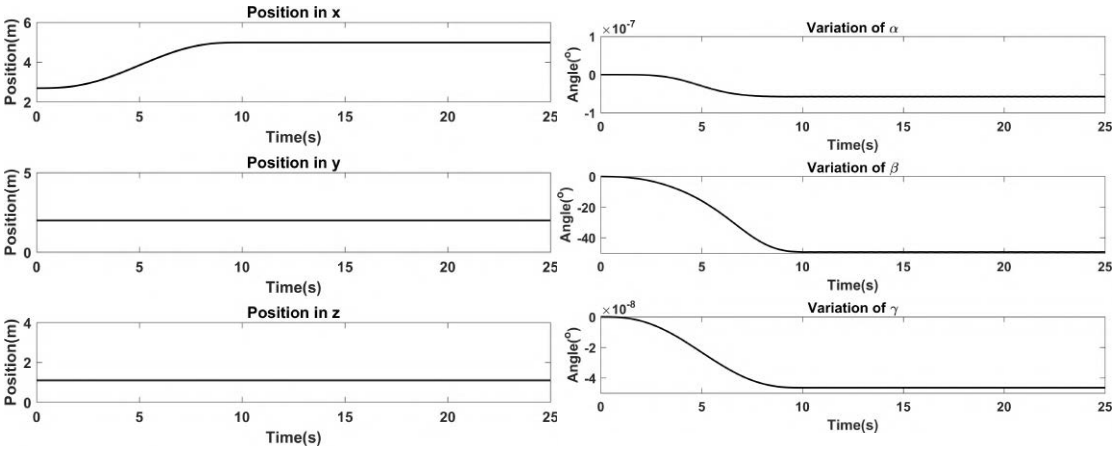

(a) MP position during the simulation using prototype dimensions

(b) MP orientation during the simulation using prototype dimensions

Figure 4.15: MP behavior during simulation using prototype dimensions

4.3 Modified IOFL

The simulation results in subsection 4.2.2 clearly indicate the strong interaction between the cable forces (inputs) and the uncontrolled degrees of freedom (α and β). The positive cable tension constraint and the underactuated nature of the CDPR make the calculation of the zero dynamics behavior challenging. The analysis presented in section 4.2.2 can be used before the prototype is fabricated. Additionally, a solution from a control point of view is presented here to address the issue of internal dynamics for the initial dimensions considered. A modified IOFL is introduced as an ad-hoc solution to improve the response of the system for the dimensions considered in table 4.1, 4.3, 4.2. Several simulation results are presented to highlight the improved performance of the system using the proposed approach.

4.3.1 Principle idea of the proposed approach

Several studies have been carried out in recent years to address the instability of zero dynamics by combining different control techniques [Isi13b]. Some of the examples include backstepping, sliding mode controller combined with backstepping approach [MB06; BS05], feedback linearization combined with sliding mode control [PKL19], flatness-based control [Léc+13] etc.. Following the approaches from these works, this modified feedback linearization control is proposed as an ad-hoc solution to stabilize the internal dynamics of the CDPR system. It is primarily based on the concept of classical input-output feedback linearization. The novelty of this approach is that instead of using two different control techniques, the same control approach is executed on two separate branches. The output from each

branch is then combined and given as the input to the system. The block diagram of the proposed control law is shown in Fig. 4.16. Two separate branches are

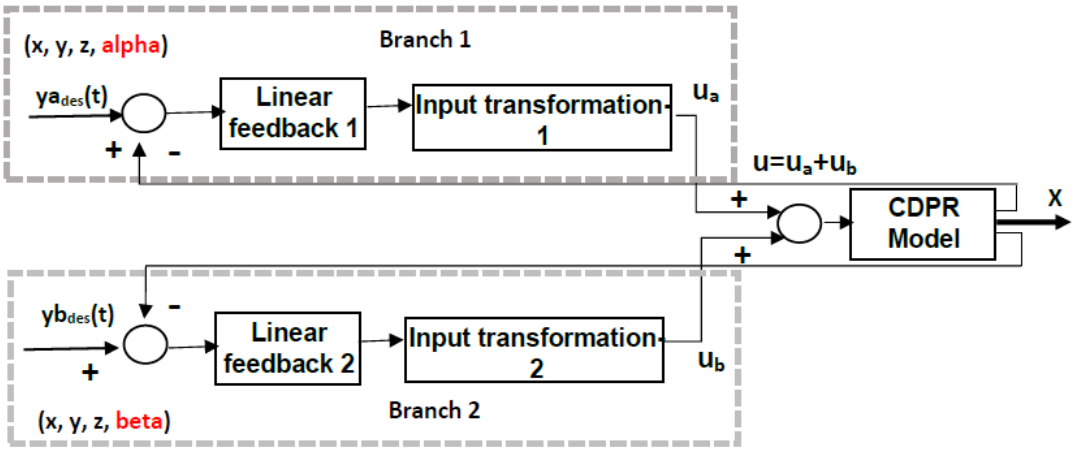

Figure 4.16: Block diagram of the Modified Feedback Linearization

formulated as shown in Fig.4.16. The selection of outputs to be controlled by each branch is based on ID from the classical I/O FL. The branches consist of a linear feedback controller and an input transformation block. Each branch is modeled to act on half of the total external wrench acting on the platform ($m * g$, in this case). The output of each branch is then added and given as the input to the dynamic model of the CDPR. The mathematical equations mostly remain as shown in IOFL approach. However, change is made in the outputs to be controlled.

$$\begin{aligned} \underline{y_{a1}} = x, \quad \underline{y_{a2}} = y, \quad \underline{y_{a3}} = z, \quad \underline{y_{a4}} = \alpha \\ \underline{y_{b1}} = x, \quad \underline{y_{b2}} = y, \quad \underline{y_{b3}} = z, \quad \underline{y_{b4}} = \beta \end{aligned} \tag{4.28}$$

where, $\underline{y_{ai}}$, $(i = 1..4)$ and $\underline{y_{bi}}$, $(i = 1..4)$, represents the outputs to be controlled by the branches 1 and 2 respectively.

Following this, the individual force values (u_a and u_b) are calculated using the steps followed in section 4.2. The final input vector (u) is then calculated as the sum of the forces from the two branches as follows:

$$u = u_a + u_b \tag{4.29}$$

4.3.2 Simulation Results

The proposed control law is applied to the CDPR system, and the simulation results are presented here. The trajectory simulated in the section before (simulation case c) is used to check the performance of the law. The cable forces

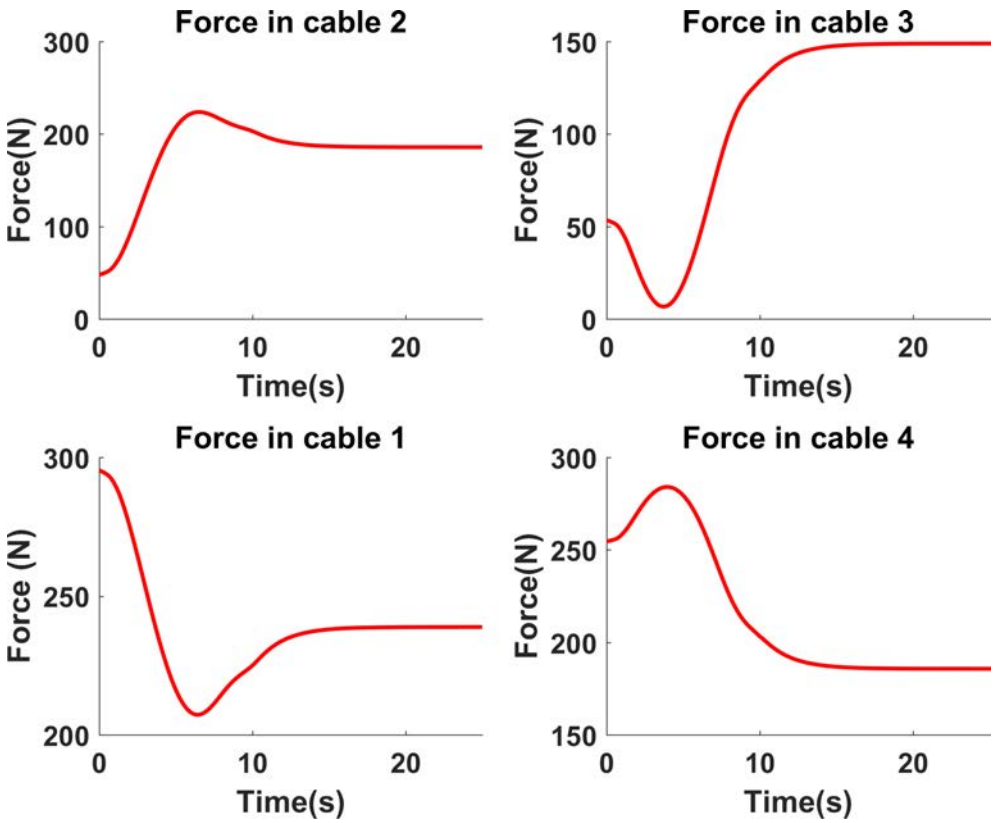

Figure 4.17: Cable forces using the modified feedback linearization

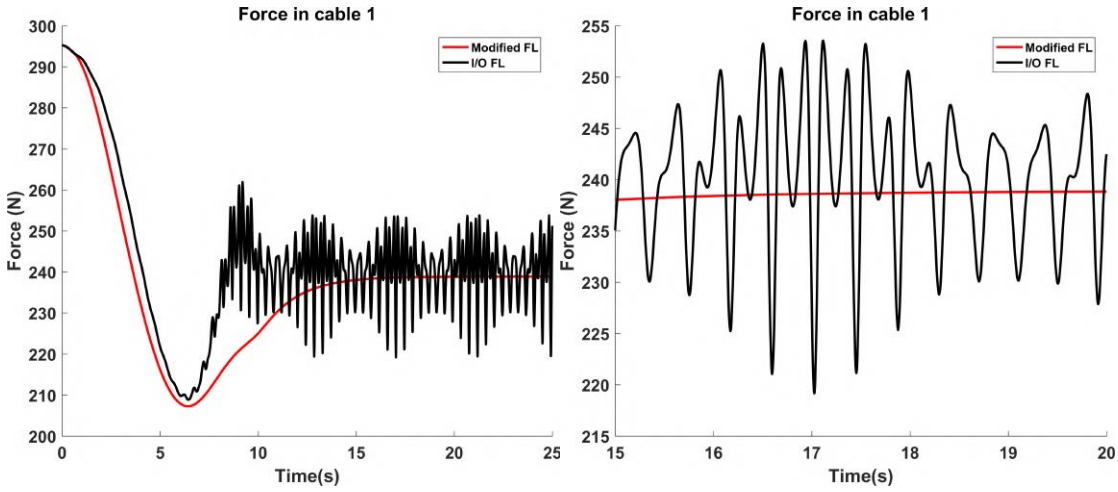

(a) Force in cable 1 (b) Enlarged view of cable forces

Figure 4.18: Comparison of cable forces generated in cable 1 during the simulation using Modified FL and IOFL

generated for the desired trajectory due to the modified control law are shown in Fig. 4.17. It is found that the values of the forces are positive and within the limits, as defined in table 4.1. Also, as seen in Fig. 4.18b, the proposed modified feedback linearization approach can maintain a stable constant value under ideal conditions (approx. 239 N) for the selected time (15 s - 20 s), whereas, the classical IOFL approach generates an oscillating value of cable force ranging from 253

N to 220 N for the selected time interval. These fluctuations can prove dangerous for the actuators and the CDPR if implemented on the real prototype. Fig. 4.20

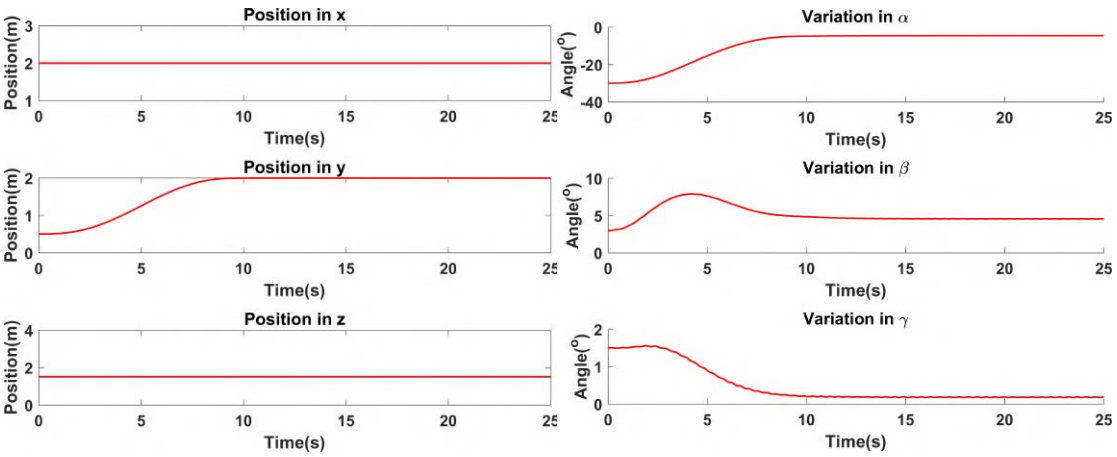

(a) MP position during simulation (b) MP orientation during simulation

Figure 4.19: MP behavior during simulation case c)

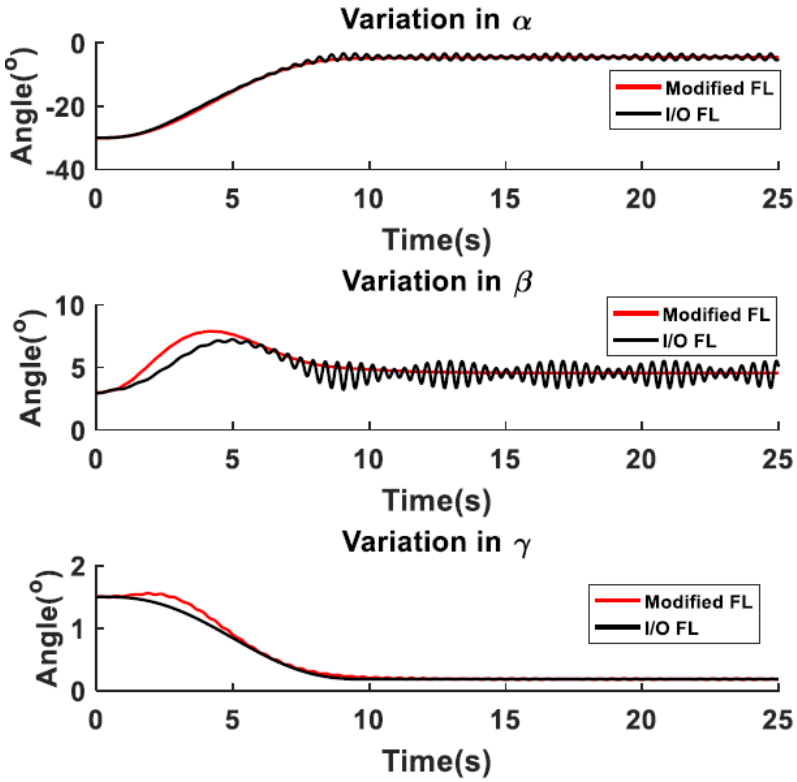

Figure 4.20: Platform orientation angle (α and β)

shows the comparison of the platform orientation values generated by the modified control law and the classical I/O feedback linearization. It is evident from Fig. 4.20 that the orientation values are stable due to the application of modified feedback linearization.

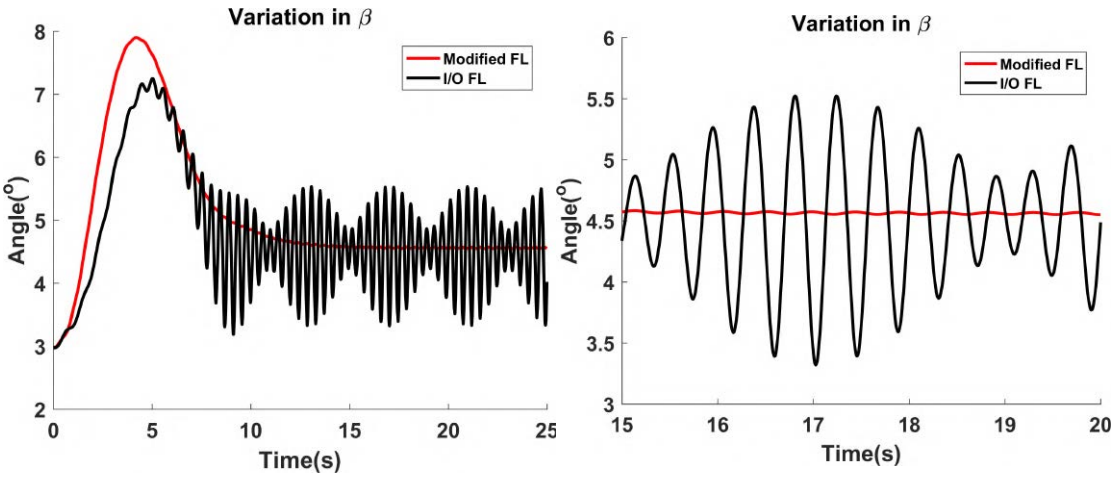

(a) Comparison plot for β

(b) Enlarged view of β

Figure 4.21: Comparison of orientation angle (β) during the simulation using Modified FL and IOFL

The performance of the proposed modified IOFL is better than the classical IOFL for the dimensions of the CDPR considered. Several simulations have been performed on other conditions mentioned in subsection 4.2.2 and the behavior of the proposed modified feedback linearization is efficient.

4.4 Inferences and Discussion

This section presents the important observations and inferences from the simulation results of the chapter. Based on the results obtained in section 4.2, certain inferences are presented here.

1) The underactuation in the CDPR design results in internal dynamics in the system. The classical IOFL technique is able to achieve the expected outcomes (using simulations) on the outputs to be controlled (x, y, z, γ). The control law is also able to generate the input values (cable forces) within limits set for the simulation. The behavior of internal dynamics is, however, not the same at every point. For the initial design considered (table 4.1 and 4.2), the uncontrolled internal dynamics results in high oscillations in cable forces which are not good for the cables and the actuators. The oscillations are also seen in the uncontrolled degrees of freedom (α, and β). This behavior is seen as the robot moves closer to the boundary of the fixed structure.

2) To reduce the oscillations in cable forces and the uncontrolled DoF, the physical dimensions of the platform were changed, and the simulation was repeated, and

the results were analyzed.

Changing the length and breadth of the MP can help in improving the platform behavior. However, this quantification requires a more in-depth analysis of various possible combinations, which is not in the scope of this work.

CoM of the MP plays an important role in maintaining the stability of the CDPR. Performing simulation before the fabrication of the prototype can help eliminate the unwanted behavior of the CDPR due to the presence of internal dynamics. Since the motors need to be placed on the MP, this simulation study provides useful insights for the fabrication of the prototype.

The room dimension also plays a significant role in reducing the impact of internal dynamics when the dimension of the MP cannot be altered due to other design constraints. A typical example occurs in this particular work where due to the motor placement, the controller fixation, and electrical wiring placements, it is easier to change the room dimension to improve the performance rather than changing the length and breadth of the MP.

3) A modified feedback linearization approach is proposed as an ad-hoc solution for the initial design parameters to reduce the oscillations in the cables, resulting in the reduction of oscillations in the platform orientation angles. It is shown that the proposed modified control works efficiently in achieving the desired results and canceling the cable oscillations. The shape of the platform (square) and the room (square) results in symmetric behavior of α and β. This results in the cancellation of the internal dynamics effects due to these orientation angles. A thorough analysis of the proposed ad-hoc control needs to be performed further to verify its applicability to other configurations of CDPRs.

4.5 Summary

This chapter presented the implementation of the classical IOFL for a four cable-driven parallel robot. Simulation studies were presented in which the behavior of the internal dynamics was shown. Following this, the role of platform dimensions in improving robot behavior was also discussed. The simulation of the IOFL with the fabricated prototype dimensions has also been demonstrated to get an insight into the performance of the MP before the validation of the model using experiments. A modified feedback linearization approach has been proposed as an ad-hoc technique to stabilize the behavior of the internal dynamics of the moving platform. The efficient performance of the proposed approach has been shown

using simulations. However, applying the proposed approach on a generic CDPR model needs to be analyzed to formulate a mathematical stability criterion.

Chapter 5

Experimental Results

Contents

This chapter presents the experimental results performed to validate the classical IOFL technique on the fabricated prototype. The first section of the chapter presents the details of the prototype. The second section gives the necessary setup done for the experimental validation. Following this, the experimental results are presented in the next section. The discussion of the results is presented in the next section, followed by the final section summarizing the chapter.

5.1 Fabricated prototype

The initial CAD design of the prototype is shown in Fig. 5.1. As mentioned in the objectives in chapter one, one of the novel features of the robot is the placement of the motors on the MP. This means that the entire actuation unit, including the gears, the winches, and the controller units, are also mounted on the MP. The main advantage of such a configuration is the simplified implementation in the workshop, as it is just sufficient to select the location of the fixed attachment points in the room.

Based on the dimensions selected in chapter four and the environment available for installing the robot, the final prototype of the CDPR fabricated for the thesis

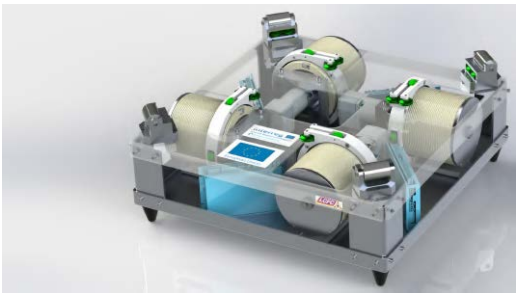

Figure 5.1: 3D model of the four cable-driven parallel robot

is shown in Fig. 5.2. The dimension of the room where the attachment points are mounted is 5.37 m $*$ 3.99 m $*$ 2.97 m. The dimension of the MP is 0.52 m $*$ 0.52 m, while the outing points of the cables for calculation are with a dimension of 0.45 m $*$ 0.45 m. The CoM of the MP was found to be at 0.09 m after performing some mechanical tests. The cables are fixed to the base structure using simple anchors as shown in Fig. 5.3. As seen in Fig. 5.4, the cables are guided by two pulleys to hold them in place as the MP moves. The total mass of the MP with all the connecting wires and the actuation unit is 22.7 kg approximately. The

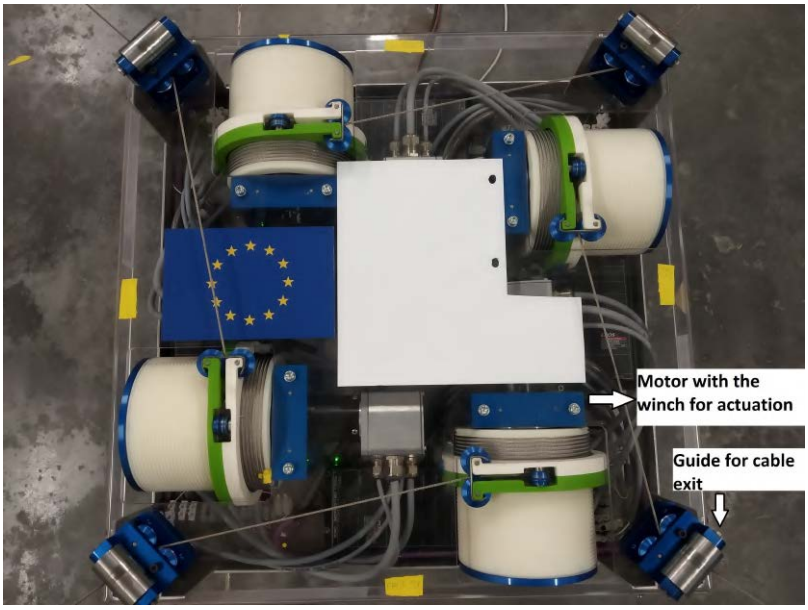

Figure 5.2: Final prototype of the four cable-driven parallel robot

hardware details are as follows:
Each actuation block for one cable consists of 1) Maxon EC brushless motor with Hall sensors, 2) a planetary gearhead unit with a reduction ratio of 74:1, 3) Encoder unit, 4) EPOS2 digital positioning controller, and, 5) K100, a tension force sensor from SCAIME.

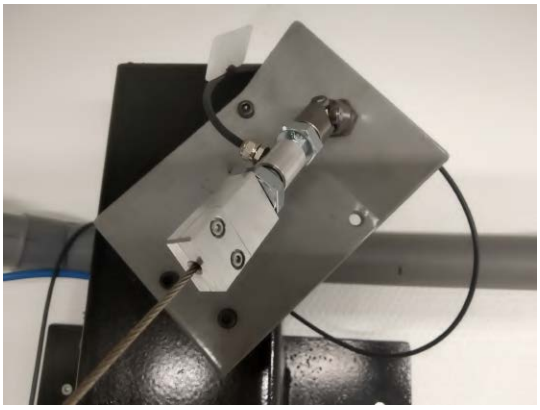

Figure 5.3: K100, a tension force sensor from SCAIME and the anchor plate for attaching the cable

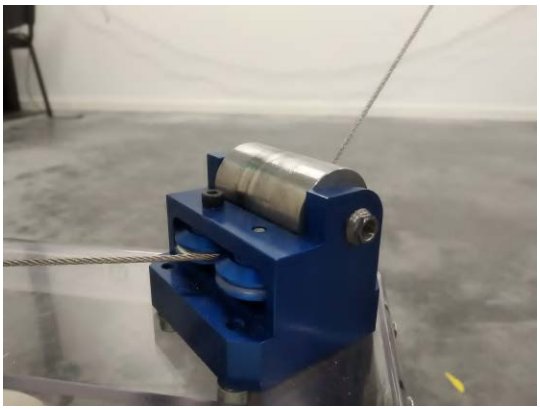

Figure 5.4: Cable guide for the CDPR

5.2 Experimental setup

The CDPR designed in this thesis is underactuated. The number of cables is four, while the number of degrees of freedom is six. It is also necessary to ensure positive cable tensions always during MP motion. A set of steps are followed before performing the experiments on the CDPR.

When the CDPR is not powered, it is normally placed at a known location on the ground. The coordinates for this location are $x = 2.685$ m, $y = 1.995$ m, and $z = 0$, which corresponds to the center of the room. This is done to ensure that the MP starts from the same point each time it is used for performing the tests. Once the CDPR is powered on, to ensure that the cables are taut and tensed, a small current is given to the motors, which guarantees minimum tension in all four cables, also known as pretension. The values of the forces in the cable (Fig. 5.5) can be seen using the interface provided by SCAIME. The magnitude of pretension in each cable depends on several factors discussed further in the discussion section of the chapter (5.4).

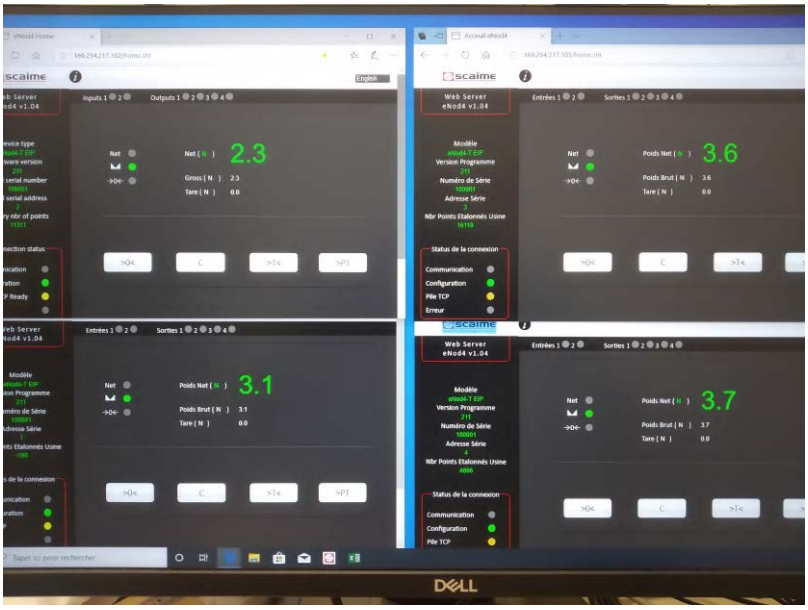

Figure 5.5: Interface to view the cable forces

A home position is defined for the CDPR from where the MP makes the needed point-to-point motion each time. This home position is selected as $x = 2.685$ m, $y = 1.995$ m, and $z = 0.214$ m as shown in Fig. 5.6 which corresponds to a distance of 10 cm from the tip of the bush fixed underneath the platform to the wooden platform on which the CDPR rests. This home position is reached from the ground by giving the necessary number of points for the motors. Certain simplifications are done for conducting the experiments to validate the control law. They are explained in the next subsection.

5.2.1 Simplifications for testing

In order to first validate the classical control law formulated, certain simplifications have been made for the experimental setup. The tests presented in this study currently consider only a translation motion along $z - axis$ from the center of the room. Due to the geometric dimensions of the environment and the moving platform, the values of the platform orientation angles (α and β) become zero while the value of γ, the orientation angle around $z - axis$ was found to be less than 1°. This simplification eliminates the addition of any sensors to measure the platform orientation. Additionally, since no movement is done along the $x - axis$ and $y - axis$, it will be possible to obtain the feedback for the control law using only the motor positions.

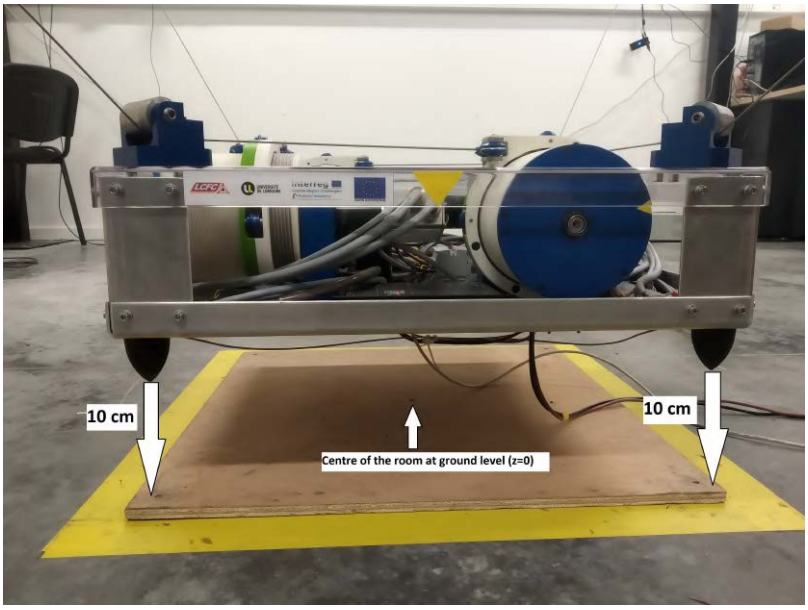

Figure 5.6: Home position for the CDPR before implementing the motion

5.2.2 Steps for testing

The interface with the controller of the robot is done using the C++ program developed in Visual Studio 2017. The block diagram for the control approach is given in Fig. 5.7. The control of the motor is done using the Interpolated Position

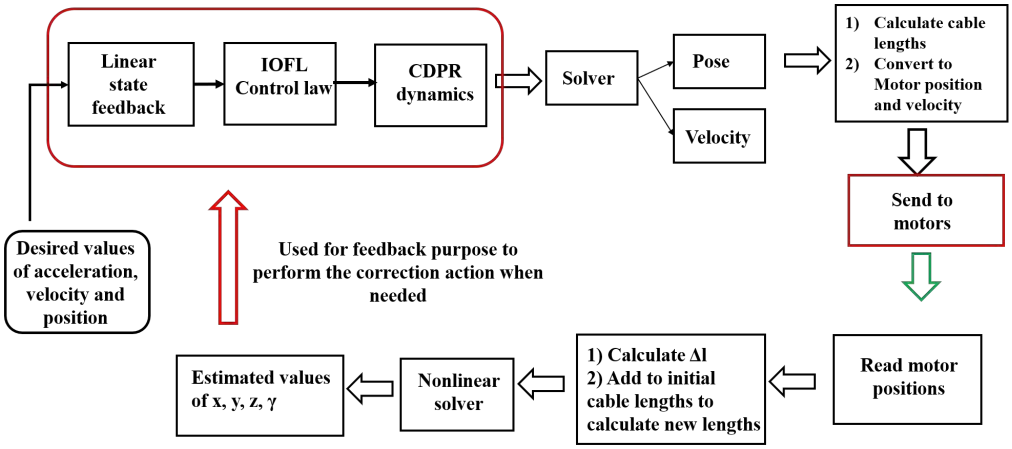

Figure 5.7: Block diagram for control approach

Mode (IPM) offered by the EPOS2 controller. In this mode, the values of motor position and velocity are being fed to the controller for performing the action at a time interval defined by the user. After performing some preliminary tests to establish a suitable sampling rate, a value of 55 ms is used for the experiments. The steps followed for performing the experiments are given further.

1) Start from ground to the *Home* position of the CDPR.

2) Select the desired height to be moved by the CDPR along with the desired

velocity value for the trajectory.
3) Initialize the values needed for the point-to-point motion. These values include the coefficients needed for the desired trajectory profile, the initial values of cable forces, the initial cable lengths, the initial values for the solver, and the initial values of the motors to set it to zero before the test.
4) Start the IPM mode by sending the desired motor position and velocity.
5) Read the current motor position values.
6) Calculate the change in length (δl_i ,$i = 1, 2, 3, 4$) from the initial position to the current measured position.
7) Calculate the new cable lengths.
8) Estimate the value of x, y, z, and γ from the new lengths using a nonlinear equation solver.
9) Send the data to the linear feedback and the control block to compute the new value of the force needed.
10)Use the estimated new force value to compute the new motor position and velocity to be sent.
11) Go back to step 5 and repeat till the final point or end of the trajectory.

The data collected from the control program (estimated value of z, the desired value of z, the estimated cable forces, the measured motor positions) and force sensors mounted on the anchor points are then compared to analyze the results and validate the experiments.

5.3 Experimental results

The experiments performed and the respective results obtained are explained in this section. The maximum speed of the prototype used according to the hardware used is $v_{max} = 0.25$ m/s. Considering the maximum velocity possible, the velocity used in this thesis is limited to 0.2 m/s. As explained in chapter four, a quintic polynomial has been used to generate the necessary values of the desired acceleration, velocity, and position for the variables that can be controlled (x, y, z, γ). A pole of 15 is used for the linear feedback block resulting in a positive gain value of 30 and 225 for the velocity and position terms, respectively (refer to chapter four, Implementation of IOFL on the CDPR system section). Several case studies are shown validating the control law. They are explained further in the section.

5.3.1 Movement from home position to a distance of $0.5m$ along z-axis

The first set of experiments presented in this chapter is done for the movement of the MP for a point-to-point motion along the $z - axis$ from the home position.

Case 1: Movement with a desired speed of $0.05m/s$

The condition for the first test is given in table 5.1.

Table 5.1: Test condition 1

Starting point	$x = 2.685$, $y = 1.995$, $z = 0.214$
Ending point	$x = 2.685$, $y = 1.995$, $z = 0.714$
Desired velocity	0.05 m/s

The total time for the test to be run depends on the velocity value set for the motion. For this case, the test runs for 10 s. Since the movement of the CDPR is only along the $z - axis$ (control variable), only the value of z is plotted in this work, assuming that there is no movement in x and y axis.

The comparison between the desired value of z (given by the user) and the rebuilt value of z from the motor position is shown in Fig. 5.8. It can be seen that the difference between the rebuilt and the desired values of z reduces as time progresses due to the convergence of the rebuilt value towards the end of the test. This indicates that the MP is able to reach the desired position. The time of convergence is not precisely 10 s as desired. There is a delay of few seconds before the MP fully reaches its final position (approx. 1.8 s). This could be due to the timing of communication between the interface and the controller.

Figure 5.9 shows the estimated values of the forces generated by the control law and the actual values of the forces in the four cables measured by the sensor.

As seen in Fig. 5.9, the measured force values oscillate during the entire point-to-point motion. There is a high spike in force values during the start of the motion, after which the level of peak reduces. This peak is due to the triggering of the motion by the controller. The force values are stable after reaching the desired time of 10 s with fewer oscillations with minimal adjustment done by the motors to reach the final desired position.

To further check the performance of the CDPR, the difference between the starting position and the ending position was checked using a handheld laser measurement device. The value measured using the device was 0.497 m, while the difference between the initial and final value of the estimated z position was 0.500904

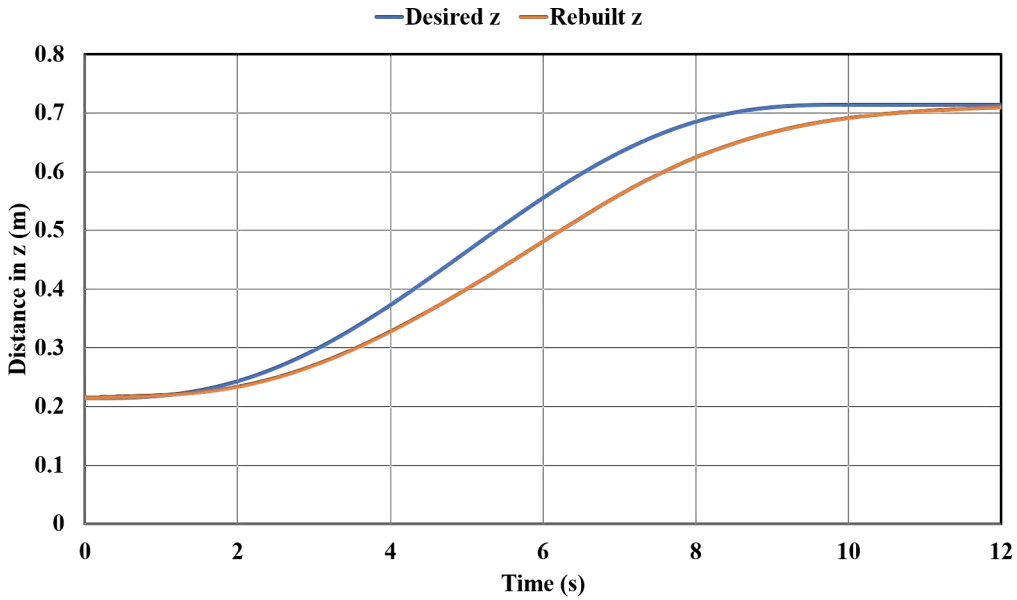

Figure 5.8: Comparison between the desired value of z and the rebuilt value of z from the motor position for a desired velocity of 0.05 m/s for the MP

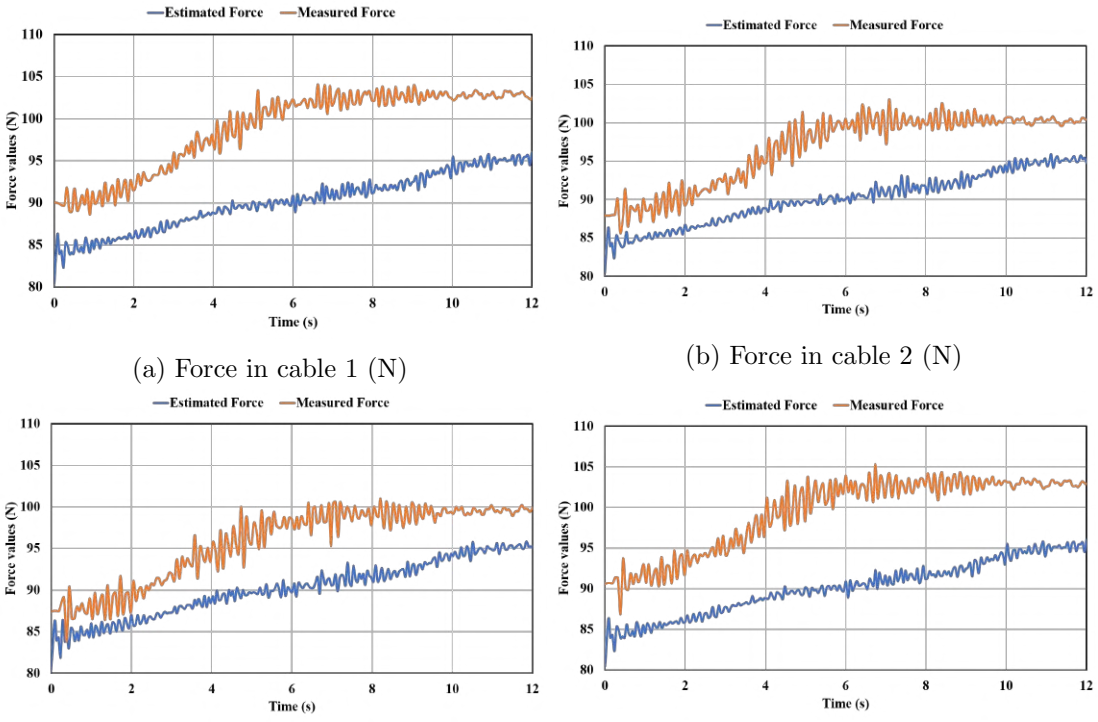

(a) Force in cable 1 (N)

(b) Force in cable 2 (N)

(c) Force in cable 3 (N)

(d) Force in cable 4 (N)

Figure 5.9: Comparison of the estimated and measured cable forces for moving the CDPR from home position to a distance of 0.5 m with a desired velocity of 0.05 m/s.

m. The difference between the measured distance value and the estimated distance value is approximately 3.9 mm.

The tests have been done three times to observe the behavior of the moving platform and the cable forces and verify its repeatability. The plots showing the

measured values of cable forces are shown in Fig. 5.10.

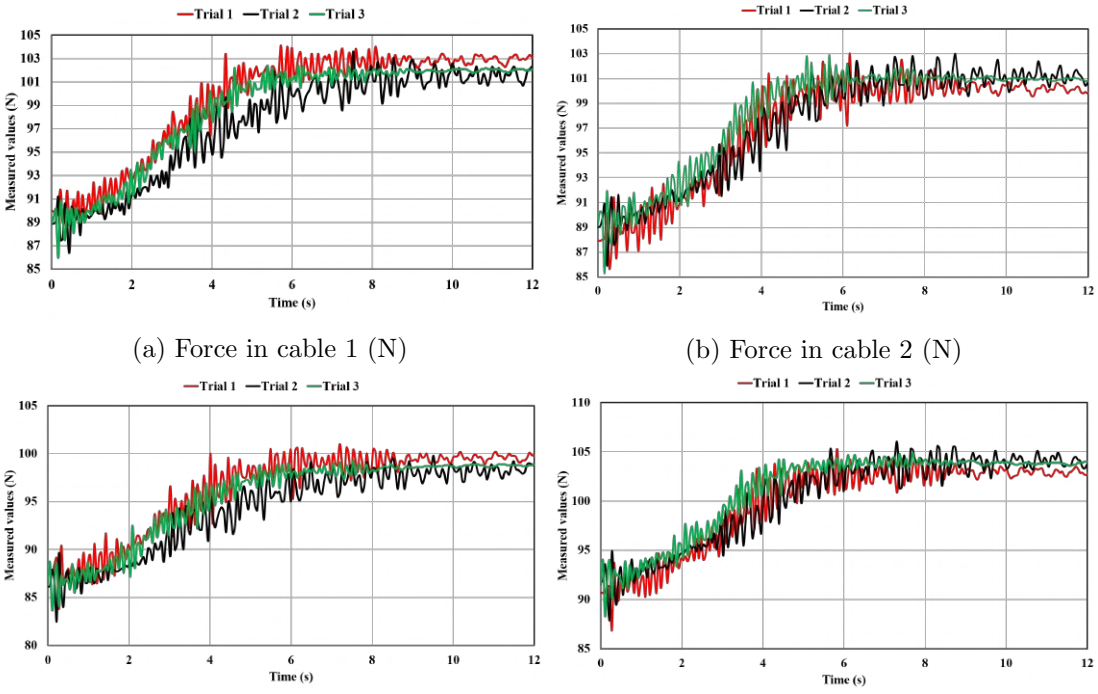

(a) Force in cable 1 (N)

(b) Force in cable 2 (N)

(c) Force in cable 3 (N)

(d) Force in cable 4 (N)

Figure 5.10: Comparison of the estimated and measured cable forces for moving the CDPR from home position to a distance of 0.5 m with a desired velocity of 0.05 m/s.

It is seen from Fig. 5.10 that the behavior of the cable forces is similar during each test. The presence of oscillations in the cables does not affect the position of the MP. Table 5.2 shows the comparison between the estimated value of z and the measured value of z during the three trials with a desired velocity of 0.05 m/s.

Table 5.2: Comparison between estimated value of z and measured value of z

Test	Measured (m)	Estimated (m)	Difference (m)	% error
Test 1	0.497	0.500904	0.00390	0.78 %
Test 2	0.497	0.500985	0.00398	0.8 %
Test 3	0.496	0.50005	0.00405	0.81 %

It can be seen from the table that the MP is almost able to reach the desired value of z during each test. The error of less than 1% can be arising due to some factors associated with the hardware of the prototype.

Case 2: Movement with a desired speed of $0.1m/s$

The condition for the second test is given in table 5.3.

Figure 5.11 shows the comparison between the desired value of z and the rebuilt value of z from the motor position. The system is able to follow the desired values of z. In order to check the time taken by the MP to reach the desired final value,

Table 5.3: Test condition 2

Starting point	$x = 2.685$, $y = 1.995$, $z = 0.214$
Ending point	$x = 2.685$, $y = 1.995$, $z = 0.714$
Desired velocity	0.1 m/s

the test was performed for a time of 9 s (5 s for the timing with the desired velocity of 0.1 m/s, 3 s of rest after reaching the final position). It can be seen that the MP converges to the final position after approximately 1.8 s.

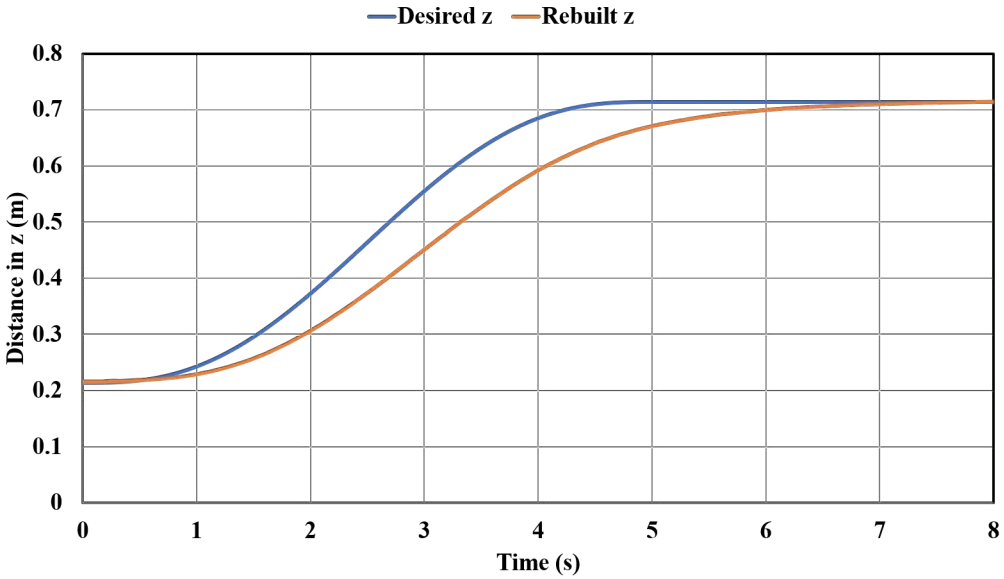

Figure 5.11: Comparison between the desired value of z and the rebuilt value of z from the motor position for a desired velocity of $0.1m/s$ for the MP

The value measured using the device was 0.497 m, while the difference between the initial and final value of the estimated z position was 0.501828 m resulting in a difference of approximately 4.8 mm.

The comparison between the values of the estimated force and the measured force is shown in Fig. 5.12. The values of the forces are in general less than the limit (500 N) set for the cables.

As seen in Fig. 5.12, the profile of the estimated force values not linear when compared to the profile in Fig. 5.9 where the desired velocity value was $0.05m/s$. The values of the estimated force reduce as the time for the final desired value approaches. The estimated force then increases gradually due to the control law and reaches a value for converging the MP position with the desired position. However, the oscillations in the force values are also seen in Fig. 5.12 with an offset range of less than 10 N for different cables.

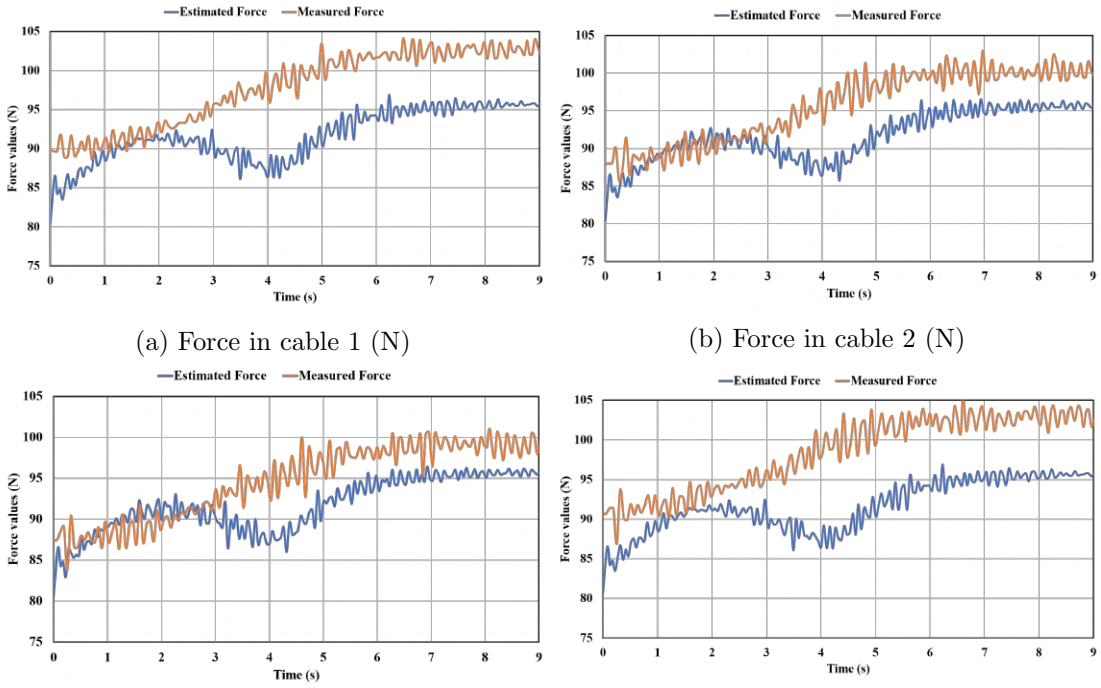

(a) Force in cable 1 (N)

(b) Force in cable 2 (N)

(c) Force in cable 3 (N)

(d) Force in cable 4 (N)

Figure 5.12: Comparison of the estimated and measured cable forces for moving the CDPR from home position to a distance of $0.5m$ with a desired velocity of $0.1m/s$.

Case 3: Movement with a desired speed of $0.2m/s$

The condition for the third test is given in table 5.4.

Table 5.4: Test condition 3

Starting point	$x = 2.685$, $y = 1.995$, $z = 0.214$
Ending point	$x = 2.685$, $y = 1.995$, $z = 0.714$
Desired velocity	$0.2\ m/s$

In this case, the value of the desired velocity is increased to 0.2 m/s, resulting in a total test time of 2.5 s. The test is conducted for an additional time of 2.5 s to check for the stability of the MP after reaching the final position and also to check for its convergence. Figure 5.13 shows the comparison between the desired value of z and the rebuilt value of z. It can be seen that the difference between the desired value and the rebuilt value during the test (moving phase) is higher than the values obtained for tests 1 and 2. The value measured using the device was 0.498 m, while the difference between the initial and final value of the estimated z position was 0.502023 m resulting in a difference of approximately 4 mm. It is also seen that the MP reaches the final position 1.8 s after the desired time.

The results of the force values measured and the force values estimated during the test are shown in Fig. 5.14.

The estimated force profile shows the same behavior as that of the previous

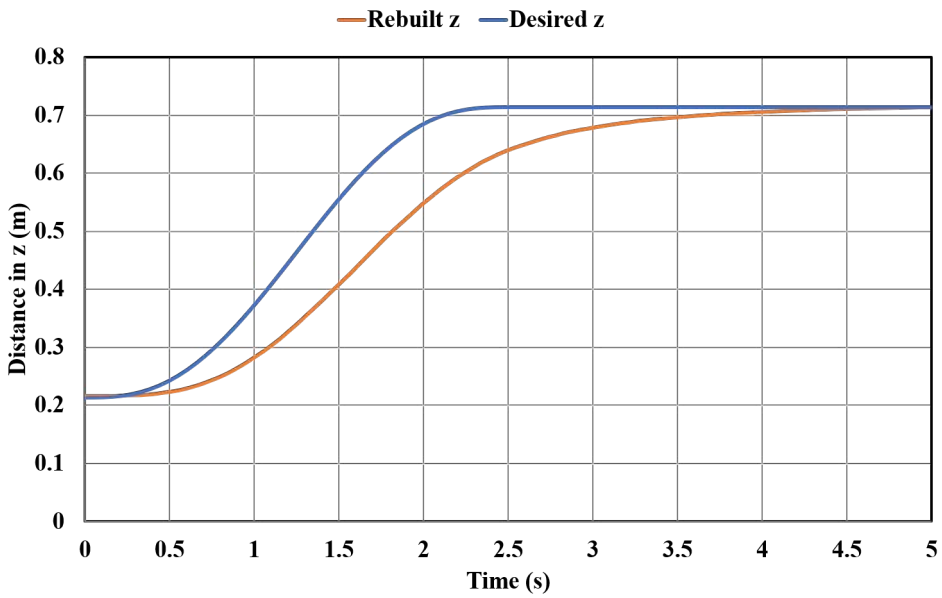

Figure 5.13: Comparison between the desired value of z and the rebuilt value of z from the motor position for a desired velocity of 0.2 m/s for the MP

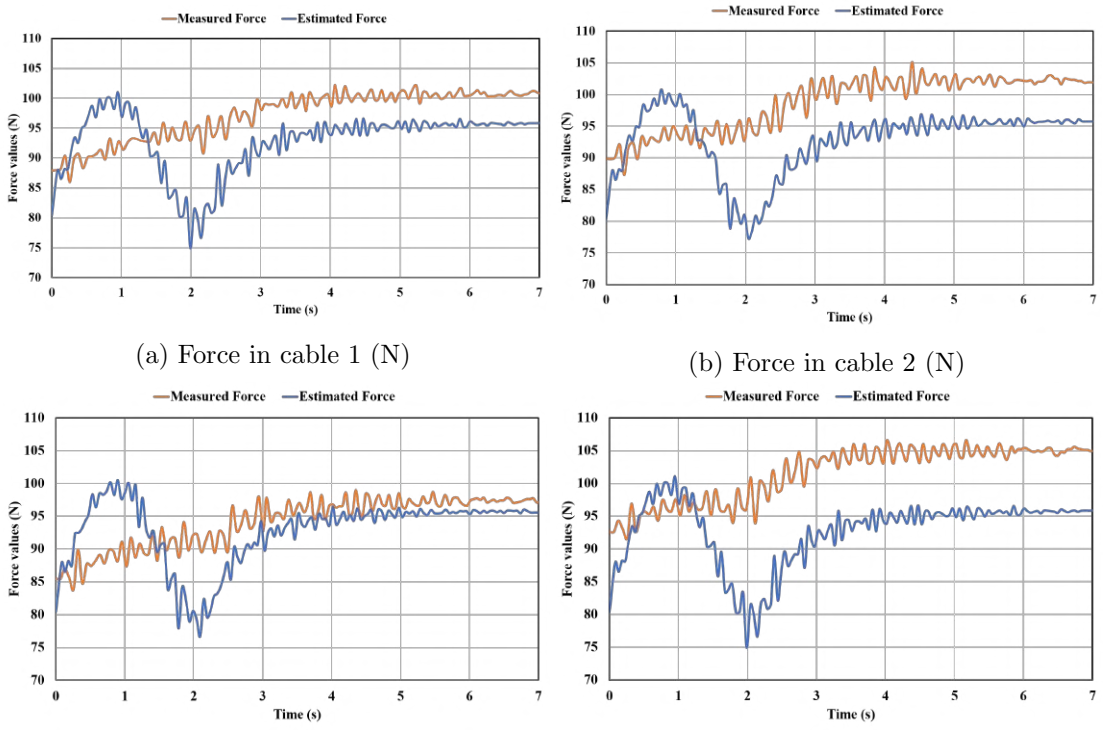

(a) Force in cable 1 (N)

(b) Force in cable 2 (N)

(c) Force in cable 3 (N)

(d) Force in cable 4 (N)

Figure 5.14: Comparison of the estimated and measured cable forces for moving the CDPR from home position to a distance of 0.5 m with a desired velocity of 0.2 m/s.

case where the desired velocity was 0.1 m/s. The values of the estimated forces reduce as the time to reach the desired value approaches. The control law then makes the necessary correction to make the values move the MP to the desired position.

The comparison between the estimated value of z and the measured value of z for the three test conditions performed is shown in table 5.5 to observe the behavior of the platform for the different speeds considered. It is seen from table

Table 5.5: Comparison between estimated value of z and measured value of z

Test	Measured (m)	Estimated (m)	Difference	% error
Test 1: 0.05 m/s	0.497	0.500904	0.0046	0.78 %
Test 2: 0.1 m/s	0.497	0.501828	0.00482	0.9 %
Test 3: 0.2 m/s	0.498	0.502023	0.00402	0.8 %

5.5 that the performance of the CDPR is satisfactory. The moving platform is able to reach the desired position without much loss. The repeatability of the robot (as shown for test case 1, table 5.2) is also good for the CDPR.

5.3.2 Movement from the home position to a distance of $0.5m$ and returning to the home position

The second set of experiments defines a motion for the CDPR where the MP is made to move to a distance of 0.5 m from the initial home position and then returns to the home position. Three tests are done as shown in previous subsection with three different velocities namely 0.05 m/s, 0.1 m/s and 0.2 m/s.

Case 1: Movement with a desired speed of $0.05m/s$

The desired velocity for this case is fixed at 0.05 m/s. The total distance to be traveled is 1 m resulting in a total experiment time of 20 s. To consider the time delay in the interface, a rest time is added in the test after reaching the first point (in this case, 0.5 m). The rest time has been changed for each test according to the time taken by the MP to reach the first position. For the first test condition, the rest time was fixed at 2.5 s.The total run time for this condition is 22.5 s. The plot showing the comparison between the desired value of z and the rebuilt value of z from the motor position is shown in Fig. 5.15.

It is seen from Fig. 5.15 that the MP was able to do the necessary translation and return to the home position. It is observed that the rest time given after reaching the first position helps the MP to handle the time delay and also for the controller to correct the position. During the return phase, the MP reaches a final position close to the home position. In other words, there is a difference between the final returned position and the home position.

The plot demonstrating the comparison between the estimated and measured cable forces for the test is shown in Fig. 5.16.

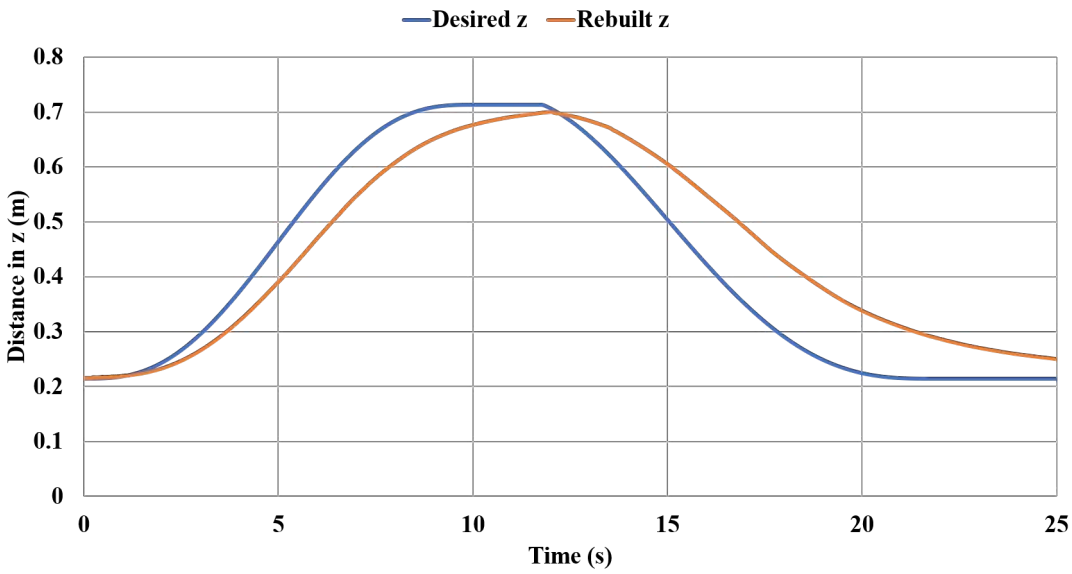

Figure 5.15: Comparison between the desired value of z and the rebuilt value of z from the motor position for a desired velocity of 0.05 m/s for the up and down movement of the MP

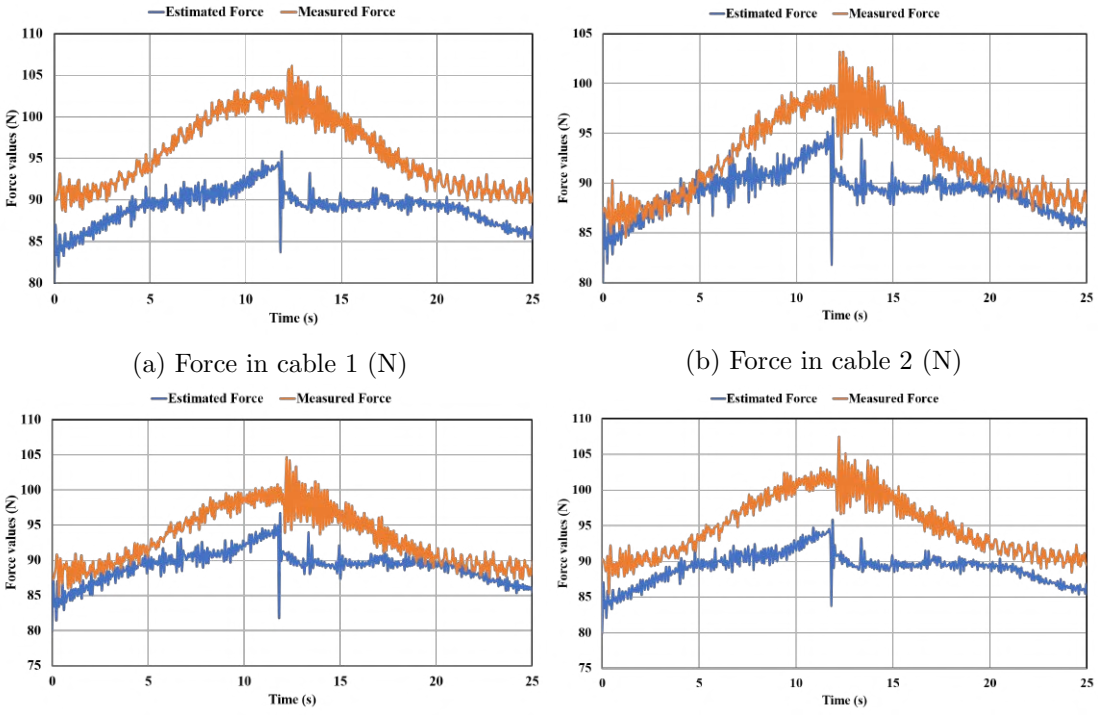

(a) Force in cable 1 (N)

(b) Force in cable 2 (N)

(c) Force in cable 3 (N)

(d) Force in cable 4 (N)

Figure 5.16: Comparison of the estimated and measured cable forces for moving the CDPR from home position to a distance of 0.5 m and returning back to the home position with a desired velocity of 0.05 m/s.

As seen in Fig. 5.16, the profile of the estimated and measured force values are almost similar. However, when the return motion of the MP commences, there is a sudden change in the values of the estimated cable forces (magnitude of force being

within 15 N), which causes strong oscillations in the measured cable forces. This behavior could be due to the nonlinear solver used by the program in calculating the cable length from the motor positions. This is augmented by the presence of the time delay in the interface program. The mismatch in the timing can trigger the return motion of the platform before it reaches its first desired position. This can generate abrupt changes in the force values, which can cause oscillations in the cables and MP.

The values obtained in the plots are compared with the measured values using the handheld measuring device to check the error between real value and estimated values.
Estimated value of z (distance) during the upward motion = 0.485014
Measured value of z (distance) during the upward motion = 0.479
Estimated value of z (distance) during the return motion = 0.461647
Measured value of z (distance) during the return motion = 0.464
Total estimated distance (m)= 0.9466
Total measured distance (m)= 0.943

From these values, it can be seen that the robot can achieve the desired translation with an error of around 5%.

Case 2: Movement with a desired speed of $0.1m/s$

The desired velocity for this case is fixed at $0.1m/s$ while the total experiment time is $10s$. In order to take into account the issue of timing, a rest time of 0.8 was added for the trajectory after reaching the first position. The plot comparing the desired value of z and the rebuilt value of z from the motor position is shown in Fig. 5.17. It is seen from Fig. 5.17 that the MP is able to reach the first position and was able to return to the home position in a time of almost 14 s.

The comparison of the estimated and measured cable forces for the test is shown in Fig. 5.18. As seen in Fig. 5.18, the profile of the cable forces is not smooth for this motion. The sudden change in the magnitude of cable forces still exists, but it is not as much as the values observed in the condition with velocity 0.1 m/s. Also, the offset between the estimated cable forces and the measured cable forces is seen in other cases. Another significant observation is that once the MP reaches close to the home position, there are oscillations in the values of the estimated cable forces. These oscillations are produced due to the correction of the control law and the difference between the desired value of z and the rebuilt value of z from the motor positions. The effect of these oscillations on the platform position is, however, found to be trivial.

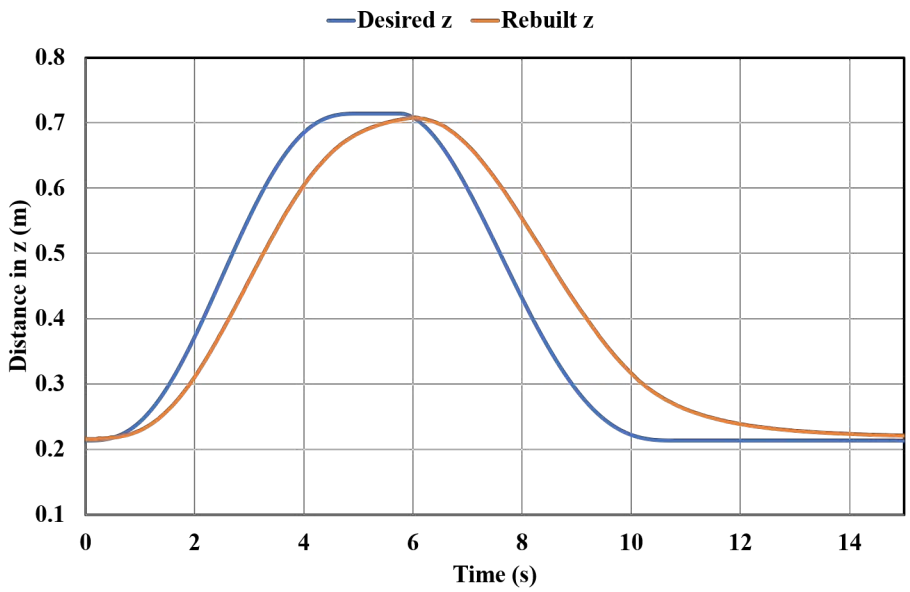

Figure 5.17: Comparison between the desired value of z and the rebuilt value of z from the motor position for a desired velocity of $0.1m/s$ for the up and down movement of the MP

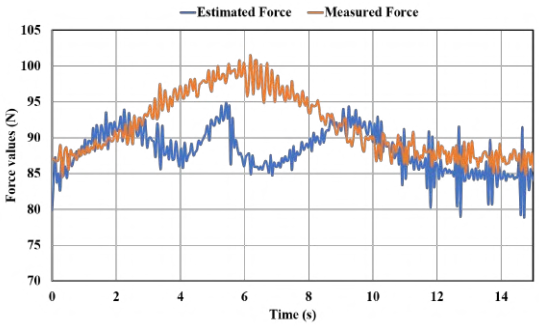

(a) Force in cable 1 (N)

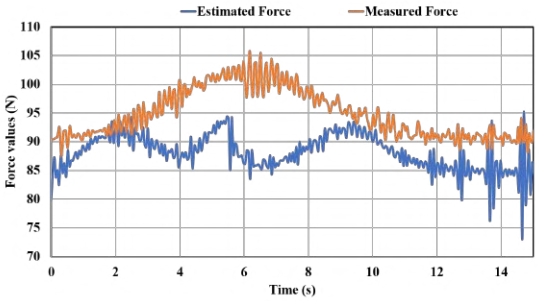

(b) Force in cable 2 (N)

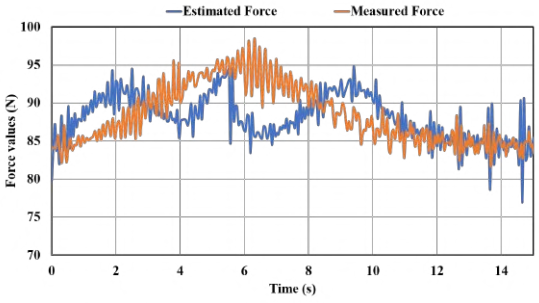

(c) Force in cable 3 (N)

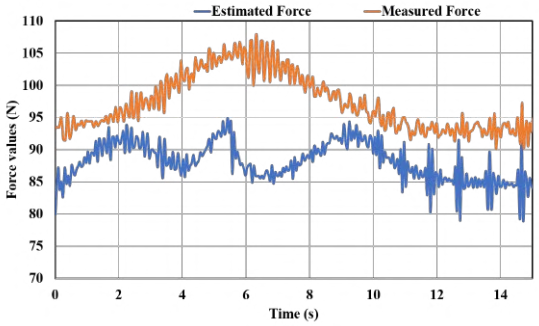

(d) Force in cable 4 (N)

Figure 5.18: Comparison of the estimated and measured cable forces for moving the CDPR from home position to a distance of $0.5m$ and returning back to the home position with a desired velocity of 0.1 m/s.

To check the difference between real values and the estimated values, a comparison is made as:
Estimated value of z (distance) during the upward motion = 0.492679
Measured value of z (distance) during the upward motion = 0.489
Estimated value of z (distance) during the return motion = 0.48849
Measured value of z (distance) during the return motion = 0.485
Total estimated distance (m)= 0.98117
Total measured distance (m)= 0.974

From these values, it can be seen that the robot can achieve the desired translation with an error of around 2.5%.

Case 3: Movement with a desired speed of $0.2m/s$

The desired velocity for this case is fixed at 0.2 m/s. The total experiment time for completing the motion of 1 m is 5 s. To observe the system behavior in the absence of rest time at the first position, this test was performed for a total time of 5 s for the translation. The values are recorded for a time of 10 s to observe the behavior of the MP and the cables forces.

The plot comparing the desired value of z and the rebuilt value of z from the motor position in Fig. 5.19. As seen in Fig. 5.19, the MP does not reach the first position completely. The platform also takes a bit longer than the other tests to reach the home position (approx. 4.8 s).

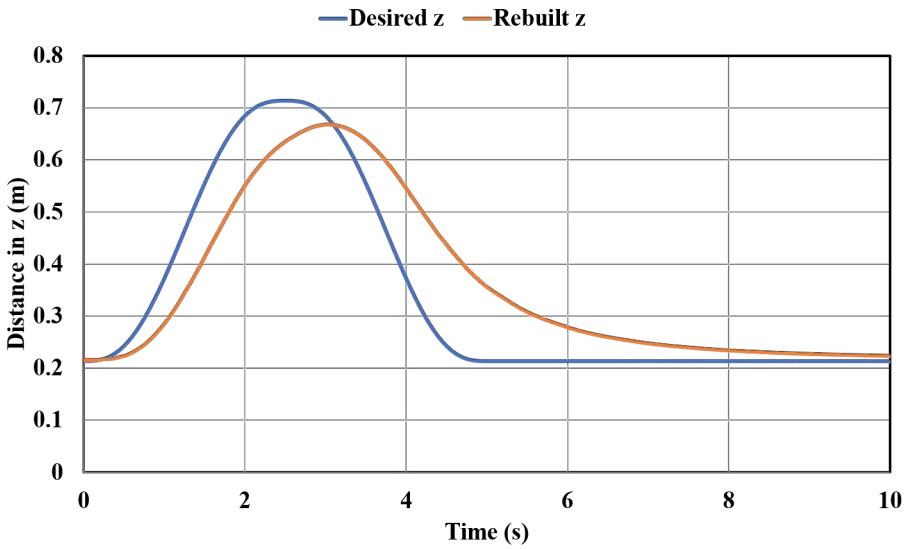

Figure 5.19: Comparison between the desired value of z and the rebuilt value of z from the motor position for a desired velocity of 0.2 m/s for the up and down movement of the MP

The comparison of the estimated and measured cable forces for the test is shown in Fig. 5.20. From Fig. 5.20, it is seen that force profile is very much

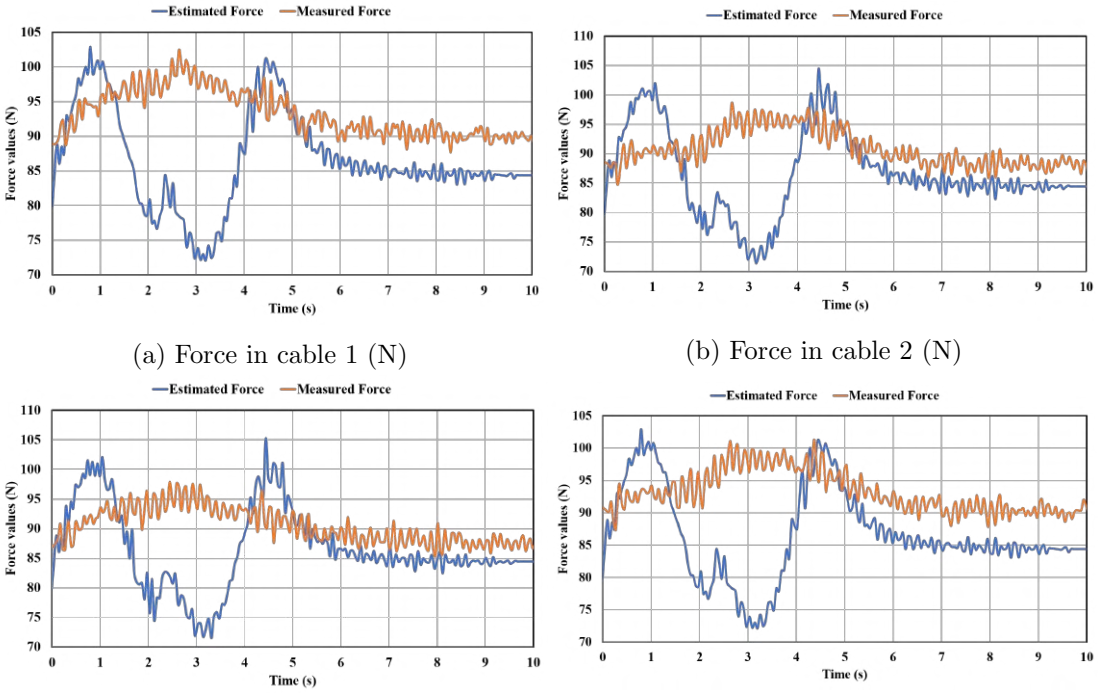

(a) Force in cable 1 (N)

(b) Force in cable 2 (N)

(c) Force in cable 3 (N)

(d) Force in cable 4 (N)

Figure 5.20: Comparison of the estimated and measured cable forces for moving the CDPR from home position to a distance of 0.5 m and returning back to the home position with a desired velocity of 0.2 m/s.

different than the other two tests results shown in Fig. 5.18 and 5.16 due to the speed set for the test. It is also seen that oscillations in the estimated cable forces during the upward motion are different from the oscillations during the return motion. It is also seen that the values of the estimated forces and measured forces are closer than the values of the forces for other tests.

The comparison between the measured values and the estimated values is given as:

Estimated value of z (distance) during the upward motion = 0.452452
Measured value of z (distance) during the upward motion = 0.458
Estimated value of z (distance) during the return motion = 0.445059
Measured value of z (distance) during the return motion = 0.455
Total estimated distance (m)= 0.8975
Total measured distance (m)= 0.913

From these values, it is observed that the robot can achieve the desired translation with an error of around 10%. From the three tests presented in this subsection for the up and down motion of the platform, it is evident that the choice of rest time and desired velocity plays an important role in cable force oscillations. When

the movement was done with a rest time after the first position, predominant oscillations are seen in the cable forces, which are not desirable for the CDPR as it can lead to complications depending on the location of the CDPR. The suitable choice for such conditions could be not to use any rest time and make the interface work faster to reduce the time delay in implementing the control even though it is minor.

5.4 Inferences and Discussion

This section presents the general inferences from the tests performed. An effort is also made to highlight how the obtained results can be improved for efficient working.

Two sets of experiments were conducted to validate the classical IOFL technique to control the four cable robot. Based on the results presented in section 5.3, some inferences are made as given below:

1) The MP can achieve the desired motion with the pole values used and reach the desired position with low error. It is indeed possible to improve the result further by tuning the values and testing it on the MP.

2) The three values of the desired velocities (0.05 m/s, 0.1 m/s, 0.2 m/s) results in three different profiles for the cable forces, but are able to satisfy the necessary behavior for the MP. These values should be adjusted according to the distance to be moved to obtain a smooth cable force profile.

3) There is an offset in the estimated values and measured values of the forces in all the tests. This is because the measurement of forces is done independently of the program used to control the robot. This results in some mismatch of the timing the readings are measured.

4) The starting values of cable forces are not always the same for each test. There is always an offset between the estimated values of the forces and the measured force values. This can be due to several reasons, some of which are discussed here.

As mentioned in section 5.2, a pretension is given to the CDPR when the robot is powered on but is at the ground. This pretension guarantees that the cables are in tension before moving to the home position but does not guarantee equal tensions in the cables. This is because when the motors are switched off, the

motor positions are not saved, and the tension in the cables is no more available. Once the motors are switched on and the positions are noted, it is not always guaranteed that the starting position of each motor remains the same. This will result in uneven cable forces among the cables. The pretension measured in the sensors also depends on how tight the cables are wound around the winches. There might be cases when the cable around the one winch might not be as tightly wound as the cable in another winch. Since the same amount of pretension current is sent to each motor, the slackness of the cable around the winch can result in different cable tension for different cables.

Another possible reason for this difference could be the error in positioning of the CDPR. The measurements to obtain the center of the room are done manually. The measurement errors might result in the robot being placed at a different place than the actual center of the room. A possible solution for this could be to make the cable forces almost equal after reaching the home position by using the interface given by the supplier to view the cable forces. However, repeating this each time might be tiresome.

5) There are some high oscillations in each cable during the start of the trajectory (for eg. Fig. 5.9 and 5.12). However, the oscillations (during the starting) are not seen when the movement is done with a velocity of 0.2 m/s (for eg. Fig. 5.14). One possible reasons for this could be the relationship between the sampling time or step time used (55 ms) for each control loop and the desired velocity needed. When the velocity value is less, the system has a larger settling time at each time step, resulting in oscillations that do not significantly affect the actual position of the moving platform but are seen profoundly in the form of cable forces. A possible solution is to improve the timing for the execution of control such that the system can receive the next position without delay and thus reducing the initial oscillations.

Another possible reason for the spike in oscillations could be due to the oscillations already present in the cables when they reach the home position from the ground level, as shown in Fig. 5.21.

As mentioned previously, a pretension is given to the system before bringing it to the home position. Due to the underactuated nature of the CDPR, the MP oscillates after reaching the home position. During the testing, care was taken to give sufficient time for the MP oscillations to reduce. These oscillations might add to the initial jerk occurring in the MP due to the settling time issue. This can magnify the oscillations resulting in some peaks during the start of the trajectory.

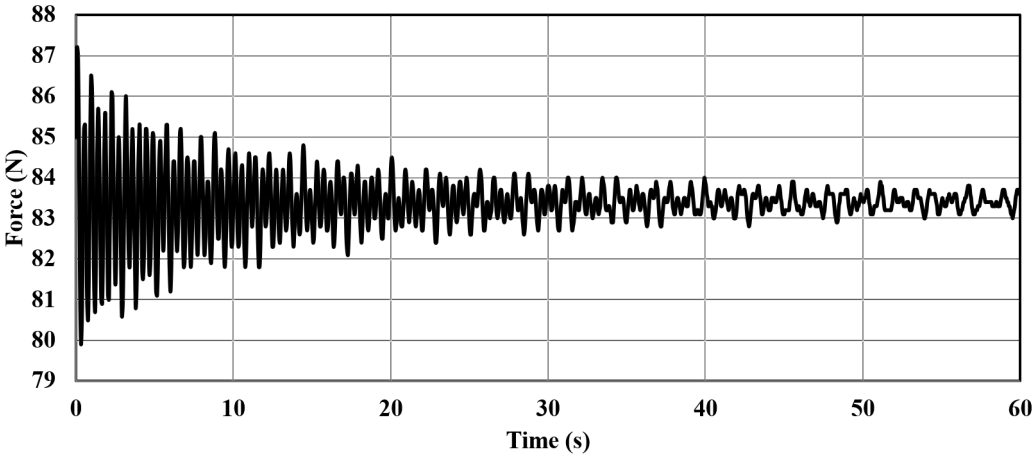

Figure 5.21: Oscillations in cable 1 force when it reaches the home position

6) As highlighted earlier, several simplifications have been done with the experimental setup to validate the control law. The first simplification being the case where only a translation along the $z - axis$ where the MP orientation angles are zero is considered. The other simplifications are mentioned here to be modified to make the CDPR more robust. The dynamic model used in the control law does not take into account the cable stiffness and the cable mass. Since the mass of the MP is considerably higher than the mass of the cables on the winches, the cable mass does not play a big role in the platform dynamics. The role of cable stiffness is significant, as seen in the oscillations seen in the cable forces. The MP is bound to oscillate due to the number of cables being four; however, including the cable stiffness and the MP stiffness as a whole in the dynamic model can result in a better behavior of the cable forces. The inertia of the MP is calculated according to the model of the robot developed using the SOLIDWORKS platform, where the electric cables and the wires are not considered. A more methodical calculation of the MP inertia could improve the mechanical parameter values entered in the program.

7) The CDPR in its current state does not have any additional sensor to measure the platform pose and orientation. This restricts the experiments that can be performed on the prototype for real-time feedback to translation along $z - axis$ only. The addition of sensors to measure the position and orientation can help make the CDPR move to different locations and perform more complex trajectories.

5.5 Summary

This chapter presented the experimental results of the tests performed to validate the classical input-output feedback linearization control technique formulated for the underactuated four cable-driven parallel robot. The prototype of the CDPR fabricated during the course of the work was shown, and the important hardware features were introduced. The experimental setup and the steps followed for implementing the control were shown with the help of a block diagram. The experimental results obtained for the different cases showed that the control law designed works satisfactorily on the CDPR and gives acceptable results. The important inferences from the results obtained and the possible challenges and solutions to further improve the working of the CDPR to make it more robust are suggested.

Chapter 6

Conclusion and Future Work

Contents

This chapter presents the general conclusions inferred from the research done during this thesis. Following this, the next steps for future work are discussed to improve the overall aspect of the prototype.

6.1 General conclusions

Underactuated CDPRs have recently attracted much interest from the research community as the reduced number of actuators makes them more profitable. However, the additional theoretical challenges in kinematics, workspace, and control are usually underestimated when starting projects on such prototypes. There is also a need for a reliable controller and design methods of under-constrained cable robots.

The research presented in this thesis is mainly related to the design and control of an underactuated cable-driven parallel robot with four cables. The CDPR prototype fabricated in this thesis is different from the other designs in the fact that the actuating motors along with the winches are placed on the moving platform. The cables are attached to the fixed structure using simple anchor points. This design presented interesting research challenges in terms of mechanical design and control points of view. A summary of the important conclusions from the various aspects of the research is presented hereby.

1) The design of a CDPR requires the computation and analysis of the CDPR capability, including the size and shape of its workspace. The static equilibrium workspace of the CDPR was calculated in **Chapter III** by defining the acceptable limits of cable tension and platform orientation angles. It was essential to get an overview of the possible values of platform orientation angles due to the under-constrained nature of the design. Several case studies were presented to highlight the change in the workspace size and shape due to the changes in the platform and fixed structure dimensions. The dynamic model of the CDPR was formulated using the classical approach where the cable mass and elasticity were ignored.

2) The formulation of the IOFL control law was presented in **Chapter IV**. This control law is one of the most widely used approaches for nonlinear systems. The behavior of uncontrolled internal dynamics was presented using phase-plane plots, and the role of platform dimensions in reducing the oscillatory nature of the internal dynamics was highlighted using simulation studies. However, it was not easy to establish a mathematical relationship between the dimensions and the internal dynamics behavior due to the complexity of the equations. As a control solution, a modified feedback linearization method was also proposed, which showed significant improvement in the performance of the CDPR behavior with the initial dimensions considered. This law was able to reduce the effect of internal dynamics, which in turn helped in eliminating the oscillations in the cable forces. Several case studies were done by varying the simulation conditions to demonstrate the stability of the proposed modified control law. The application of this modified control law on other CDPR configurations needs to be verified so that a mathematical stability criterion can be developed accordingly.

3) The experimental validation of the IOFL was presented in **Chapter V**. The experimental set-up and the simplifications to perform the tests were explained. The point-to-point motion of the CDPR is made only along the $z - axis$ at the center of the room. This was done to validate the control by making use of only the motor positions and velocities. Two different sets of experiments were done with different desired velocities for the moving platform (0.05 m/s, 0.1 m/s, 0.2 m/s) to raise the moving platform to a distance of 0.5 m from the defined *home* position. The control of motors was done using the interpolated position mode offered by the EPOS2 controller. The values of the distance moved by the moving platform along $z - axis$ rebuilt using the motor positions were compared with the desired values of z. The estimated force values and the measured cable forces

were also compared to analyze the final results obtained. The CDPR was able to perform the point-to-point motion along the desired trajectory. However, the forces in the cables were oscillating throughout the motion. These forces did not adversely affect the movement of the moving platform.

6.2 Perspectives

This manuscript focuses on the design and control of an underactuated cable-driven parallel robot with four cables. The standard static equilibrium conditions and the classical dynamic modeling equation of the CDPR have been used to analyze the workspace and dynamic behavior. Following this, a prototype has been fabricated, and control laws have been formulated to control and stabilize the behavior of the CDPR. Based on the previous discussions and developments, summarised in Sec. 6.1, some perspectives for future work are proposed hereafter.

6.2.1 Modeling

A simple linear model of the cable has been used for the geometric and dynamic modeling of the CDPR. This simple model should be replaced by elastostatic [Gag16] and elastodynamic cable models [Bak+19] which take into account the elasticity of the cables. The use of such cable models can help to analyze the displacement of the moving platform due to the non-rigid nature of the cables or the compliance of the moving platform.

The mass of the cables is negligible due to the mass of the moving platform and the dimensions of the experimental set-up. However, if the prototype is scaled to a bigger set-up, the mass of the cables and the sagging will play a significant role. Hence the formulation of the sagging cable model should be done for the CDPR to uniquely define the quasi-static model and analyze its behavior. The stiffness matrix (active and passive) should be formulated and used in the dynamic model to account for the possible errors that can occur due to the cable length.

6.2.2 Control of CDPR

The validation of the IOFL control is done by testing the MP movement along the $z - axis$ without the addition of any sensors. The use of sensors to measure the platform orientation angles (α and β) should be done to investigate further the behavior of the CDPR at different locations of the working environment. This will

help in understanding the performance of such underactuated CDPRs and result in increasing the working zone of the robot.

The control of CDPR is done using the interpolated position mode of the electronic controller. A control strategy should be developed to perform force control on the CDPR. This will include the formulation of the relationship between the cable forces and motor current. Several tests should be done to estimate a reliable relationship to demonstrate the performance regarding control accuracy, stability, and positional accuracy. Using this approach will eliminate the need for the nonlinear solver currently in place to calculate the motor positions and velocity for the IPM mode. The study of platform oscillations using current control can be interesting depending on the accuracy of the mathematical model formulated.

The use of other control laws to study the behavior of the CDPR should be done to compare the results with the classical IOFL technique. Control combining different laws is being used increasingly on underactuated systems. Possible use of some combined control laws and validating them on the CDPR can lead to interesting outcomes. The preliminary focus of the new control laws should be on the possibility of reducing the oscillations of the moving platform during the point-to-point trajectories. The experimental validation of the proposed modified feedback linearization should also be done to check if it can be applied in general on an underactuated CDPR. The mathematical stability conditions should be formulated for this approach, and more case studies should be done to strengthen the understanding of the approach further.

6.2.3 Integration with Haptic Device

The overall final objective of the project is to make the CDPR collaborative by allowing the industry worker to interact with the robot for handling the industrial product. The first step in this direction has been completed in this thesis in the form of the prototype in which the position of the moving platform can be controlled using the control law formulated. The next step is to integrate the haptic device (already designed by another researcher as a part of master thesis work) with the CDPR. This will need the formulation of a robust control which will work along with the manual effort of the worker with the haptic device in achieving the desired movement.

6.2.4 Safety measures

The final step to make the CDPR a fully functional collaborative robot should include the necessary strategy to be implemented in case of a cable failure to ensure the safety of the worker and also to prevent damage to the robot. A standard set of safety protocols could be developed for collaborative cable-driven robots installed in a manufacturing line in the future.

Bibliography

[AA02a] AB Alp and Sunil K Agrawal. "Cable suspended robots: Feedback controllers with positive inputs". In: *Proceedings of the 2002 American Control Conference (IEEE Cat. No. CH37301)*. Vol. 1. IEEE. 2002, pp. 815–820.

[AA02b] Jorge Angeles and J Angeles. *Fundamentals of robotic mechanical systems*. Vol. 2. Springer, 2002.

[Abb] *IRB 360 - Industrial Robots (Robotics) - Industrial Robots From ABB Robotics*. https://new.abb.com/products/robotics/industrial-robots/irb-360.

[ABD93] James Albus, Roger Bostelman, and Nicholas Dagalakis. "The NIST Robocrane". In: *Journal of robotic systems* 10.5 (1993), pp. 709–724.

[AY17] Hamed Jabbari Asl and Jungwon Yoon. "Robust trajectory tracking control of cable-driven parallel robots". In: *Nonlinear Dynamics* 89.4 (2017), pp. 2769–2784.

[Bak+19] Sana Baklouti et al. "Vibration reduction of Cable-Driven Parallel Robots through elasto-dynamic model-based control". In: *Mechanism and Machine Theory* 139 (2019), pp. 329–345.

[Bar+17] Luca Barbazza et al. "Design and optimal control of an underactuated cable-driven micro–macro robot". In: *IEEE Robotics and Automation Letters* 2.2 (2017), pp. 896–903.

[BCC19] Sana Baklouti, Stéphane Caro, and Eric Courteille. "Elasto-dynamic model-based control of non-redundant cable-driven parallel robots". In: *ROMANSY 22–Robot Design, Dynamics and Control*. Springer, 2019, pp. 238–246.

[BFV16] Nicole Barry, Erin Fisher, and Joshua Vaughan. “Modeling and control of a cable-suspended robot for inspection of vertical structures”. In: *Journal of Physics: Conference Series*. Vol. 744. 1. IOP Publishing. 2016, p. 012071.

[BG15] Eric Barnett and Clément Gosselin. “Large-scale 3D printing with a cable-suspended robot”. In: *Additive Manufacturing* 7 (2015), pp. 27–44.

[BK06] Saeed Behzadipour and Amir Khajepour. “Cable-based robot manipulators with translational degrees of freedom”. In: *Industrial Robotics: Theory, Modelling and Control*. IntechOpen, 2006.

[BKA19] Javad Bolboli, Mohammad A Khosravi, and Farzaneh Abdollahi. “Stiffness feasible workspace of cable-driven parallel robots with application to optimal design of a planar cable robot”. In: *Robotics and Autonomous Systems* 114 (2019), pp. 19–28.

[BKT15] Reza Babaghasabha, Mohammad A Khosravi, and Hamid D Taghirad. “Adaptive robust control of fully-constrained cable driven parallel robots”. In: *Mechatronics* 25 (2015), pp. 27–36.

[BKT16] Reza Babaghasabha, Mohammad A Khosravi, and Hamid D Taghirad. “Adaptive robust control of fully constrained cable robots: singular perturbation approach”. In: *Nonlinear Dynamics* 85.1 (2016), pp. 607–620.

[Bos+07] Paul Bosscher et al. “Cable-suspended robotic contour crafting system”. In: *Automation in construction* 17.1 (2007), pp. 45–55.

[Bru+12] Tobias Bruckmann et al. “Development of a storage retrieval machine for high racks using a wire robot”. In: *ASME 2012 International Design Engineering Technical Conferences and Computers and Information in Engineering Conference*. American Society of Mechanical Engineers Digital Collection. 2012, pp. 771–780.

[Bru+13] Tobias Bruckmann et al. “Design and realization of a high rack storage and retrieval machine based on wire robot technology”. In: *DINAME* (2013).

[BS05] Samir Bouabdallah and Roland Siegwart. “Backstepping and sliding-mode techniques applied to an indoor micro quadrotor”. In: *Proceedings of the 2005 IEEE international conference on robotics and automation*. IEEE. 2005, pp. 2247–2252.

[CA09] Daniel Cunningham and H Harry Asada. "The winch-bot: A cable-suspended, under-actuated robot utilizing parametric self-excitation". In: *2009 IEEE International Conference on Robotics and Automation*. IEEE. 2009, pp. 1844–1850.

[Cao+11] Yi Cao et al. "Accurate numerical methods for computing 2d and 3d robot workspace". In: *International Journal of Advanced Robotic Systems* 8.6 (2011), p. 76.

[Cho96] W Choe. "A Design of Parallel Wire Driven Robots for Ultrahigh Speed Motion Based on Stiffiness Analysis". In: *Proc. of the Japan-USA Symposium on Flexible Automation*. 1996, pp. 159–166.

[CLP18] Jorge Ivan Ayala Cuevas, Édouard Laroche, and Olivier Piccin. "Assumed-mode-based dynamic model for cable robots with non-straight cables". In: *Cable-Driven Parallel Robots*. Springer, 2018, pp. 15–25.

[CN12] David W Crawford and Edward A Nemeth. *Amusement park ride with cable-suspended vehicles*. US Patent 8,147,344. 2012.

[Con85] Lawrence L Cone. "Skycam-an aerial robotic camera system". In: *Byte* 10.10 (1985), p. 122.

[COR14] Gianni Castelli, Erika Ottaviano, and Pierluigi Rea. "A Cartesian Cable-Suspended Robot for improving end-users' mobility in an urban environment". In: *Robotics and Computer-Integrated Manufacturing* 30.3 (2014), pp. 335–343.

[CSS14] A Capua, A Shapiro, and S Shoval. "SpiderBot: a cable-suspended walking robot". In: *Mechanism and Machine Theory* 82 (2014), pp. 56–70.

[Cui+13] Xiang Cui et al. "Closed-loop control for a cable-driven parallel manipulator with joint angle feedback". In: *2013 IEEE/ASME International Conference on Advanced Intelligent Mechatronics*. IEEE. 2013, pp. 625–630.

[DD14] QJ Duan and Xuechao Duan. "Workspace classification and quantification calculations of cable-driven parallel robots". In: *Advances in Mechanical Engineering* 6 (2014), p. 358727.

[DPL07] Lionel Dominjon, Jérôme Perret, and Anatole Lécuyer. "Novel devices and interaction techniques for human-scale haptics". In: *The Visual Computer* 23.4 (2007), pp. 257–266.

[EGGC15] Gamal El-Ghazaly, Marc Gouttefarde, and Vincent Creuze. “Hybrid cable-thruster actuated underwater vehicle-manipulator systems: A study on force capabilities”. In: *2015 IEEE/RSJ International Conference on Intelligent Robots and Systems (IROS)*. IEEE. 2015, pp. 1672–1678.

[Gag+15] Lorenzo Gagliardini et al. “A reconfigurable cable-driven parallel robot for sandblasting and painting of large structures”. In: *Cable-Driven Parallel Robots*. Springer, 2015, pp. 275–291.

[Gag16] Lorenzo Gagliardini. “Discrete reconfigurations of cable-driven parallel robots”. PhD thesis. 2016.

[GAT08] Pooneh Gholami, Mohammad M Aref, and Hamid D Taghirad. “On the control of the KNTU CDRPM: A cable driven redundant parallel manipulator”. In: *2008 IEEE/RSJ International Conference on Intelligent Robots and Systems*. IEEE. 2008, pp. 2404–2409.

[HDT+19] Mohammad Reza Jafari Harandi, Hamed Damirchi, Hamid Dokht Taghirad, et al. “Point-to-Point Motion Control of an Underactuated Planar Cable Driven Robot”. In: *2019 27th Iranian Conference on Electrical Engineering (ICEE)*. IEEE. 2019, pp. 979–984.

[Hig88] T. Higuchi. “Application of Multi-Dimensional Wire Crane in Construction”. In: *Proc. 5th Int. Symp. on Robotics in Construction*. Vol. 661. 1988.

[Ho+15] Wei Yang Ho et al. “Haptic interaction with a cable-driven parallel robot using admittance control”. In: *Cable-Driven Parallel Robots*. Springer, 2015, pp. 201–212.

[HW06] Thomas Heyden and Christoph Woernle. “Dynamics and flatness-based control of a kinematically undetermined cable suspension manipulator”. In: *Multibody System Dynamics* 16.2 (2006), p. 155.

[Hwa+16a] Sung Wook Hwang et al. “Trajectory generation to suppress oscillations in under-constrained cable-driven parallel robots”. In: *Journal of Mechanical Science and Technology* 30.12 (2016), pp. 5689–5697.

[Hwa+16b] Sung Wook Hwang et al. “Trajectory generation to suppress oscillations in under-constrained cable-driven parallel robots”. In: *Journal of Mechanical Science and Technology* 30.12 (2016), pp. 5689–5697.

[IBC19] Edoardo Idà, Tobias Bruckmann, and Marco Carricato. "Rest-to-Rest Trajectory Planning for Underactuated Cable-Driven Parallel Robots". In: *IEEE Transactions on Robotics* 35.6 (2019), pp. 1338–1351.

[Idá+18] Edoardo Idá et al. "Rest-to-rest trajectory planning for planar underactuated cable-driven parallel robots". In: *Cable-Driven Parallel Robots*. Springer, 2018, pp. 207–218.

[IS94] Masahiro Ishii and Makoto Sato. "A 3D spatial interface device using tensed strings". In: *Presence: Teleoperators & Virtual Environments* 3.1 (1994), pp. 81–86.

[Isi13a] Alberto Isidori. *Nonlinear control systems*. Springer Science & Business Media, 2013.

[Isi13b] Alberto Isidori. "The zero dynamics of a nonlinear system: From the origin to the latest progresses of a long successful story". In: *European Journal of Control* 19.5 (2013), pp. 369–378.

[Iza+13] Jean-Baptiste Izard et al. "Integration of a parallel cable-driven robot on an existing building façade". In: *Cable-driven parallel robots*. Springer, 2013, pp. 149–164.

[Kaw+97] Sadao Kawamura et al. "Development of an ultrahigh speed robot FALCON using parallel wire drive systems". In: *Journal of the Robotics Society of Japan* 15.1 (1997), pp. 82–89.

[KD04] Wisama Khalil and Etienne Dombre. *Modeling, identification and control of robots*. Butterworth-Heinemann, 2004.

[KI93] Sadao Kawamura and Ken Ito. "A new type of master robot for teleoperation using a radial wire drive system". In: *Proceedings of 1993 IEEE/RSJ International Conference on Intelligent Robots and Systems (IROS'93)*. Vol. 1. IEEE. 1993, pp. 55–60.

[Kin+07] Hithoshi Kino et al. "Robust PD control using adaptive compensation for completely restrained parallel-wire driven robots: Translational systems using the minimum number of wires under zero-gravity condition". In: *IEEE Transactions on Robotics* 23.4 (2007), pp. 803–812.

[KKW00] Sadao Kawamura, Hitoshi Kino, and Choe Won. "High-speed manipulation by using parallel wire-driven robots". In: *Robotica* 18.1 (2000), pp. 13–21.

[KT11] Mohammad A Khosravi and Hamid D Taghirad. "Dynamic analysis and control of cable driven robots with elastic cables". In: *Transactions of the Canadian Society for Mechanical Engineering* 35.4 (2011), pp. 543–557.

[KT13] Mohammad A Khosravi and Hamid D Taghirad. "Experimental performance of robust PID controller on a planar cable robot". In: *Cable-Driven Parallel Robots*. Springer, 2013, pp. 337–352.

[KT14] Mohammad A Khosravi and Hamid D Taghirad. "Dynamic modeling and control of parallel robots with elastic cables: singular perturbation approach". In: *IEEE Transactions on Robotics* 30.3 (2014), pp. 694–704.

[KT15] Mohammad A Khosravi and Hamid D Taghirad. "Dynamic analysis and control of fully-constrained cable robots with elastic cables: variable stiffness formulation". In: *Cable-Driven Parallel Robots*. Springer, 2015, pp. 161–177.

[KT16] MA Khosravi and Hamid D Taghirad. "Stability analysis and robust PID control of cable driven robots considering elasticity in cables". In: *AUT Journal of Electrical Engineering* 48.2 (2016), pp. 113–126.

[KTH17] SA Khalilpour, HD Taghirad, and Hossein Habibi. "Wave-based control of suspended cable driven parallel manipulators". In: *2017 5th International Conference on Control, Instrumentation, and Automation (ICCIA)*. IEEE. 2017, pp. 173–178.

[Kuk] *Industrial robot*. https://www.kuka.com/en-de/products/robot-systems/industrial-robots.

[Kum+19] Atal Anil Kumar et al. "Workspace Analysis of a 4 Cable-Driven Spatial Parallel Robot". In: *ROMANSY 22–Robot Design, Dynamics and Control*. Springer, 2019, pp. 204–212.

[Lan85] Samuel Ernest Landsberger. "A New Design for Parallel Link Manipulators". In: *Proc. of the IEEE International Conference on Systems*. 1985, pp. 812–814.

[Léc+13] Vincent Léchappé et al. "Partial linearization of the PVTOL aircraft with internal stability". In: *52nd IEEE conference on decision and control*. IEEE. 2013, pp. 2564–2569.

[LG13] Johann Lamaury and Marc Gouttefarde. “Control of a large redundantly actuated cable-suspended parallel robot”. In: *2013 IEEE International Conference on Robotics and Automation*. IEEE. 2013, pp. 4659–4664.

[Li+09] Bing Li et al. “Vibration suppression of a 3-PRR flexible parallel manipulator using input shaping”. In: *2009 International Conference on Mechatronics and Automation*. IEEE. 2009, pp. 3539–3544.

[LL16a] Jonqlan Lin and Guan-Ting Liao. “A modularized cable-suspended robot: Implementation and oscillation suppression control”. In: *Proceedings of the Institution of Mechanical Engineers, Part I: Journal of Systems and Control Engineering* 230.9 (2016), pp. 1030–1043.

[LL16b] Jonqlan Lin and Guan-Ting Liao. “Design and oscillation suppression control for cable-suspended robot”. In: *2016 American Control Conference (ACC)*. IEEE. 2016, pp. 3014–3019.

[LNC07] Casey Lambert, Meyer Nahon, and Dean Chalmers. “Implementation of an aerostat positioning system with cable control”. In: *IEEE/ASME Transactions on Mechatronics* 12.1 (2007), pp. 32–40.

[MA12] Ying Mao and Sunil Kumar Agrawal. “Design of a cable-driven arm exoskeleton (CAREX) for neural rehabilitation”. In: *IEEE Transactions on Robotics* 28.4 (2012), pp. 922–931.

[Mae+99] Kiyoshi Maeda et al. “On design of a redundant wire-driven parallel robot WARP manipulator”. In: *Proceedings 1999 IEEE International Conference on Robotics and Automation (Cat. No. 99CH36288C)*. Vol. 2. IEEE. 1999, pp. 895–900.

[May+05] David Mayhew et al. “Development of the MACARM-a novel cable robot for upper limb neurorehabilitation”. In: *9th International Conference on Rehabilitation Robotics, 2005. ICORR 2005.* IEEE. 2005, pp. 299–302.

[MB06] Tarek Madani and Abdelaziz Benallegue. “Backstepping control for a quadrotor helicopter”. In: *2006 IEEE/RSJ International Conference on Intelligent Robots and Systems*. IEEE. 2006, pp. 3255–3260.

[MD10a] Jean-pierre Merlet and David Daney. “A Portable, Modular Parallel Wire Crane for Rescue Operations”. In: *Robotics and Automation (ICRA), 2010 IEEE International Conference On*. IEEE, 2010, pp. 2834–2839. ISBN: 1-4244-5038-1.

[MD10b] Jean-pierre Merlet and David Daney. “A portable, modular parallel wire crane for rescue operations”. In: *2010 IEEE International Conference on Robotics and Automation*. IEEE. 2010, pp. 2834–2839.

[Mer06] Jean-Pierre Merlet. *Parallel robots*. Vol. 128. Springer Science & Business Media, 2006.

[Mer08] Jean-Pierre Merlet. “Kinematics of the wire-driven parallel robot MARIONET using linear actuators”. In: *2008 IEEE International Conference on Robotics and Automation*. IEEE. 2008, pp. 3857–3862.

[Mer17] Jean-Pierre Merlet. “Simulation of discrete-time controlled cable-driven parallel robots on a trajectory”. In: *IEEE Transactions on Robotics* 33.3 (2017), pp. 675–688.

[Min94a] Aiguo Ming. “Study on Multiple Degree-of-Freedom Positioning Mechanism Using Wires (Part I)-Concept, Design and Control”. In: *International Journal of the Japan Society for Precision Engineering* 28.2 (1994), pp. 131–138.

[Min94b] Aiguo Ming. “Study on Multiple Degree-of-Freedom Positioning Mechanism Using Wires (Part I)-Concept, Design and Control”. In: *International Journal of the Japan Society for Precision Engineering* 28.2 (1994), pp. 131–138.

[MKK97] Tetsuya Morizono, Kazuhiro Kurahashi, and Sadao Kawamura. “Realization of a virtual sports training system with parallel wire mechanism”. In: *Proceedings of International Conference on Robotics and Automation*. Vol. 4. IEEE. 1997, pp. 3025–3030.

[MKK98] Tetsuya Morizono, Kazuhiro Kurahashi, and Sadao Kawamura. “Analysis and control of a force display system driven by parallel wire mechanism”. In: *Robotica* 16.5 (1998), pp. 551–563.

[MV17] Forrest Montgomery and Joshua Vaughan. “Suppression of cable suspended parallel manipulator vibration utilizing input shaping”. In: *2017 IEEE Conference on Control Technology and Applications (CCTA)*. IEEE. 2017, pp. 1480–1485.

[NDD] Nurhayati Mohd Nur, Siti Zawiah Dawal, and Mahidzal Dahari. “The Prevalence of Work Related Musculoskeletal Disorders Among Workers Performing Industrial Repetitive Tasks in the Automotive Manufacturing Companies”. en. In: (), p. 8.

[OA05] So-Ryeok Oh and Sunil Kumar Agrawal. "Cable suspended planar robots with redundant cables: Controllers with positive tensions". In: *IEEE Transactions on Robotics* 21.3 (2005), pp. 457–465.

[ÖKO16] Julian Öltjen, Jens Kotlarski, and Tobias Ortmaier. "On the reduction of vibration of parallel robots using flatness-based control and adaptive inputshaping". In: *2016 IEEE International Conference on Advanced Intelligent Mechatronics (AIM)*. IEEE. 2016, pp. 695–702.

[Ort+02] Romeo Ortega et al. "Stabilization of a class of underactuated mechanical systems via interconnection and damping assignment". In: *IEEE transactions on automatic control* 47.8 (2002), pp. 1218–1233.

[Oti+08] Martin J-D Otis et al. "Hybrid control with multi-contact interactions for 6dof haptic foot platform on a cable-driven locomotion interface". In: *2008 Symposium on Haptic Interfaces for Virtual Environment and Teleoperator Systems*. IEEE. 2008, pp. 161–168.

[Par+06] Juyi Park et al. "Design of learning input shaping technique for residual vibration suppression in an industrial robot". In: *IEEE/ASME Transactions on Mechatronics* 11.1 (2006), pp. 55–65.

[PG08] Simon Perreault and Clément M Gosselin. "Cable-driven parallel mechanisms: Application to a locomotion interface". In: *Journal of Mechanical Design* 130.10 (2008).

[PKL19] Dinh Ba Pham, Jaejun Kim, and Soon-Geul Lee. "Combined control with sliding mode and partial feedback linearization for a spatial ridable ballbot". In: *Mechanical Systems and Signal Processing* 128 (2019), pp. 531–550.

[Pot18] Andreas Pott. *Cable-driven parallel robots: theory and application*. Vol. 120. Springer, 2018.

[Ras+18] Tahir Rasheed et al. "Tension distribution algorithm for planar mobile cable-driven parallel robots". In: *Cable-Driven Parallel Robots*. Springer, 2018, pp. 268–279.

[RHK15] Levi Rupert, Phillip Hyatt, and Marc D Killpack. "Comparing model predictive control and input shaping for improved response of low-impedance robots". In: *2015 IEEE-RAS 15th International Conference on Humanoid Robots (Humanoids)*. IEEE. 2015, pp. 256–263.

[Rob] *Die einzige Robotix Academy in Europa*. https://robotix.academy/.

[SOA94] Yusi Shen, Hisashi Osumi, and Tamio Arai. "Set of manipulating forces in wire driven systems". In: *Proceedings of IEEE/RSJ International Conference on Intelligent Robots and Systems (IROS'94)*. Vol. 3. IEEE. 1994, pp. 1626–1631.

[SZB07] Dragoljub Surdilovic, Jinyu Zhang, and Rolf Bernhardt. "STRING-MAN: Wire-robot technology for safe, flexible and human-friendly gait rehabilitation". In: *2007 IEEE 10th International Conference on Rehabilitation Robotics*. IEEE. 2007, pp. 446–453.

[TMC08] Cristina Tavolieri, Jean-Pierre Merlet, and Marco Ceccarelli. "A workspace analysis of a overconstrained cable-based parallel manipulator by using interval analysis". In: *3rd International symposium on Multibody Systems and Mechatronics*. 2008, pp. 1–13.

[TN08] Hamid D Taghirad and Meyer Nahon. "Kinematic analysis of a macro–micro redundantly actuated parallel manipulator". In: *Advanced Robotics* 22.6-7 (2008), pp. 657–687.

[Tsa99] Lung-Wen Tsai. *Robot analysis: the mechanics of serial and parallel manipulators*. John Wiley & Sons, 1999.

[Ver04] Richard Verhoeven. "Analysis of the workspace of tendon based stewart platforms". PhD thesis. Publisher not ascertainable, 2004.

[VHT98] Richard Verhoeven, Manfred Hiller, and Satoshi Tadokoro. "Workspace, stiffness, singularities and classification of tendon-driven stewart platforms". In: *Advances in robot kinematics: Analysis and Control*. Springer, 1998, pp. 105–114.

[Wan+15] Naige Wang et al. "Design and trajectory analysis of incompletely restrained cable-suspension swing system driven by two cables". In: *International Journal of Advanced Robotic Systems* 12.12 (2015), p. 189.

[Wor10] European Agency for Safety and Health at Work, ed. *OSH in figures: work-related musculoskeletal disorders in the EU - Facts and figures*. en. European risk observatory report. OCLC: 838180059. Luxembourg: Office for Official Publ. of the Europ. Communities, 2010. ISBN: 978-92-9191-261-2.

[Yi+16] Jiang Yi et al. "Vibration suppression based on input shaping for biped walking". In: *2016 IEEE-RAS 16th International Conference on Humanoid Robots (Humanoids)*. IEEE. 2016, pp. 236–241.

[Yoo+16] Jonghyun Yoon et al. “Multi-mode input shaping for vibration suppression of over-constrained cable-driven parallel robots with cable stiffness”. In: *2016 7th International Conference on Mechanical and Aerospace Engineering (ICMAE)*. IEEE. 2016, pp. 363–367.

[Yua15] Han Yuan. “Static and dynamic stiffness analysis of cable-driven parallel robots”. PhD thesis. Rennes, INSA, 2015.

[YYM02] Noritaka Yanai, Motoji Yamamoto, and Akira Mohri. “Anti-sway control for wire-suspended mechanism based on dynamics compensation”. In: *Proceedings 2002 IEEE International Conference on Robotics and Automation (Cat. No. 02CH37292)*. Vol. 4. IEEE. 2002, pp. 4287–4292.

[YYM04] Motoji Yamamoto, Noritaka Yanai, and Akira Mohri. “Trajectory control of incompletely restrained parallel-wire-suspended mechanism based on inverse dynamics”. In: *IEEE transactions on robotics* 20.5 (2004), pp. 840–850.

[Zan+14] Damiano Zanotto et al. “Sophia-3: A semiadaptive cable-driven rehabilitation device with a tilting working plane”. In: *IEEE Transactions on Robotics* 30.4 (2014), pp. 974–979.

[ZG12] Nathaniel Zoso and Clément Gosselin. “Point-to-point motion planning of a parallel 3-dof underactuated cable-suspended robot”. In: *2012 IEEE International Conference on Robotics and Automation*. IEEE. 2012, pp. 2325–2330.

[Zha+16] Yu Zhao et al. “Zero time delay input shaping for smooth settling of industrial robots”. In: *2016 IEEE International Conference on Automation Science and Engineering (CASE)*. IEEE. 2016, pp. 620–625.

[Zi+08] Bin Zi et al. “Dynamic modeling and active control of a cable-suspended parallel robot”. In: *Mechatronics* 18.1 (2008), pp. 1–12.

[ZSC17] Bingyuan Zhang, Weiwei Shang, and Shuang Cong. “Dynamic control with tension compensation of a 3-DOF cable-driven parallel manipulator”. In: *2017 IEEE International Conference on Cybernetics and Intelligent Systems (CIS) and IEEE Conference on Robotics, Automation and Mechatronics (RAM)*. IEEE. 2017, pp. 508–513.

Appendix A

Useful equations

A.1 Quintic polynomial equation

A fifth order polynomial also known as quintic polynomial is used in this work for defining the desired acceleration, velocity and position for the outputs to be controlled. The advantage of using a fifth order polynomial is that we can obtain a smooth profile for acceleration which will prevent any impulsive jerk occurring during the motion.

For a fifth order polynomial, to move from one point to another, we have six constraints (one each for initial and final positions, initial and final velocities, and initial and final accelerations). Once the six constraints are defined by the user the following equations (Eq. A.1) are used to generate the necessary values of position, velocity and acceleration:

$$\begin{aligned} q(t) &= a_0 + a_1 t + a_2 t^2 + a_3 t^3 + a_4 t^4 + a_5 t^5 \\ v(t) &= a_1 + 2 * a_2 t + 3 * a_3 t^2 + 4 * a_4 t^3 + 5 * a_5 t^4 \\ acc(t) &= 2 * a_2 + 6 * a_3 t + 12 * a_4 t^2 + 20 * a_5 t^3 \end{aligned} \tag{A.1}$$

where, $q(t)$, $v(t)$, and $acc(t)$ are the position, velocity and acceleration at time t, a_0, a_1, a_2, a_3, a_4, a_5 are coefficients that will be calculated from the constraints set for the motion.

Given the six constraints $q_0(t_0)$, $v_0(t_0)$, and $acc_0(t_0)$ for the initial values of position, velocity and acceleration at initial time t_0, and $q_f(t_f)$, $v_f(t_f)$, and $acc_f(t_f)$ for the final values of position, velocity and acceleration at the final time t_f, the

values of the coefficients are calculated by the solving the equation

$$\begin{bmatrix} 1 & t_0 & {t_0}^2 & {t_0}^3 & {t_0}^4 & {t_0}^5 \\ 0 & 1 & 2t_0 & 3{t_0}^2 & 4{t_0}^3 & 5{t_0}^4 \\ 0 & 0 & 2 & 6t_0 & 12{t_0}^2 & 20{t_0}^3 \\ 1 & t_f & {t_f}^2 & {t_f}^3 & {t_f}^4 & {t_f}^5 \\ 0 & 1 & 2t_f & 3{t_f}^2 & 4{t_f}^3 & 5{t_f}^4 \\ 0 & 0 & 2 & 6t_f & 12{t_f}^2 & 20{t_f}^3 \end{bmatrix} \begin{bmatrix} a_0 \\ a_1 \\ a_2 \\ a_3 \\ a_4 \\ a_5 \end{bmatrix} = \begin{bmatrix} q_0 \\ v_0 \\ acc_0 \\ q_f \\ v_f \\ acc_f \end{bmatrix} \tag{A.2}$$

The implementation of the quintic polynomial in the generation of the desired position, velocity and acceleration for the desired movement of a point from an initial value of 0.5 m to a final value of 1.5 m in a time of 10 s is shown in Fig. A.1. The initial and final values of velocity and acceleration are set as 0 for the motion.

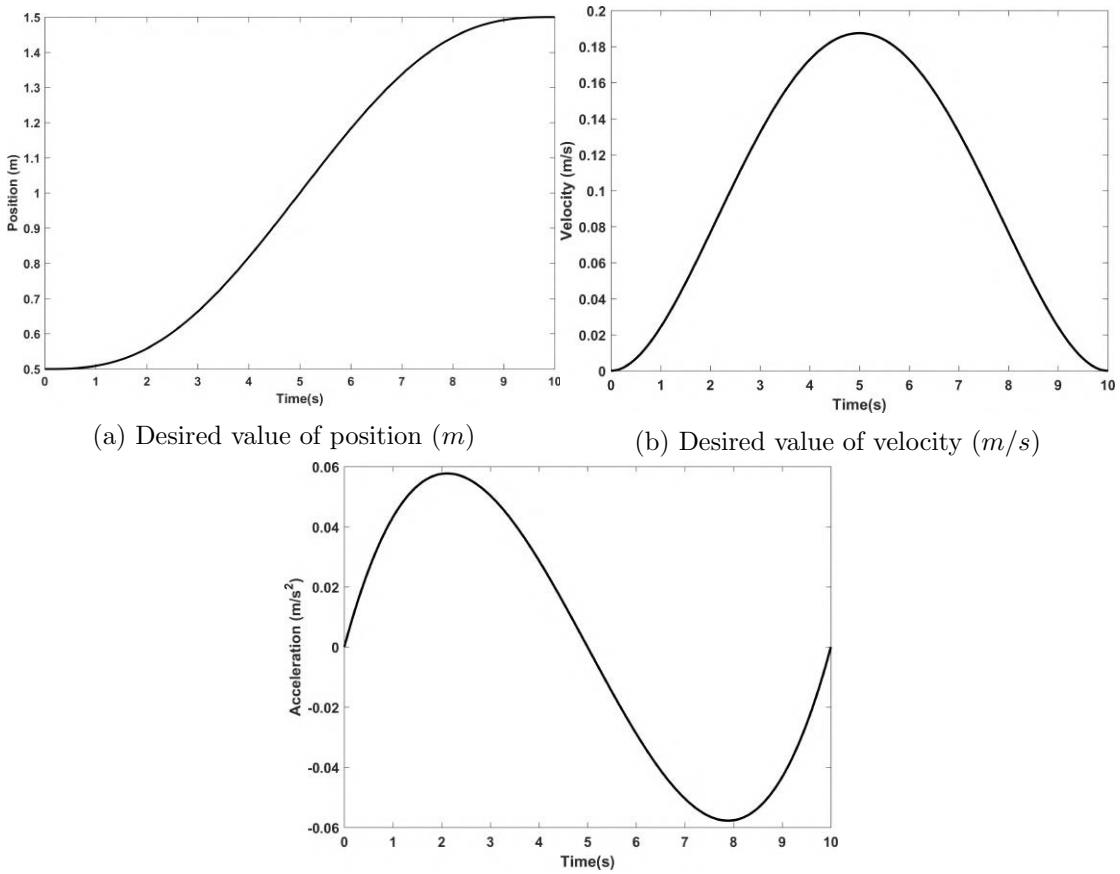

(a) Desired value of position (m)

(b) Desired value of velocity (m/s)

(c) Desired value of acceleration (m/s^2)

Figure A.1: Desired values of position, velocity and acceleration generated using the quintic polynomial

Appendix B

Hardware details

This appendix gives a brief information about the hardware components used and the interpolated position mode used to control the motors.

B.1 Hardware specifications

The important hardware specifications are mentioned in this section.

B.1.1 Motor specifications

The actuation of the winches is done by a DC brushless motor (Fig. B.1) supplied by Maxon. The important specifications needed for the work are given in table B.1.

Figure B.1: Maxon EC brushless motor with Hall sensor

Table B.1: Motor specifications

Details	Values
Nominal voltage	48 V
No load speed	6160 rpm
No load current	244 mA
Stall torque	3530 mNm
Nominal speed	5490 rpm
Max. efficiency	86 %
Torque constant	73.9 mNm/A
Rotor inertia	209 gcm^2
Weight	1100 g

B.1.2 Gearhead specifications

A planetary gearhead of ceramic version (Fig. B.2) is used for reduction in the actuation unit. The important specifications of the gearhead are given in table B.2.

Figure B.2: Planetary gearhead unit

Table B.2: Gearhead specifications

Details	Values
Reduction	74:1
Number of stages	3
Max. continuous torque	30 Nm
Max. intermittent torque	45 Nm
Average backlash no load	1°
Max. efficiency	75 %
Axial play	0-0.3 mm
Radial play	max. 0.06 mm, 12 mm from flange
Weight	770 g

B.1.3 Encoder specifications

The details of encoder (Fig. B.3) used in this work is given in table B.3. These specifications are used in the calculation of motor positions for the desired movement and also when the length of the cables are calculated from the motor positions during feedback.

Figure B.3: Planetary gearhead unit

Table B.3: Encoder specifications

Details	Values
Counts per turn	74:1
Number of channels	3
Max. angular acceleration	250000 rad/s^2
Signal rise time	180 ns
Signal fall time	40 ns

B.1.4 EPOS2 positioning controller

The control of motors is done by a small-sized, full digital, smart motion controller known as EPOS2 positioning controller (Fig. B.4).

Figure B.4: Positioning controller

Table B.4: EPOS2 specifications

Details	Values
Digital outputs	5
Operating voltage V_{cc} (min)	11 V
Operating voltage V_{cc} (max)	70 V
Max. efficiency	94 %
Installation program	EPOS setup
Interface	RS232, USB 2.0, CAN
Operating mode	Current, Speed and Position

Appendix C

List of publications

C.1 Publications in conference

1) Kumar, A. A., Antoine, J.F., I& Abba, G. Control of an Underactuated 4 Cable-Driven Parallel Robot using Modified Input-Output Feedback Linearization presented at the 21st IFAC World Congress, 2020, (IFAC 2020).

2) Kumar, A. A., Antoine, J.F., Zattarin, P., I& Abba, G. (2020). Modified Feedback Linearization for Underactuated Cable Robot Control: Case studies. Robotix Academy Conference for Industrial Robotics (RACIR), Luxembourg.

3) Kumar,A.A., Antoine, J.F., Zattarin, P., I& Abba, G. (2019). Workspace Analysis of a 4 Cable-Driven Spatial Parallel Robot. In ROMANSY, 22-Robot Design, Dynamics and Control (pp. 204-212). Springer, Cham.

4) Kumar, A. A., Antoine, J.F., I& Abba, G. (2019). Input-Output Feedback Linearization for the Control of a 4 Cable-Driven Parallel Robot – Published in 9th IFAC Conference Manufacturing Modelling, Management and Control MIM 2019, Berlin, Germany.

5) Kumar, A. A., Antoine, J.F., I& Abba, G. (2019). Linéarisation à rétroaction partielle d'un robot parallèle commandé par câble- 24ème Congrès Français de Mécanique(CFM), Brest, France.

6) Kumar, A. A., Antoine, J.F., I& Abba, G. (2019). Control of underactuated cable robot – presented in Robotix-Academy Conference on Industrial Robotics

2019 (RACIR 2019), Liege, Belgium.

7) Kumar, A. A., Antoine, J.F., Zattarin, P., I& Abba, G. (2018). Influence of payload and platform dimensions on the static workspace of a 4-cable driven parallel robot. Robotix Academy Conference for Industrial Robotics (RACIR), Luxembourg.